Archives of Computational Methods in Engineering
https://doi.org/10.1007/s11831-018-9257-4

ORIGINAL PAPER

Image Segmentation Using Computational Intelligence Techniques: Review

Siddharth Singh Chouhan[1] · Ajay Kaul[1] · Uday Pratap Singh[2]

Received: 12 June 2017 / Accepted: 26 January 2018

Abstract
Image segmentation methodology is a part of nearly all computer schemes as a pre-processing phase to excerpt more meaningful and useful information for analysing the objects within an image. Segmentation of an image is one of the most conjoint scientific matter, essential technology and critical constraint for image investigation and dispensation. There has been a lot of research work conceded in several emerging algorithms and approaches for segmentation, but even at present, no solitary standard technique has been proposed. The methodologies present are broadly classified among two classes i.e. traditional approaches and Soft computing approaches or Computational Intelligence (CI) approaches. In this article, our emphasis is to focus on Soft Computing (SC) techniques which has been adopted for segmenting an image. Nowadays, it is quite often seen that SC or CI is cast-off frequently in Information Technology and Computer Technology. However, Soft Computing approaches working synergistically provides in anyway, malleable information processing competence to manipulate real-life enigmatic circumstances. The impetus of these methodologies is to feat the lenience for ambiguity, roughness, imprecise acumen and partial veracity for the sake to attain compliance, sturdiness and economical results. Neural Networks (NNs), Fuzzy Logic (FL), and Genetic Algorithm (GA) are the fundamental approaches of SC regulation. SC approaches has been broadly implemented and studied in the number of applications including scientific analysis, medical, engineering, management, humanities etc. The paper focuses on introducing the various SC methodologies and presenting numerous applications in image segmentation. The acumen is to corroborate the probabilities of smearing computational intelligence to segmentation of an image. The available articles about usage of SC in segmentation are investigated, especially focusing on the core approaches like FL, NN and GA and efforts has been also made for collaborating new techniques like Fuzzy C-Means from FL family and Deep Neural Network or Convolutional Neural Network from NN family. The impression behind this work is to simulate core Soft Computing methodologies, along with encapsulating various terminologies like evaluation parameters, tools, databases, noises etc. which can be advantageous for researchers. This study also identifies approaches of SC being used, often collectively to resolve the distinctive dilemma of image segmentation, concluding with a general discussion about methodologies, applications followed by proposed work.

1 Image Segmentation

Segmentation of an image is the mechanism of segregating it into numerous segments as batch of pixels with some homogeneous features for instance texture, intensity, color which are more meaningful and easier to analyse objects within the image [1, 2]. The extent of homogeneity of the segmented region can be measured using some image property (e.g. Pixel intensity) [3]. Image Segmentation methodology is a part of almost all computer vision systems as a pre-processing step because it is one of the most common scientific issue, core technology and critical in image analysis and processing [1, 4, 5]. The level to which the subdivision is carried out be subjected to on the

✉ Siddharth Singh Chouhan
siddharth.lnct@gmail.com

Ajay Kaul
ajay.kaul@smvdu.ac.in

Uday Pratap Singh
usinghiitg@gmail.com

[1] Shri Mata Vaishno Devi University, Kakrayl, Katra 182320, India

[2] Madhav Institute of Technology and Science, Gwalior 474005, India

Published online: 07 February 2018

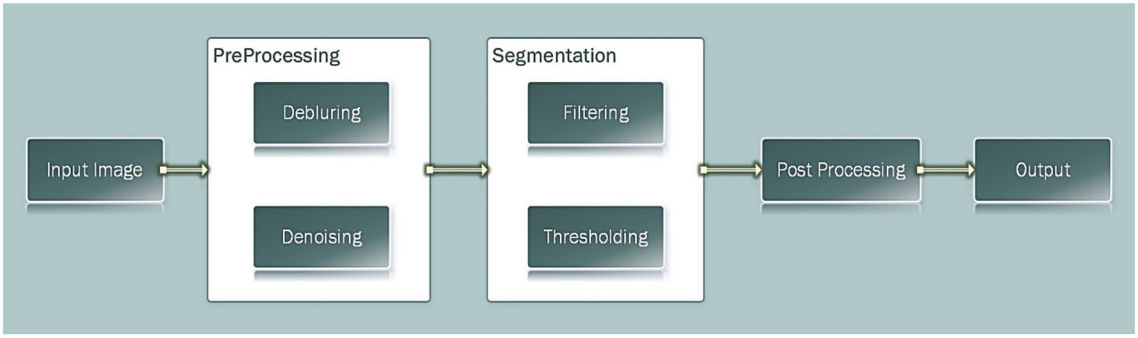

Fig. 1 Image segmentation process

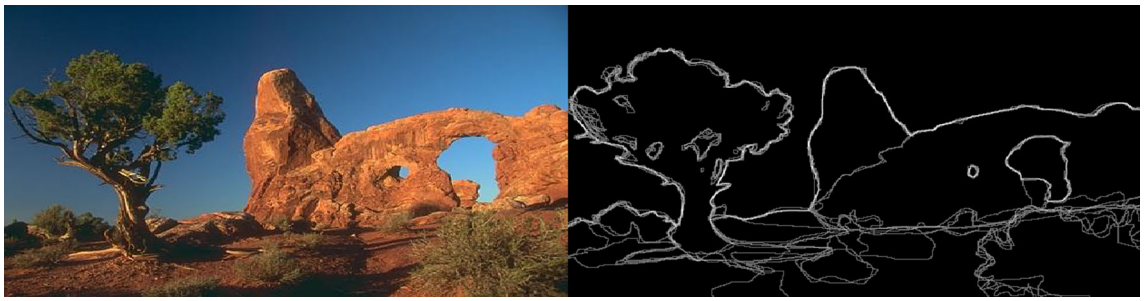

Fig. 2 Image segmentation result from BSD [6]

problem being solved. That is, segmentation should stop when the objects of interest in for an application have been isolated. Mathematically, if I designate the image, subdivision is the partition of I into N_s identical segments S_i such that Eq. 1:

$$\bigcup_{i=1}^{N_s} S_i = I, S_i \cap S_j = \emptyset, \quad i \neq j \tag{1}$$

An overview of an image processing has been shown Fig. 1. It consists of mainly five steps input, pre-processing, segmentation, post processing and output. At the first step an image is taken as input which is deblurred and denoised at pre-processing level then by applying filtering and thresholding at segmentation step followed by post processing to get the output result. An example of segmented image taken from BSD database [6] has been shown in Fig. 2. Shows that by adopting the theory of segmentation it becomes easier to extract more information from the given image and this is useful in various applications, like for medical images to locate tumors, measure of tissue volumes, study of anatomical structure etc., locating objects in satellite images like roads, forests, crops etc. and so on [7].

Extensive research has been carried out in developing different algorithms and methods for image segmentation but even today, no single standard method of image segmentation has emerged. Rather, there are assortments of hybrid methods that have received some degree of popularity. However, all the research work performed on image segmentation can be classified into two broad categories i.e. Traditional methods or Hard Computing (HC) and Soft Computing (SC) methods [8, 9]. Taxonomy of the traditional approaches distinguishing the following categories: Thresholding techniques (based on pixel intensity), Morphological methods (deformable), edge-based segmentation (boundary localization), Normalized Cut method (NC), Efficient graph-based method (EG), Mean shift method (MS), Level-set method (LS), Ratio-contour method (RC) etc. and the taxonomy of the different Soft Computing algorithms distinguishing the following categories: Fuzzy Logic (FL), Artificial Neural Network (ANN), Genetic Algorithm (GA), Ant Colony optimization (ACO), Particle swarm optimization (PSO) etc. type Evolutionary algorithms (EA) [10, 11].

Soft segmentation methodologies are flattering due to the flexibility of working with ownership functions. Moreover, from these ownership functions, the retrieval of its equivalent hard formulation is straightforward [9]. Soft Computing algorithms because of their adaptive nature and accuracy are predominantly used and preferred by researchers for segmentation [1]. They are tolerant of imprecision, uncertainty, partial truth, and approximations unlike hard computing and provide inexact solutions to the

problems [12]. Soft Computing approaches has been extensively studied and implemented in the last three decades for scientific research, engineering, medical, management, humanities etc. [10]. The principal methodologies of SC are FL, NN and GA. Soft computing working in hybrid manner that is combining the benefits of HC and SC or collaborating SC approaches as FL + NN, NN + GA and FL + GA [13] also has great impending for developing cost-effective, high-performance, and steadfast computing methods that provide pioneering results to problems [14]. Here in this article we are focusing on the core approaches of Soft Computing which has been adopted for the purpose of segmenting an image. Along with this we have also spotted the recent and the hybrid techniques like Fuzzy C Means, Deep learning or CNN.

After introduction, organization of the article follows as Sect. 2 compromises of methodology behind this article followed by Sect. 3 which introduces Fuzzy Logic, Neural Network, Genetic algorithm, and other methods, in Sect. 4 Literature review on the basis of Soft Computing approaches, Sect. 5 present the outcomes like problem domain for segmentation, databases used, evaluation parameters, future work etc., Sect. 6 is Discussions, followed by Sect. 7 consists of numerous future works, Sect. 8 enlightens our proposed work, Sect. 9 concludes this article followed by references.

2 Methodology

The research methodology comprises reviewing papers for SC methods introduced to the related developments in image segmentation.

2.1 Sources and Search Methods

The databases that had been concerned in this study consist of IEEE Digital library, Elsevier, and Springer. The reviewed papers were sorted out from more than 75 journals and magazine such as IEEE Access, IEEE Transactions on Aerospace And Electronic Systems, IEEE Journal of Selected Topics in Applied Earth Observations and Remote Sensing, IEEE Transactions on Cybernetics, IEEE Computational Intelligence Magazine, IEEE Transactions on Information Technology in Biomedicine, IEEE Transactions on Fuzzy Systems, IEEE Transactions on Image Processing, IEEE Transactions on Biomedical Engineering, IEEE Transactions on Consumer Electronics, IEEE Transactions on Systems, Man, And Cybernetics, IEEE Transactions on Medical Imaging, IEEE Transactions on Pattern Analysis And Machine Intelligence, Pattern Recognition, Applied Soft Computing, Future Generation Computer Systems (FGCS), Pattern Recognition Letters, Computer Methods and Programs in Biomedicine, IRBM, Neurocomputing, Knowledge-Based Systems, Alexandria Engineering Journal, Egyptian Informatics Journal, ISPRS Journal of Photogrammetry and Remote Sensing, Journal of Computer Science and Technology, Automatic Control and Computer Sciences, Signal, Image and Video Processing, Soft Computing, Soft Computing: Methodologies and Applications, and so on.

Given the specific interest in how soft computing techniques have been applied to image segmentation. Keywords which were used to cross-search related papers in specific databases are soft computing approaches for image segmentation or object detection using fuzzy logic, neural network, genetic algorithm along with neuro-fuzzy, fuzzy genetic such hybrid approaches. Some of the recent conference papers from IEEE conferences proceeding has also been considered in this article. As a result, the total number of 276 articles published in referred journals and conferences where finally referenced.

2.2 Scope and Contribution

The concept of Image Segmentation or Object Retrieval from an image using Soft Computing has been evaluated by many researchers from numerous perceptions. However, it is beyond the extent of this paper to address all difficulties in detail. So in an effort to provide a more severe review of existing papers in this area, paper mainly focuses on image segmentation using soft computing approaches such as FL, NN and GA are the major focus in this research.

Here in this paper we attempt to enlighten the soft computing methodologies used for the purpose of image segmentation being the most important and critical task as a pre-processing step in image processing. Our work is focused on the core approaches like FL, NN and GA. Since these techniques gives the approximate results, are used in number of critical applications like extracting WM, GM, CSF and background from an MRI brain image, finding out objects from complex real world scenes etc. Our contribution lies in the fact that we had done literature survey from number of papers introducing recent approaches like FCM, DNN or CNN etc. The application researchers were interested in, the evaluation parameters for inspecting segmentation accuracy, the results comparison of several approaches, the databases used by the researches, the future work, other parameters like noises used, tools or software used for implementation purposes were surveyed for the purpose of helping researchers to carry out research in this domain.

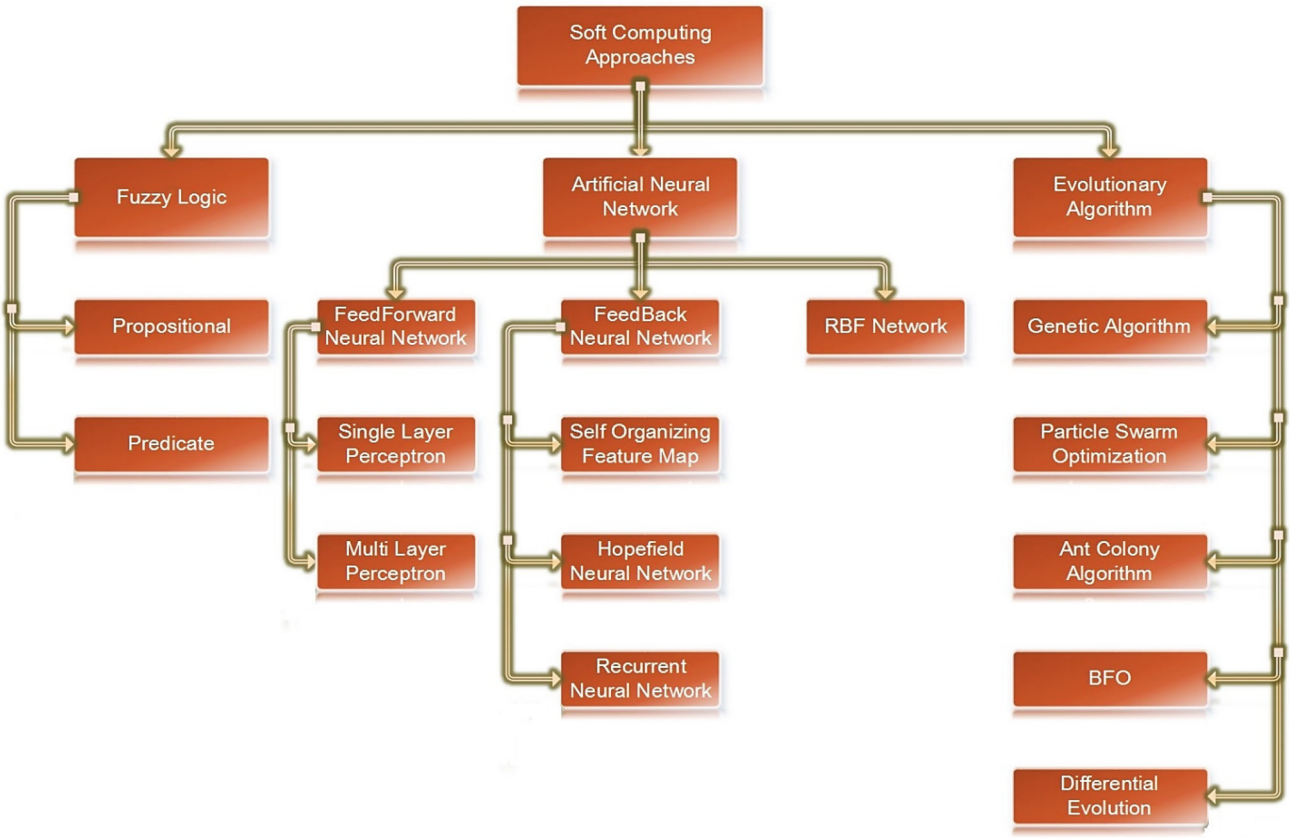

Fig. 3 Soft computing taxonomy

3 Soft Computing

Soft computing (SC) delivers the opportunity to represent vagueness in human thinking with the ambiguity in the real world complex problems [13] working synergistically with artificial intelligent methods. It is a combination of computing techniques and biological structures that provide new methods for more competent, vigorous, and dependable solutions [14]. According to Zadeh known as the father of Soft Computing and Fuzzy Logic (FL) initiated SC in the 1990s [13, 14], defines SC that, it is mainly a consortium of Fuzzy Logic, Artificial Neural Network, and Genetic Algorithm together termed as to be artificial intelligence [15] that has the capability to abide uncertainty, roughness, and incomplete truth to attain controllability and sturdiness with a low-cost solution for simulating human decision-making behaviour [10]. In Fig. 3 we have presented a taxonomy for various soft computing methods which has been categorize mainly into three parts that is FL, ANN and Evolutionary Algorithm. The FL is further classified into two that is propositional and predicate logic, ANN into Feedforward Neural Network (single and multiplayer perceptron), Feedback Neural Network (Self organizing feature map (SOFM), Hopfield Neural Network (HNN), Recurrent Neural Network (RNN)) and Radial Basis Function (RBF) networks, EA (Genetic Algorithm (GA), Particle Swarm Optimization (PSO), Bacterial Foraging Optimization (BFO), Ant Colony Optimization (ACO), Differential Evolution) and so on [10]. Differing from the hard computing (HC) where each time the exact result is guaranteed, SC is a technology which deals with inexact solutions to the problems such as the problem of NP-complete where no computing method solves the problem in given polynomial time. The difference between hard computing and soft computing is given in Table 1. As hard computing provides exact models working with symbolic logic reasoning and numeric modelling SC provides approximate models working with approximate reasoning and modelling [12] as shown in Fig. 4.

Some of the applications of SC which has also been seen from the literature in various fields are, in [16] ANN is used to calculate the highest power created by the non-linear and intermittent behaviour of PV/wind input sources management and control, [10] context-based video retrieval, [17] detection of plant leaf diseases, [18] for coastal study, [19] prediction of monthly regional groundwater, [20] RNN and CNN has been used for multimodal affect analysis, [21] the

Table 1 Differences between HC and SC

Hard computing	Soft computing
Used where an exact result is desired	Used where an inexact result is desired
Conventional mathematical and analytical model	Does not uses conventional mathematical and analytical model
Follows Binary logic or Boolean logic [0, 1]	Multivalued logic (Boolean logic + Fuzzy logic) results can be between 0 and 1
Precision, certain, tractable	Imprecision, uncertain, intractable
Exact input data	Ambiguous and noisy data
Sequential computations	Parallel computations
Example: computer	Example: human

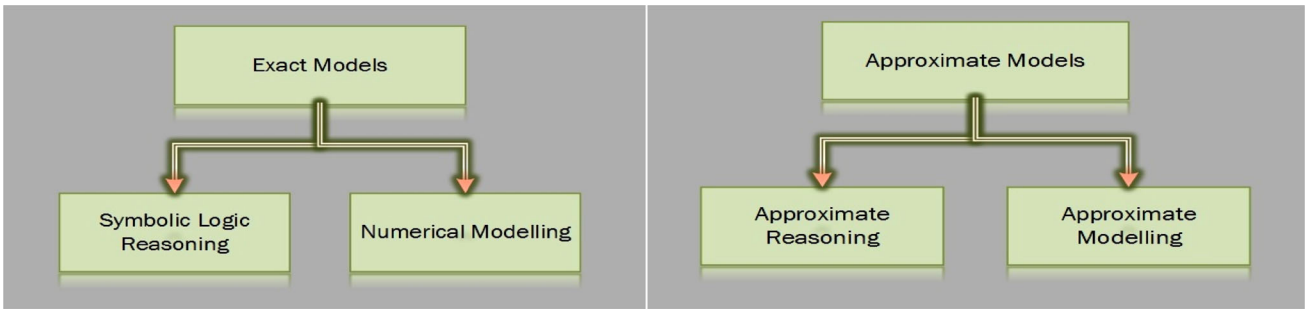

Fig. 4 Hard and soft computing conceptual model

plant disease detection system for automatically detecting the symptoms that appear on the leaves and stem, [22] soft computing has been used for classification of weeds, [23] to determine the quality of water in river and to help to extract the key features and problems with the existing systems for water treatment, [15] MR brain image segmentation, [24] intellectual forecasting of the enactments in PV/T collectors, in [25] for segmentation in strategic marketing, [26] identification of plant species, SC has been adopted [14] in the field of biological and agricultural engineering especially for the soil and water for crop management and decision support in precision agriculture [27], SC approaches for grid connected PV system, [28] segmentation of green plants, [13] for medical related problems, [29] for supply chain management, [30] SC methods for maximum power point stalking of SPV system, [31] in engineering design, in [32] fusion of HC and SC has been used for control of large-scale industrial plants, in [33] for brain MRI segmentation, to segment SAR images in [34], for moving object segmentation in [35], for Dermoscopy images in [36], Nucleus segmentation from brain tumor, Neuroendocrine tumor (NET) and breast cancer images in [37, 38] Feed forward neural network is adopted for English hand letter recognition, in [39] for 3D segmentation of lung from CT images using SC technique and so on.

3.1 Fuzzy Logic (FL)

Clustering is an unsupervised procedure of grouping a set of entities into classes of alike features [40]. It has been extensively applied in a number of fields, such as geology, engineering systems, machine learning, statistics, medicine, etc. [41]. Among various clustering algorithms, fuzzy algorithms, FCM, Gustafson–Kessel (GK) and non-fuzzy algorithms like k-means (KM), are most popular [42]. Meanwhile, clustering techniques group consists of following methods shown in Fig. 5.

The k-means or Hard C-Means is an iterative method which can be run several times to reduce the sensitivity caused by initial random selection of centroids that were introduced by MacQueen in 1967. It is a partitioning algorithm applied to classify data into $c(1 \leq c \leq N)$ clusters and each object (observation) can only belong to one cluster at a given point of time. Consider a dataset Z with N observations. Each observation is an n-dimensional row vector $z_k = [z_{k1}, z_{k2}, \ldots z_{kn}] \in R^n$. The dataset Z is represented as $N \times n$ matrix. The rows of Z represent samples (observations) and the columns are measurements for these samples (objects). K-means model achieves its partitioning by the iterative optimization of its objective function (a squared error function) given in Eq. 2.

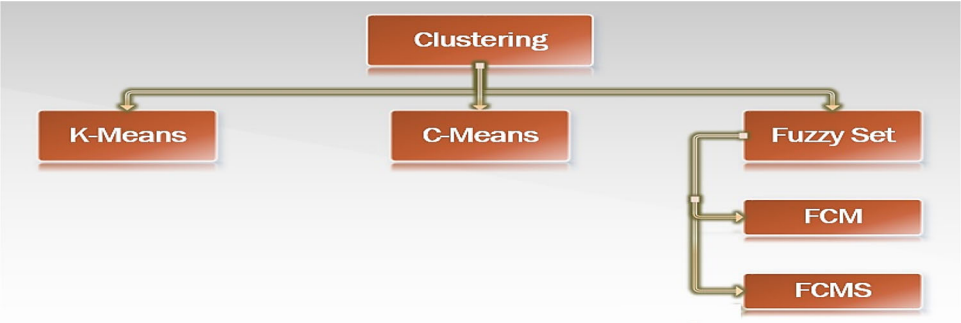

Fig. 5 Clustering techniques

$$J(V) = \sum_{i=1}^{c} \sum_{k=1}^{N} ||z_k - v_i||^2 \tag{2}$$

where $||z_k - v_i||^2$ is the Euclidean distance calculated between kth object, z_k and ith centroid, v_i [42].

Although it is the most favourable technique, it does have some weaknesses like its dependency on initialization, sensitive to outliers and skewed distributions causing converge to a local minimum or may miss a small cluster. There are a number of clustering procedures proposed to overwhelm the above-mentioned weaknesses such as C-Means. Partitioning the data into C-clusters is carried out by compacting data in the same clusters and separating data in different ones. C-means clustering provides crisp segmentation which does not take into account fine details of infrastructure such as hybridization or mixing of data [43, 44]. Another and most widely used method to reduce the deficiency of the other clustering approach is the fuzzy model.

Fuzzy set was proposed in 1965, which is an extension of the classical set theory. A paper to smear fuzzy on biology was the first application of fuzzy when Zadeh published a paper in 1969. FL provisions mathematical competence for the impersonation of the thought and perception procedures acts as the elementary theory of SC [45]. Its application predominantly in control engineering since the model of the system is anonymous. Over the interval [0, 1], FL is a set by means of graded membership [10]. Whereas in classical set theory the elements are either part of sets or not, considered as hard or crisp sets having Boolean membership [10]. Fuzzy logic is an exact multi-valued logic concept which practices fuzzy set theory. Its objective is to formalize the tools of almost precise perceptive [10, 46]. A fuzzy set, is denoted mathematically by Eq. 3 [10, 47, 48].

$$A = \int_{A} \frac{\mu_A(x)}{x} \tag{3}$$

where $A =$ fuzzy set, $X =$ universe of discourse, $\mu_A(x)$ is a membership function describing the degree of membership of points in X in the fuzzy subset A.

Fuzzy logic is among the indispensable approaches of SC techniques which can deal with impreciseness of input data and domain information to give rapid, modest and frequently adequate good approximations of the anticipated results. FL is dissimilar from probability theory for the reason that FL is deterministic instead of probabilistic. Imprecision is modelled via fuzzy sets, linguistic variables, membership functions, inferences, and defuzzification. These concepts are all controlled in an entirely deterministic manner. There exist several forms of formal FL like, fuzzy set theory, and fuzzy control systems. The principle fundamentals of FL classifier system [46] are depicted in Fig. 6.

- *Fuzzifier* The Fuzzifier accomplishes a mapping from the crisp input to fuzzy set. The input is characterized by a membership function.
- *Fuzzy rule base* The Fuzzy rule base consists of a set of linguistic rules like "IF a set of conditions are satisfied, THEN a set of consequences are inferred".
- *Fuzzy inference engine* The Fuzzy inference engine is decision-making logic that employs fuzzy rules from the fuzzy rule bases to determine a mapping from the fuzzy sets in the input space to the fuzzy set in the output space.
- *Defuzzifier* The Defuzzifier performs a mapping from the fuzzy set in the output to crisp output.

The advantages of fuzzy logic are as follows [13]

- As compared with model-based or other controllers to perform same task use of fuzzy is economical.
- Fuzzy is could be at ease to understand, modify and also they can be articulated in natural linguistic so could be altered rendering to individual prospects.
- Fuzzy is simple to learn and implement.
- Fuzzy can be simulated with conventional techniques.

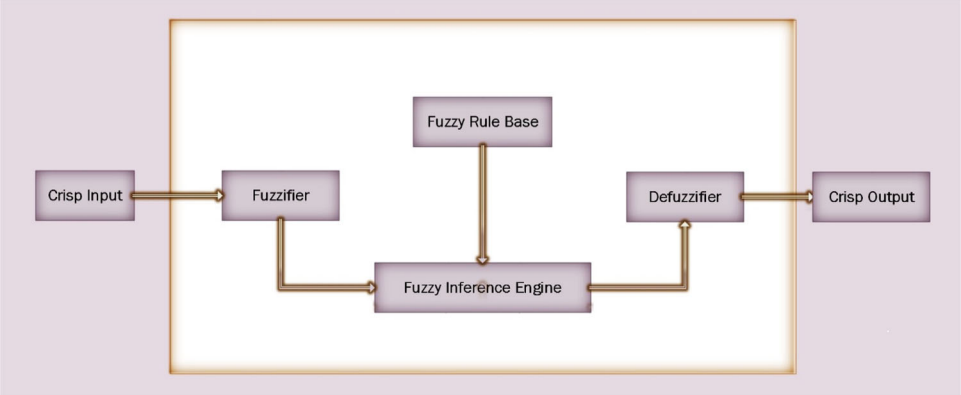

Fig. 6 Fuzzy classifier system

Fuzzy logic has widely been applied in several areas mainly to deal with qualitative, inexact, uncertain and complicated processes the fuzzy logic system can be well-adopted since it exhibits human-like thinking process. In current years, imaging has required the use of fuzzy technology to pay off for the ambiguity accompanying with class definitions, boundaries, and inexact gray levels. Fuzzy clustering as a soft segmentation technique [49] has been extensively studied and successfully applied in image subdivision [2, 50]. Amongst the fuzzy clustering approaches, FCM algorithm is the prevalent technique used in image subdivision as it has vigorous characteristics for vagueness and can recollect much more statistics than hard segmentation approaches [3, 50–53].

Data clustering is the important task in many of the application so a new approach devised by Dunn in 1973 and modified by Bezdek in 1981 depending on FS named Fuzzy c-means algorithm (FCM) was introduced [44, 54–56]. This approach is intended to knob the obligatory crisp grades of membership of pixels to dissimilar clusters [57]. So, FCM has emerged to be an efficient mechanism when it comes for data clustering [3, 52]. In this approach a portion can belong to two or many clusters [50, 56, 57]. It has proven to be an effective tool for partial volume effect [56, 58], but it does suffer from the problems such as drifting of center of clusters, sensitiveness among classes due to intensity overlap [59]. FCM algorithm accomplishes unsupervised clustering [54, 60], makes it possible for segmenting images automatically under circumstances of vagueness and fuzziness [59]. Because of the reason FCM does not contemplate spatial evidence for a given image it does suffer from noise [53, 61]. Other than this FCM has proven to be efficient algorithm in number of fields such as in pattern recognition, machine learning etc. FCM has also been adopted for categorizing an image into its substituent parts quite effectively. FCM is a nonlinear iterative optimization approach which is built on an objective function and also minimizing it [50, 53, 54, 56, 57]. The motivation behind FCM is to treasure centroids (cluster centers) so that dissimilarity function can be minimized. The objective function (weighted distance), is well-defined as for segregating $\{x_k\}_k = 1 : N$ into c cluster is given in Eq. 4.

$$J_{FCM} = \sum_{i=1}^{c} \sum_{k=1}^{N} u_{ik}^{p} = ||x_k - v_i||^2 \tag{4}$$

where c = no. of clusters (predefined), N = no. of pixels from given image, x_k = gray value of the k-th pixel, v_i = center of the i-th cluster, u_{ik} = membership of the k-th pixel in the i-th cluster, having every pixel constriction $= \sum_{i=1}^{c} u_{ik} = 1$; p = is the amount of fuzziness generally higher then 1; $\| \|$ = the standard Euclidean distance [50–53, 62, 63]. Lagrange multiplier method is used for objective function minimization [8, 32]. In a traditional FCM producing initial cluster is a crucial step if it is done then the algorithm achieves fast convergence, less computational time, less iteration process because of initial cluster helps in finding final cluster [53].

The use of fuzzy family on number of applications for image segmentation are segmenting images with various textures [2], Segmenting gray scale and color images [43], Underwater image segmentation [54], For brain MRI segmentation [62], To segment leukocytes in blood smear images [64], Segmentation of various images with spatial constraints [11], Automatically detecting facial images segmenting it into forehead/eyes and mouth [65], Retinal vessel segmentation [46], infrared ship image segmentation [66], To segment urban information from VHSR multispectral images [67], Specific object detection in complex scenes [61], Tissue segmentation from MRI brain images [68], To segment M-FISH [69], To segment MRI into background, CSF, WM, or GM [49], To segment building, road, vegetation, tree, water and land area [70], To segment various images [50], Segment the suspicious nodules from

CT images [51], Clustering of noisy data and to remove [52] and so on.

3.2 Artificial Neural Network (ANN)

Artificial Neural Networks (ANN) is a highly parallel connectionist organisations modelled on biological neurons. The concept of ANN investigation was revealed nearly 50 years ago, but it is only in the last 20 years that applications of ANNs are already becoming a fairly renowned technique within computer science [14]. The basic objective is to impersonate the human vision processing scheme which is highly robust, reluctant to noise, work with even insufficient information, searching for the optimum results working with a problem such as a brain tissue segmentation. ANN learns from the past and does not use any rule sets [71, 72]. Based on external or internal statistics that streams through the network all through the learning phase ANN is adaptive to the system and changes its structure. The learning can either be supervised or unsupervised [14]. The learning process tries to discover a set of connections that give a mapping that fits the training set well. There are 3 layers in an ANN 1. Input 2. Hidden 3. Output as depict in Fig. 7. Between the layers of units are connections containing weights also known as synaptic weight. ANN simulates the brain in two respects: (1) By learning phase knowledge acquired by the network (2) Synaptic weights (interneuron connection strengths), used to store the acquired knowledge. These weights serve to proliferate signals through the network. Learning of network is completed using a method which can imitate of as gradient descent in the connection weight space. Once the learning has been accomplished, given any set of inputs and outputs, the network reproduces the outputs. Error Back Propagation (EBP) method is used for finding the weights which produce correct outputs for given inputs and adjusting the same.

NN can be treated as a simple matrix–vector multiplier, it has been proven by Bhattacharyya and Maulik to provide

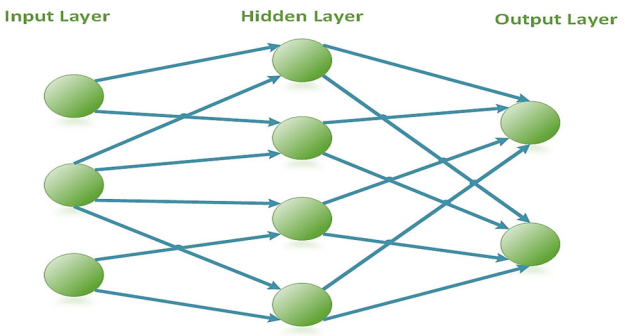

Fig. 7 NN architecture

a mathematical model of NN. Denoted by let z inputs $\{r_1, r_2,\ldots, r_z\}$ coming at a getting from z previous neurons falls in a vector space A_z. If the interconnection weight matrix $W_{y\times z} = \{w_{ij}, i = 1, 2, 3,\ldots, z; j = 1, 2, 3,\ldots, y\}$, from y such receiving neurons to their z preceding neurons is signified by [10], i.e.

$$B = \begin{bmatrix} w_{11} & w_{12} & w_{13} & . & . & w_{1z} \\ w_{21} & w_{22} & w_{23} & . & . & w_{2z} \\ w_{31} & w_{32} & w_{33} & . & . & w_{3z} \\ . & . & . & . & . & . \\ . & . & . & . & . & . \\ w_{y1} & w_{y2} & w_{y3} & . & . & w_{yz} \end{bmatrix} \times \begin{bmatrix} r_1 \\ r_2 \\ r_3 \\ . \\ . \\ r_z \end{bmatrix} \quad (5)$$

vector specified by

$$B = \begin{bmatrix} b_1 \\ b_2 \\ b_3 \\ . \\ . \\ b_y \end{bmatrix}$$

Thus, each jth (j = 1, 2, 3,…, y) neuron is nourished through a constituent of the vector $[b_1, b_2, b_3,\ldots,b_y]$ T forming the summing mechanism. By means of processing task, each such jth (j = 1, 2, 3,…, y) neuron then smears the equivalent activation function (f_a) to the elements of this vector to produce the equivalent output response Y_j, j = 1, 2, 3,…, y, as shown in Eq. 5. Thus, specified a set of inputs in A_z, the interconnection weight matrix $W_{y\times z} = \{w_{ij}, i = 1, 2, 3,\ldots, z; j = 1, 2, 3,\ldots, y\}$ along with the activation function f_a decide the output replies of the neurons and thus the NN maneuvers as a simple matrix–vector multiplier.

$$Y = f_a \begin{bmatrix} b_1 \\ b_2 \\ b_3 \\ . \\ . \\ b_y \end{bmatrix}$$

Though NN precludes mathematical calculations, physical or impractical models for simulating real world complex glitches they do have some shortcomings [10]. Below are the listed some advantages as well as disadvantages of NN [13].

Advantages

- NN have the capability of learning to obtain information and acquaintance for a problem.
- They can deal with continuous data which contains many variables.
- Can be a black box methodology.
- NN can handle noisy input data.

Disadvantages

- The data used for training purposes should cover the entire range of the system.
- Limitation of theoretical concepts to design NN.
- Does not guarantee an exact solution.

The parameters of NN are given in Table 2.

In order to simulate the thinking and classification power of human being for extracting interesting features a lot of research has been done from the several decades for a system to be as smart as human. Deep learning among a new concept under AI which is having the capability of learning high level features from low level feature is being the area of interest for such kind of applications of target recognition and classification. Deep learning has a unique capability of initialization through unsupervised learning and then fine tuning through supervised fashion [73–80]. Deep learning algorithms predominantly Convolutional neural networks (CNNs) have revealed their sturdier feature depiction power in a wide range of computer vision applications [77, 81]. CNNs have been severely used once in the 1990s. Hinton and Salakhutdinov initiated again it in 2006 [74]. In 2012, Krizhevsky et al. made CNNs regain focus by showing superior image classification truthfulness on the ImageNet Large Scale Visual Recognition Challenge (ILSVRC) data set revolution through the efficient use of GPUs, ReLUs, new dropout regularization, and effective data augmentation [73, 82].

CNN stimulated by neuroscience is a distinctive kind of Deep NN [74]. CNN is a hierarchically organized (generally three layers) FFNN [83, 84]. Using local association among the neurons of nearby layers CNN exploits local correlation [74, 75]. For image classification, the CNNs are almost of the same two-stage architecture, while the differences are their configurations, the depth, the number of units, and the form of nonlinear functions. The first stage of CNNs acts as a feature extractor, which learns rich hierarchical features mainly using a Convolutional operation, and the last stage is a multilayer perceptron classifier [82]. CNN has the capability of reducing number of parameters with the help of local influences by significantly extracting the shared weights and spatial information [73, 75]. Supervised CNN is better feature extractor when compared with unsupervised CNN because supervised CNN uses class specific information provided with training samples [74, 83]. The structural design of CNN is dissimilar from former deep learning models [73, 82]. CNN is hard to train but there are two important facts lies in the design of CNN i.e., local connections and shared weights. CNNs are a special kind of NN for processing data that has a recognized, grid-like topology. CNN is organized as a sequence of phases revealed in Fig. 8. Input layer, convolution layer, pooling layer, fully connected layer are the basic layers of CNN [74, 75, 77–79, 82–90]. By piling numerous convolution layers and pooling layer CNN is constructed to form a deep architecture. Convolutional layer works on small local receptive fields of input data in a sliding window fashion.

Each filter acts as a specific feature detector, in each layer multiple convolution filters exists, that work in parallel. By using a set of weights each neuron is associated to previous layer through local patches [74, 82]. It is important to set proper weight (connections) of CNN since the power of CNN comes from that. Cost function or an error measure has to be set properly before setting an updating rule which can be done by using a mini-batch update. The outcome of this locally weighted sum is then put into an activation function [73, 74]. Which acts as a non-linear transformation that prevents CNN from learning trivial linear groupings of the inputs. The aim of convolution layer is to perceive local groupings of features as of the preceding layer. The pooling layer helps in reducing the

Table 2 Parameters of NN

Parameters	Description
Neurons number in hidden layer	It defines the no. of neurons at hidden layer excluding input and the output layer
Learning rate (α)	It is the total amount of weight and bias adjustment done at each step of learning or training. It ranges between 0 and 1
Momentum	It is used to make update in current weight by a fraction m of previously updated weight so that it will not converge to local minima
MSE-mean square error	Sum of the squares of the dissimilarity among the actual output plus the target output. As the MSE reaches zero, training will be stopped
Training type	There are two types of training performed in a NN to decide the no. of iterations: (1) Based on Epoch (2) Based on MSE
Vigilance parameter (p)	It is used to control the similarity of patterns that are in the same cluster
Weight	A neuron is connected to another neuron through a weighted link and the number assigned to it is known as the weight which contains the information about input signal

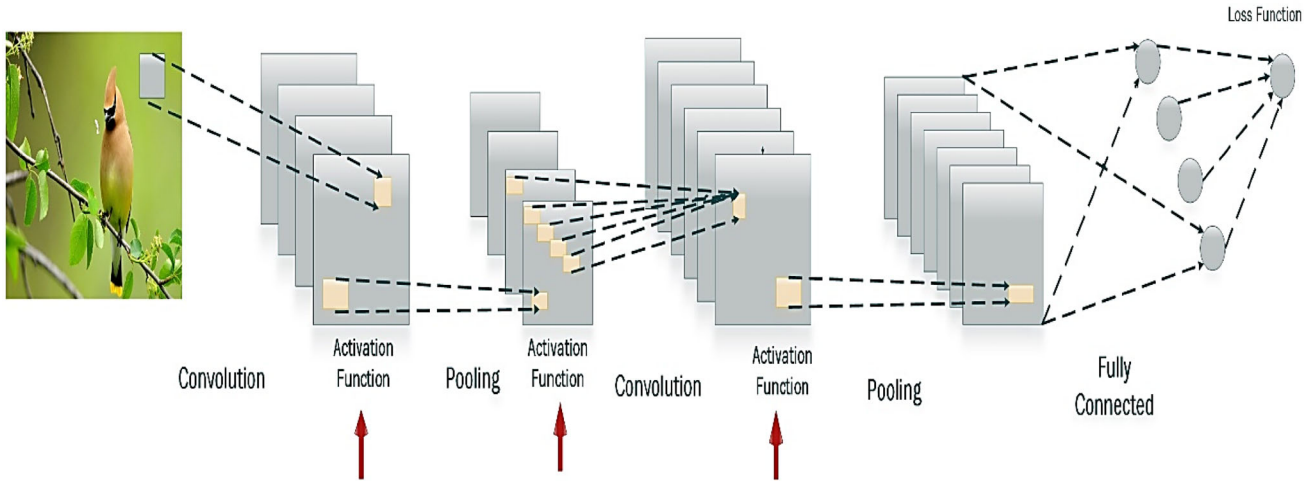

Fig. 8 Convolutional neural networks (CNN)

data size by merging semantically analogous features into one it also has two important assistances 1. It does only allows output to change very little as input changes in appearance and position and 2. Having many layers pooling can cut off cost of the CNN [74, 75, 82–87]. Max pooling is furthermost common pooling. The output of CNN can be measured with the help of a loss function which is the difference between a true image and output of CNN. Thus a good training of CNN minimizes the loss function and CNNs performance is improved which is generally obtained with the help of stochastic gradient descent (SGD). [74, 83]. Applications deep CNNs to many pattern recognition tasks, image classification, object detection, medical imaging, feature extraction or representation learning, face recognition, pedestrian detection, recognition of handwriting and vehicle detection [74–79, 81–84, 86, 90, 91].

Some of the applications of neural networks are QBDSONN for instantaneous object segmentation in [92], in [93] NN to segment CT images thyroid and volume estimation. MLP used for brain tumor segmentation in [71], segmentation of carbon nanotube images in [72]. Some of the applications of PCNN are for Dark-Spot Detection from SAR in [94], a region-based object in [95], SAR segmentation in [96], and digital image segmentation in [97]. SOFM for Object extraction in [92], segmentation of tumor in [98], Partial Volume Segmentation in Brain MR Image in [99].

3.3 Genetic Algorithm (GA)

The father of original GA was John Holland who invented it in the 1960s [100]. GAs are effective, parallel, adaptive, vigorous search and optimization methods, inspired from the genetic adaptation of natural evolution and have implicit parallelism which is finding application in a number of practical complex problems [10, 14]. Various segmentation approaches have been recommended in the past that make use of evolutionary algorithms, and predominantly genetic algorithms (GA) [14]. The most important characteristic of GA is being a global optimization technique [100]. GA uses payoff values known as fitness to guide the search which makes it blind optimization technique that do not need derivatives to explore the search space. This quality can make GAs more robust than other local search procedures such as gradient descent or greedy techniques used for combinatorial optimization [101, 102]. The vital constituents of GAs are chromosomes known as a representation strategy, a chromosomes population, a fitness function used for validating each string, procedure for selection or reproduction and genetic operators. The fitness function (FF) is used to find the best candidate node so that the candidate node represents a maximum number of vectors of the training set, and has minimum distances to these represented vectors. A simple GA consists of four operations: Selection, Genetic operation, Hill Climbing and Replacement. Genetic operations are the crossover (reproduction) where two parents are selected to mate in order to reproduce new siblings [101, 102] and mutation is the process of changing one gene (parent) from one type to another. Replacement is the process of replacing parents with newly evolved sibling. The role of Hill-climbing process is to investigate adjacent points in the search space, and to move in the direction of giving the greatest increase in fitness [103]. Optimal solutions can only be attained at the expense of large population sizes and after a large number of generations [101, 102]. The simple GA structure is shown in Fig. 9 and parameters description in Table 3.

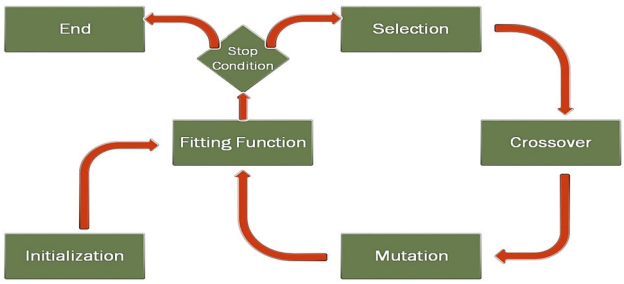

Fig. 9 Genetic algorithm structure

GA phases are as under:

- Prepare the population.
- By means of fitness function calculate fitness values after decoding the strings.
- Stop the procedure if cessation measure is achieved.
- For a novel mating pool reproduction has to be done.
- Using crossover and mutation produce another population.
- Be present at Step II [100, 104].

By considering an elitist selection approach, where r and s = probabilities, $s = 1 - r$, A = max. no. of generations, P_i = no. of generations before buffer refreshment in the ith evolution, $i \geq 1$ then expected convergence = C is given by Eq. 6 [10].

$$C = \frac{r(1-s)^{(A-1)}}{1-(1-r)^{(A-1)}} \tag{6}$$

Advantages [100]

- GA is derivative-free technique.
- GA can be used for both continuous and discrete optimization problems
- GA adopts stochastic operators, so will not get into local minima situation.
- GA works directly with binary strings like population, solution set but not with the parameters themselves.

The applications of genetic programming can be texture segmentation, object detection, image classification, image segmentation and so on. Some of the genetic applications which have been applied in the past are Genetic Sequential Image Segmentation (GeneSIS) for object extraction form SAR images in [105], Adaptive genetic algorithm (AGA) by improving it to adaptive genetic algorithm (IAGA) was proposed for image segmentation in many applications [106], in [103] the genetic-based GFCM on multiple Graphic Processing Units (GFCM2G) method is proposed and so on.

4 Literature Review

In this section an attempt has been made to present the research work done by the researchers in the past. We have principally divided complete literature into three parts i.e. segmentation using fuzzy theory, segmentation using artificial neural networks and segmentation using genetic algorithm. Again categorizing fuzzy theory into fuzzy c means and neural network into convolutional neural network. Further classifying the work on the basis of applications generally dividing them into three medical, satellite and others.

Table 3 GA parameters

Parameters	Description
Population size (P)	It is the collection of individuals being tested. Population size should be selected in such a way that it converges to solution optimally
Fitness function	It is used to evaluate the goodness of any solution and closeness of chromosome to get optimal solution
Crossover probability (P_c)	It defines how often will be crossover performed. $P_c = 100\%$, then all offspring are prepared by crossover and $P_c = 0\%$, then new generation is the duplicate of chromosomes from the past population
Crossover type	It is the mechanism of recombination of two chromosomes
Mutation probability (P_m)	Chance of getting chromosome mutated. If $P_m = 100\%$, then complete chromosome is replaced, and when $P_m = 0\%$ nothing is replaced
Mutation type	It is the mechanism used to recover the lost genetic material
Selection type	It is the process of selecting two chromosomes for reproducing offspring
No. of Generations (N)	It defines the number of new population generated from old population
Coding schemes	It is the representation of genes as numbers, bits, arrays, trees, or any other object which is dependent on the type of application
Operator types	It defines the type of operation that has to be performed for generating the solution

4.1 Segmentation Using Fuzzy Logic and Its Variants

4.1.1 Medical Images Segmentation

Fuzzy sets and rough set were applied to handle the rough regions of the image with better segmentation results by Namburu et al. [107] named as SFRCM. Because of the multifaceted and inefficient flora of the Fuzzy set, Soft fuzzy rough sets using Meng's method has been applied to quantify the uncertainty pertaining to which extent the previous cluster and the present clusters obtained are alike along with a histogram based initialization of cluster prototype is used to choose the appropriate centroids which help in calculation of upper and lower approximations. Vishnuvarthanan et al. [108] proposed a hybrid SOM-FKM procedure that supports the radio surgeon by with an automatic tissue and tumor segmentation, thus enhancing radio therapeutic techniques. In [68], Ji et al. for brain MRI subdivision proposes the fuzzy local GMM (FLGMM) algorithm with the objective function defined as the combination of the weighted GMM energy functions over the complete image along with a abridged Gaussian kernel function which is cast-off to impose the spatial constraint, and fuzzy memberships are in a job to balance the support of each GMM to the segmentation procedure. The automatic segmentation clustering technique with multiobjective variable string length (permitted to accomplish the no. of clusters automatically) genetic fuzzy clustering (MOVGA) method which is used on several simulated T1-weighted, T2-weighted and proton density-weighted normal and MS lesion MRI brain images was proposed by Mukhopadhyay and Maulik [109]. The fuzzy segmentation and fuzzy maximum intensity projection method (FMIP) was proposed by Hata and Kobashi [110] for volume visualization of 3D MR images. FMIP can project a 3D dataset onto a 2D plane for fuzzy segmented images. A fuzzy segmentation algorithm for the segmentation of endorrhachis in MR images was proposed. Kannan [111] proposes a Fuzzy membership C-mean algorithm (FMCM) clustering technique for subdivision of MRI. A precise way to hypothesis initial membership matrix for initialized clusters with associated to samples in data set and a way to discover out the initial membership matrix according to the asset of elements in data set which is to be grouped by unsupervised clustering approaches utilized by the authors. An approach that is applicable to any set of multi-feature images of the same location is derived by Zhang et al. [60]. The work was carried out on repeated camera images of the same area; medical images of a region of the body; and satellite images of a region. A set of training images and domain knowledge for the segmentation and labelling has been used to turn out an image segmentation system that can be used without transform on images of the same region collected over time. An automated method for segmenting an MR image of a human brain based on fuzzy logic was proposed in [112] by Hata et al.

Baazaoui et al. proposes a semi-automated method, named as an entropy-based fuzzy region growing (EFRG) in [113] for segmenting a tumor and multiple tumor in the liver CT images. The proposed method iteratively computes the region mean entropy and the resulted tumor region are obtained using a fixed threshold-based membership degree. Manikandan and Bharathi [51] implemented fuzzy clustering to subdivision the suspected nodules from the CT images. By adopting fuzzy cluster which uses its initial cluster by itself and working with soft fuzzy membership based segmentation this process becomes completely automatic. Simhachalam and Ganesan [42] presents, a comparative study of k Means, FCM and Gustafson–Kessel (GK) working with real world data sets.

Detection of lesion from skin image is a complex task Cordeiro et al. [114] by adopting fuzzy based GrowCut technique performs this in [114]. This approach works in 2 phases 1. By applying differential evolution optimization algorithm for automatic selection of internal points 2. In a way to deal with complexity to define lesion borders with the use of Gaussian fuzzy membership functions modification of cellular automata evolution rules has been done. Using fuzzy logic, SVM, ANN, and classifier fusion for the subdivision of blood vessels from the retinal images is presented for the Diagnosis of diabetic retinopathy at an early stage by Barkana et al. [46]. Employing Skeletonization and a threshold selection based on Fuzzy Entropy for analysis of retina blood vessels has been presented by Rezaee et al. [115]. Wiener's filter is used for removing blurring noises and then adaptive filtering is applied for the extraction of blood vessels from the retina. And at last, by employing fuzzy entropy an optimal threshold for discriminating main vessels of the retina from other parts of the tissue is achieved. Ananthi and Balasubramaniam presents a new automatic subdivision technique grounded on interval-valued intuitionistic fuzzy similarity measure called as IVIFSs to fragment leukocytes in blood smear images in [64]. Hernandez-Matamoros et al. [65] proposes a Facial Expression Recognition (FER) algorithm by segmenting face into two regions—the forehead/eyes and mouth regions making it more feasible to make accurate decisions even if one of the two ROIs is partially or totally obstructed. To obtain an $L \times NM$ feature matrix, $L =$ no. of training images, later the ROI estimation, with a set of Gabor functions each region is segmented into a set of $N \times M$ blocks that are correlated. The outcome factures matrix is then applied to a PCA for dimensionality reduction. A classifier that has low

computational cost based on a fuzzy logic has been used providing recognition rates similar to those provided by other high-performance classifiers. Chaira [116] presents a novel thresholding technique that uses Attanassov intuitionistic fuzzy set theory (IFS) to segment blood vessels and blood cells in pathological images. The IFS is constructed using Sugeno type intuitionistic fuzzy generator with a new membership function using restricted equivalence function. To find the optimum threshold values a distance measure called intuitionistic fuzzy divergence is used. In this article a new fuzzy clustering technique intended for lip image segmentation is offered by Leung et al. [117] for lip image analysis. With the help of an elliptic shape function, the clustering method takes together the color statistics and the spatial distance into consideration. Because of the function, the new method is capable to discriminate the pixels having identical color information but positioned in diverse regions.

4.1.2 Satellite Images Segmentation

A fuzzy weighted active contour model for SAR image segmentation is proposed by Javed et al. [118]. A Based on local variance and entropy fuzzy inference engine (FIE) is castoff to allocate weights to pixels of the level set function. The RSF model fails to propagate the contour of the water region, but offered method is capable to fragment the water also the land region. Using Fast-Scale Invariant Feature Transform (F-SIFT) and Fuzzy-Relevance Vector Machine (F-RVM) algorithm along with Gaussian Filter (GF) and the PSO-Affine based image registration for feature extraction in [70] proposed by Priya et al. for the efficient image segmentation multi-temporal satellite image. A feature dependent infrared ship image segmentation approach utilizing the fuzzy inference system is proposed for sea surveillance system presented by Bai et al. [66]. The unimodal threshold is used for intensity feature extraction to preserve the low contrast pixels. Then by using saliency detection, region growing and morphology processing the local feature is extracted to find the shape of the target. Partial region growing and weighted distance transformation to suppress the background and to extract the global spatial feature has been used. Integrating with fuzzy inference system based upon expert knowledge the complete target could be directly extracted. An automatic or semi-automatic approach named as object oriented image analysis (OBIA), intended to replicate and/or to surpass the human interpretation of images was proposed by Sebari and He [67] (1) creation of primitives from pixels and (2) creation of objects from primitives are the two approaches of OBIA for segmenting: natural classes such as tree, lawn, soil, and water and for manmade classes building, road, parking area.

4.1.3 Segmentation for Different Applications

Using a bi-level segmentation operator, which combines fuzzy 2-partition entropy maximization with binary GC optimization the algorithm, uses the super pixels as segmentation primitives and partitions all the super pixels iteratively by Yin et al. [43]. Li et al. [119] proposed a Fuzzy-based modified discrete Grey wolf optimizer and aggregation (FMDGWOA) captivating fuzzy Kapur's entropy by way of the optimal objective function, practices pseudo trapezoid-shaped to bearing fuzzy membership initialization so as to accomplish object extraction finally via limited information aggregation. Zhang et al. [55] presents a multiobjective evolutionary fuzzy clustering (MOEFC) algorithm permissibly to attain the robust enactment of conserving important image information while eliminating noise for image subdivision into multiobjective problems. For improving the performance and search capability, an adaptive weighted fuzzy factor with a mixed population initialization and Opposition-based learning is utilized. Mondal et al. [120] article, proposes a robust fuzzy energy based active contour using both global and local information to segment (noisy and blurred) images with high-intensity inhomogeneity or non-homogeneity. The local information is generated based on both the spatial distance and the pixel intensity. To overcome the sensitivity of image noise and to obtain effective segmentation results, a multiobjective spatial fuzzy clustering algorithm (MSFCA) for image segmentation is proposed by Zhao et al. [121]. In this method, the non-local spatial information derived from the image is introduced into the fitness functions which respectively consider the global fuzzy compactness and fuzzy separation among the clusters. MSFCA uses Non-dominated Sorting Genetic Algorithm-II (NSGA-II) as the underlying optimization strategy. After obtaining the final non-dominated solution set, the best solution is selected according to a cluster validity index with the non-local spatial information in MSFCA. In [48] Choy et al. presents a multiphase fuzzy region competition model that takes spatial and frequency information for synthetic, natural textures and real world images segmentation. Each region is represented by a fuzzy membership function and a data fidelity term that calculates the conformity of spatial and frequency data inside each region. The strategy of the Iteratively Fuzzy Region Competition (IFRC) model is used to perform a two-phase Fuzzy Region Competition model iteratively for multiphase $N-1$ times and to compute one fuzzy membership function per round for image segmentation proposed by Borges et al. [9]. Sulaiman and Isa [40] present's a new clustering approach known as Adaptive Fuzzy-K-means (AFKM) clustering for to deliver an enhanced and further

adaptive clustering procedure, this work employs the concepts of fuzziness and belongingness.

An unsupervised fuzzy model-based learning algorithm using Generalized Gaussian Density (GGD) model in an optimization framework for segmentation has been presented by Choy et al. [2]. Maj and Roy [122] presents a new methodology by integrating judiciously the merits of the rough-fuzzy-possibilistic c-means algorithm and multiresolution image analysis, for segmenting the text part from the graphics region based on textural cues. The rough-fuzzy possibilistic c-means combines c-means algorithm, rough sets, and probabilistic and possibilistic memberships of fuzzy sets. The use of wavelet theory via M-band wavelet packet decomposition of images provides a multiscale multidirectional representation of the image and yields a large number of frequency channels. No assumption is made about the font size, orientation, and script of the text; that is, the proposed approach is purely unsupervised. Caponetti et al. [123] using a neuro-fuzzy methodology for performing the classification processes, propose a new document page segmentation method, capable of differentiating between text, graphics, and background. Chi and Yan [124] a technique for map image subdivision founded on fuzzy rules and thresholding is offered which outperforms the commonly employed adaptive thresholding method by incorporating a thresholding method which is easy to implement and fast. In [61] Chen and Juang proposes a new method for object detection, firstly a two new color-based entropy features that represent the color components of an object (the ECC) and the geometric distribution of each composing color cluster in an object (the EGCD) are proposed along with a two-phase filtering approach based on the two new features is recommended. There are two phases in this work (1) the ECC computed from the color histograms is used to filter test patterns and generate object candidates and (2) filters the candidate objects by feeding their EGCD features into an FC. The performance of the two entropy features is verified through comparisons with other detection methods. Secondly, a new FC classifier that uses the SSC and the linear SVM to learn fuzzy rule antecedent and consequent parameters, respectively, is put forward. The new FC is called FC-SSCSVM. Herrera et al. [125] a novel pixel-based strategy of segmentation and stereovision matching for obtaining disparity maps from hemispherical images captured with fish-eye lenses from forest environments. The interest of the authors is focused on the trunks of the trees because they contain the higher concentration of wood. This method works in 2 phases at a first the method identifies textures of interest to be either matched or discarded and extracts six attributes of each pixel as features by applying both Otsu and fuzzy k-Means methods and at second a stereovision matching process is designed based on the application of 3 stereovision matching constraints: epipolar, similarity, and uniqueness. The novelty comes from the point of view of combination of strategies to automate the process, i.e. applying the OM combined with the elimination of leaves textures that makes the FKM is automatic. Pednekar and Kakadiaris [126] present a modification and extension to dynamically adjust the linear weights in the functional form of fuzzy connectedness and to introduce directional sensitivity to the homogeneity-based component a method called fuzzy connectedness using dynamic weights (DyW). Dynamic computation of the weights relieves the user of the extensive search process to find the finest combination of weights suited to an exacting application.

4.1.4 Discussion

Fuzzy logic has been deployed in various segmentation task for example in segmenting MRI, CT, SAR, real world images, text-graphic images, document page etc. FL collaborating with some mathematical models or other soft computing approaches performs it. Some of the variants are Gaussian mixture model, generalized Gaussian density function, discrete grey wolf optimizer, M band wavelet packet, entropy based, dynamic weights, fast scale invariant feature transform (F-SIFT), intuitionistic theory, fuzzy with multi-objective functions, relevance vector machine (RVM), Growcut algorithm, rough theory along with some soft computing approaches like ANN, GA. The most crucial part for implementing any of the approach is to find out the suitable threshold value, once it is fixed than it's become comfortable to perform the research. The next parameter plays an important role working with fuzzy is fuzziness factor generally denoted by m its ranges from 0 to 3. Another parameter is number of cluster denoted by c which has to be decided by the researcher and sometimes it does have adaptive nature depends on the implementation of algorithm for example while segmenting an MRI image interest is to divide it into 3 or 4 parts so in this case value of c can be 3 or 4 respectively. Tables 4 and 5 shows summary of the various articles used for segmentation using fuzzy logic.

4.2 Segmentation Using Fuzzy C Means and Its Variants

4.2.1 Medical Images Segmentation

Chen et al. [62] proposes an improved anisotropic multivariate student t-distribution based hierarchical fuzzy C-means method (IAMTHFCM) for segmenting MR images into GM, WM, and CSF. A more flexible objective function by considering the improved dissimilarity

Table 4 Summary of FL articles with parameter

Ref no.	Methodology	Parameter	Domain	Dataset/result
[2]	Fuzzy generalized gaussian density (GGD)	Regularization parameter $\lambda = 0.1$, initial group $k = 20$	Segment images with various textures	GGD and Weizmann/SE = 4.35%, JI = 0.9022, time of about 5.0 to 8.0 s
[43]	Fuzzy c-partition entropy	tuning factor α for gray scale image = 13, tuning factor α for color image = 14, level of variation $\sigma = 1$, $T_{MSE} = 19$	Grayscale and color images	BSD/F-measure for bird, camera, flower and boats color with super pixels = 4.5595 (avg) and without super pixels = 5.8777 (avg), PRI, VoI, GCE, BDE are 0.7769, 2.3067, 0.2215 and 10.66 and 10.8 s for color images on average
[113]	Entropy-based fuzzy region growing (EFRG)	no. of iterations = 15, diffusion constant = 1/7, edge detector kernel = 30, conduction coefficient functions = 2, membership function $\beta = 0.06$, nw = 3 × 3	Multiple tumor region using CT images	Image CT1 AOE %, RAD %, DSM is 12.78, 9.72, 0.93, for image CT2 10.99, 8.83, 0.94, for image CT3 8.83, 5.34, 0.95, CT4 tumor 1, 24.38, 27.93, 0.86, CT4 tumor 2, 38.78, 26.12, 0.75, CT4 tumor 3, 23.67, 14.77, 0.86
[119]	FMDGWOA	population size = 50, threshold = 2, 3, 4, 5, no. of iterations = 150, lower bound = 1, upper bound = 256	Multilevel image threshold problem for different images	BSD500/performance is improved averagely on PSNR, MEAN and STD values for six different images
[118]	Active Contours and Fuzzy Logic	$\lambda1 = \lambda2 = \mu$=1, threshold = 0.1, $\eta = 0.001 \times (255)^2$, $\rho = 3$, u1 = v1 = 3, $\kappa = 2$	Water and Land from SAR images	Ajkwa river/PRI and GCE were used for result validation with RSF model. Method has successfully performed in the water and land segmentation. Computational time has also been increased
[55]	Multi-objective evolutionary fuzzy clustering (MOEFC)	nw = 3 × 3, population size = 100, max. generations = 30, neighbourhood size = 20, crossover = 1, mutation = 0.5	Various images	Synthetic, medical, natural and SAR/The avg. accurate rate (AR) = 97.01% and Adjusted rand index (ARI) = 93.14% and *t* test confidence level = 95%
[107]	Soft fuzzy rough c-means (SFRCM)	Cluster c = 4, fuzziness m = 2, threshold = [0, 1], exit criteria = 0.99	MR brain image	Brain Web/20, IBSR/20, BRATS/10/ Segmentation accuracy (SA) = 0.8930, Jaccard similarity (JS) = 0.8930
[120]	Active contour and Fuzzy	$\lambda1 = \lambda2 = 1.0$, factor controlling global and local energies β = [0, 1]	To detect objects in a given image based on curve evolution	Various images/segmentation was performed on 22 images JI, P_r, R_e, F-measure and region entropy and execution time along with statistical analysis the proposed method outperforms other 8 methods
[42]	Fuzzy and non-fuzzy classification methods	No. of iterations = 100, threshold $\varepsilon = 0.00001$, m = 2	Liver image segmentation	Liver disorder with 341 samples and Wine with 178 samples/Accuracy for K-means = 76%, Fuzzy c-Means = 71% and Gustafson–Kessel = 83%
[121]	Multi-objective spatial fuzzy clustering algorithm (MSFCA)	threshold $\varepsilon = 10^{-5}$, nw = 3 × 3, crossover = 0.9, mututaion = 0.1, no. of generations = 100, population size = 50	Synthetic and real images segmentation	BSD/on the basis of the clustering accuracy (CA), ARI compared with other 5 algorithms proposed MSFCA algorithm performs better
[122]	Rough-fuzzy-possibilistic c-means (RFPCM) and M-band wavelet packet analysis	nw = 9 × 9, m = 2, weight w = 0.95	Text-graphics segmentation	Document (real life) images/equated with 6 procedures and numerous feature extraction techniques with JI, DSC, Sen. And Spec. resulted better accuracy when tested for 50 document images
[61]	FC-SSCSVM	Threshold = [2.6, 5], cluster c = 15, 60	Exact object recognition from multifaceted scenes	5 different images including beverage can, red cup, notebook, cosmetic bag, and toy fish

Table 4 (continued)

Ref no.	Methodology	Parameter	Domain	Dataset/result
[68]	Fuzzy local Gaussian mixture model (FLGMM)	m = 2, SD of kernel function $\tau = 4$, neighbourhood radius of kernel function $\rho = 10$	Tissue from MR brain images	BrainWeb, IBSR/JS for GM = 0.8138 and WM = 0.9339, Mean ± SD for 2D images = 21.18 ± 2.36, 25.82 ± 3.33, 3D = 875.19 ± 27.25, 655.63 ± 42.84
[48]	Fuzzy Region Competition with Spatial/Frequency Information	nw = 5 × 5, m = 1, 5, threshold $\varepsilon = 10^{-4}$, $\lambda = 10$, $\tau = 0.025$, $\theta = 1.0$	Multiphase image segmentation model	Weizmann/Error = 1.01%, SA, the errors of Region Competition RC method results in (a): (4.02%, 1.13%) and (b): (11.7%, 0.55%)
[125]	Otsu and FKM	threshold $\varepsilon = 0.1$	Stereovision matching in hemispherical images (Forest environment)	A set of 2700 samples/Avg. % of error and SD (σ) For 2 Class based on sa (correlation) 30.1 and 2.9, sb (color) 16.2 and 1.3, sc (texture) 18.1 and 1.7, sd = 14.3 and 1.1, se = 35.2 and 3.6, sf (Laplacian) 32.1 and 3.1 and some Decision making strategies such as for % and σ, YAG 13.3 and 1.9, CFI 11.2 and 1.3, SFI 11.2 and 1.3, DES 11.2 and 1.6, FMCDM 9.3 and 0.9, VC 8.9 and 0.8
[116]	Intuitionistic fuzzy set theory (IFS)	membership degree = 1, non-membership degree = 0, m = 0, nw = 3 × 3, $\lambda = 0.8$, $\sigma = 0.5$	Segmentation of medical images	Pathological images/Segmentation error 0.0102 (1.02%)
[109]	Multi-objective variable string length genetic fuzzy clustering (MOVGA) technique	crossover = 0.8, mutation = 0.01, generation = 20, population size = 20, no. of iterations = 400	Segmenting several MRI brain images	BrainWeb database/CA % = 92.4366, average ARI = 0.7713 and for MS lesions brain planes Z10, Z60, Z72, Z108 and Z120 average, Results for images for Z2, Z40, Z90, Z125 and Z140 planes average CA % = 92.6018 and average ARI = 0.7839
[117]	Fuzzy clustering method	c = m = 2	Lip image segmentation	5000 lip images/FCMS is about 1.78 times faster than that of FCM, with average SE for 3 images = 2.23%, SE for 27 images = 2.72%

function itself as a sub-FCM and the improved anisotropic spatial information is proposed is used to outcome the effect of the noise and preserve more detail information. Sarkar et al. [59] proposed a hybrid clustering approach as Rough Possibilistic Type-2 Fuzzy C-Means clustering (RPT2FCM) with Random Forest (RF). Rough sets are used to handle ambiguity and imprecision for noisy data, to deal with uncertainty and other numerous delicate qualms and RF for getting enhanced clustering results by categorizing rough points. [49] Deng et al. put forward an innovative method named RCLFCM for bias field correction and image segmentation of synthetic and MRI images, which incorporates a neighbourhood and spatial information of an image. The novel technique redefines the impact factor among the central pixel and its neighbour pixels, adjusts the objective function of FCM, and cartels it with the bias field estimation model. Feng et al. [127] presents a bias correction embedded FCM (BCEFCM) to subdivision 3D MRI sequences of each time point separately and estimate the bias field simultaneously. Segmentation consistency of the recommended technique is restrained by a non-locally spatiotemporal regularization which is well-defined on similarities of intensities amongst voxels and cluster centroids. In [128] Aparajeeta et al. proposed three to segment the given MR image while estimating the bias field. The problem is compounded when the MR image is corrupted with noise in addition to the inherent bias field. The notions of possibilistic and fuzzy membership have been combined to take care of the modelling of the bias field and noise. The weighted typicality measure together with the weighted fuzzy membership has been used to model the image resulted in Bias Corrected Possibilistic Fuzzy C-Means (BCPFCM) strategy. Further reinforcing the neighborhood data to the modeling aspect has resulted in the two other strategies namely Bias Corrected Possibilistic Neighborhood Fuzzy C-Means (BCPNFCM) and Bias-Corrected Separately weighted Possibilistic Neighborhood Fuzzy C-Means (BCSPNFCM). (1) To make initial centers close to the optimal ones and decrease the possibility of falling into local minima initial cluster

Table 5 Summary of FL articles without parameters

Ref no.	Methodology	Domain	Dataset/result
[64]	IVIFS	Leukocytes from blood smear images	100 images through 1 WBC, 270 images through 2 WBC/The accuracy rate is compared to both the databases as D1
[70]	F-SIFT and F-RVM	To segment building, road, vegetation, tree, water and land area	Indian Pines/The OA and the avg kappa coefficient of the are 98.2 and 98.89%
[51]	FACMM	Suspect nodules from the CT images	56 malignant, 50 normal cases 56 malignant nodules, 745 benign nodules/TPR = 100%, TNR = 93%, Accuracy = 94% with a false positive of 0.38/patient
[65]	Clustering and FL	Facial images segmenting it into forehead/eyes and mouth	KDEF/recognition rate increases to 99% for ROI form 98%
[46]	FL, ANN, SVM, and classifier fusion	Retinal vessel segmentation	DRIVE and STARE/The fuzzy classifier achieved OA = 93.82%
[66]	FIS	Infrared Ship image segmentation	80 infrared ship images/ME = 0.0183, RAE = 0.3734, computational complexity = 5.8187
[115]	Skeletonization and threshold based on Fuzzy Entropy	Analysis of retina blood vessels	DRIVE and STARE
[108]	SOM + FKM	Tumor and tissue present brain	Images from 4 patients, and from Harvard Brain Repository/Compared with FCM. Avg. MSE value = 2.151, avg. PSNR value = 41.85
[114]	Fuzzy semi-supervised version of the GrowCut algorithm	Mammographic images (Lesion segmentation)	A total of 57 images from MiniMIAS mammography database
[9]	IFRC	Multiphase segment different images	MIAS, BSD/The SA was 84.45%
[67]	OBIA	Urban information from VHSR multispectral images	Ikonos image of Sherbrooke/An overall segmentation rate of 80% was observed. The accuracy of segmentation accuracy manmade classes are of 81, 75 and 60%
[40]	AFKM	To segment various images	Various images/evaluated using F(I), F'(I) and Q(I) and compared with FCM and MKM approaches
[110]	FMIP	Endorrhachis in magnetic resonance images	Five dataset from Ishikawa Hospital
[111]	FMCMs	MRI brain images	Avg. silhouette width for FMCM = 0.59, FCM = 0.51
[123]	Neuro-Fuzzy methodology	Document page segmentation	Document Image Database/SA = 97.51%, with noises ranging from [0, 1] SA = 85.68%
[126]	Fuzzy connectedness using dynamic weights (DyW)	Segmentation using Dynamic weights	Phantom/SA = 99.15%
[60]	Fuzzy Clustering Algorithms	Segmentation of MR images	–
[112]	Fuzzy information granulation and fuzzy inference	Segmentation of Brain MR images	54 patients in 3 groups
[124]	Thresholding and Fuzzy rules	Grayscale geographic map images	22 grayscale map images

centers are computed by peak detection and interval analysis (2) the spatial information of the given image will strengthen the robustness to image artifacts because of the improved FCM with spatial information is performed (3) by selecting the misclassified pixels and reallocating them based on the local information of the original image the segmentation results are refined in the proposed work by Zhang et al. [56] presents an improved fuzzy algorithm for synthetic images and MR image segmentation. An enhanced intuitionistic fuzzy c-means (IIFCM) algorithm by introducing local spatial information in IFCM a novel intuitionistic fuzzy factor is presented by Verma et al. [129] for brain image segmentation. In [130] Adhikari proposes a conditional and spatial fuzzy C-means (csFCM) clustering algorithm that can effectively segment MRI brain images with the presence of noise and intensity

inhomogeneity. By incorporating local spatial interaction among adjacent pixels in the fuzzy membership function in such a way that if the neighboring pixels share similar characteristics, the center pixel should have a higher probability of grouping to the same cluster as of the neighboring pixels. A novel clustering procedure which can preserve the benefits of an intuitionistic FCM clustering technique to maximize benefits and reduce noise influences through neighbourhood membership with a GA cast-off concurrently to select the optimal parameters, named NIFCMGA (Novel Intuitionistic fuzzy c-means clustering algorithm) was proposed by Huang et al. [131] for subdivision of CT and MRI images was proposed. The projected technique works in 3 phases in 1. Noise elimination as a preprocessing step extracting out the texture features 2. Then by using SVM a classification has been done resulting about 99% accuracy and then in 3. Using the proposed multi-phase method by Ain et al. [132] tumor region is haul out from the given MR image with FCM. Balla-Arabe et al. presents an approach in [45] is based on the LBM Partial Differential Equation (PDE) solver. Using a modified FCM objective function, a new fuzzy external force (FEF) was designed to solve the Level Set Equation (LSE) using the lattice Boltzmann method (LBM). FCM gives it advantage of the latitude to stop the evolving curve according to the membership degree of the current pixel with the advantages of the LSM which allow it to handle complex shapes, topological changes, and different constraints on the contour smoothness, size, speed, and shape which are simply specified alongside the advantages of the LBM which make it very suitable for parallel programming due to its local and explicit nature. Yang [133] proposes a robust modified FCM with a new objective function along for noisy image segmentation. The algorithm which is an extension of the 2-D adaptive fuzzy C-means algorithm (2-D AFCM) for the segmentation of two-dimensional (2-D) and three-dimensional (3-D) multispectral magnetic resonance (MR) images that have been altered by intensity in homogeneities, also known as shading artifacts has been presented by Pham and Prince [58]. A segmentation method based on information theory using fuzzy was proposed by Bakhshali [52] for segmentation of MR images. Ji et al. [134] have proposed the weighted image patch-based FCM (WIPFCM) algorithm for synthetic images and clinical brain MR segmentation. In this algorithm, they have used the image patches to replace pixels in the fuzzy clustering, and construct a weighting scheme to able the pixels in each image patch to have anisotropic weights. Thus, the proposed algorithm incorporates local spatial information embedded in the image into the segmentation process, and hence improves its robustness to noise.

Zhou and Zhou [57] propose a modified approach for image subdivision has been performed in this work by considering FCM and working in 2 steps i.e. at first it directly obtain the centroids of pixels and then applying fuzzy the assignment of neighbor pixels of the extracted part being given to the conforming clusters. In [135] Chen and Zhang proposes two variants of FCM_S with an intent to simplify the computation of parameters and then extend them, together with the original to corresponding kernelized versions FCM_S1, by the kernel function substitution KFCM_S2. Aim for adopting kernel functions are (1) to more likely reveal inherent non-Euclidean structures in data (2) to retain simplicity of computation (3) to induce a class of new robust distance measures for the input space and then replace non robust measure to cluster data or segment images more effectively. In [136] Shen et al. used NN model with a cost function for optimizing the degree of attraction and segmentation based on the fact that a environs desirability, which is in need of the comparative location and features of adjacent pixels to enhanced the segmentation results can be employed.

Segmentation of lung nodules by Nithila and Kumar [41] was proposed using a method incorporating region-based active contour model and FCM. Selective binary and Gaussian filtering with new signed pressure force function (SBGF-new SPF) along with clustering technique for nodule segmentation reconstruction of parenchyma has also been utilized. Segmentation of brain tumors from MRI using new c-means algorithm based on IVIFS is presented by Ananthi et al. [47]. Images are enhanced using median filter to reduce noise and brain is extracted using the skull stripping method. From the IFS, which are attained from FS, the IVIFS for the enhanced brain MR image is generated. Then by applying the proposed interval-valued intuitionistic FCM (IVIFCM) clustering method IVIFS is clustered. Rezaei et al. [137] aims to improve the identification of Thin-cap fibroatheroma (TCFA) or "vulnerable plaque" from Virtual Histology Intravascular Ultrasound (VH-IVUS) images using a hybrid method named HFCM-kNN. The proposed approach is adequate of eliminating outliers and detecting clusters with different densities in VH-IVUS image.

4.2.2 Satellite Images Segmentation

For precaution not to get FCM into local minima the proposed scheme first achieves the initial cluster with clone and then by reducing noise by applying improved nonlocal filters by adjusting some parameters SAR images are segmented by proposed method CKS_FCM in [53] by Shang et al. In [44] Ji and Wang first propose fuzzy clustering algorithm with enhanced nonlocal spatial information (FCM_INLS), which has adaptive distance measure and

self-tuning filtering degree parameter integrating with the nonlocal spatial information attained by the nonlocal mean technique into the FCM.

4.2.3 Segmentation for Different Applications

By using the features of SOM and EFCM a hybrid approach named as Self-Organizing Map based Extended Fuzzy C-Means (SEEFC) presented by Aghajari and Chandrashekhar [8] along with it DWT is used for the segmentation of various images taken from BSD500 database. FCM with spatial constraints (LCFCM_S) and simplifying it to corresponding robust version LCFCM_S1 Jiang et al. [11] proposes a novel level set algorithm for segmentation of synthetic and medical images. LCFCM_S and LCFCM_S1 based clustering algorithm can provide enough robustness to noise and outliers because of the correntropy criterion which can reduce the weights of the samples that area way from their corresponding cluster centers. C-means clustering algorithm by incorporating both local membership relative entropy (MRE) and modified local spatial data information to form two algorithms namely LMREFCM and LDMREFCM was proposed by Gharieb et al. [63]. The modified objective clustering function of the algorithm was obtained by minimizing the standard C means function with two MRE functions for fuzzification and regularization. Tripathy and Mittal [138] combine the notions of kernel and possibilistic approach together in a distributed environment provided by ApacheTMHadoop. They integrated this combined notion with map-reduce paradigm of Hadoop and put forth three novel algorithms; Hadoop based possibilistic kernelized rough c-means (HPKRCM), Hadoop based possibilistic kernelized rough fuzzy c-means (HPKRFCM) and Hadoop based possibilistic kernelized rough intuitionistic fuzzy c-means (HPKRIFCM) for segmenting images of metal coin, colored brain MRI, satellite image, blood cancer cells, brain MRI. In this paper by Tan et al. [139] the HA initialization scheme is proposed to overcome the sensitiveness of FCM algorithm to the initialization condition of clusters number and initial cluster centers as they have significant impacts on the segmentation quality. Region Splitting and Merging Fuzzy C-means Hybrid Algorithm (RFHA) that consists of two main modules: Region Splitting and Merging (RSM) and FCM is an adaptive unsupervised clustering approach for color image segmentation was proposed by Tan et al. [140]. An automatic fuzzy clustering algorithm (AMFCM) for automatically grouping the pixels of an image into different homogeneous regions when the number of clusters is not known beforehand is proposed by Li and Shen [3]. Zhou et al. [141] presents an innovative 2D FCM clustering method for image subdivision by transforming it into an optimization problem. The fitness function containing neighbor information was set up based on the gray information and the neighbor relations between the pixels described by the improved two-dimensional histogram. By making use of the global searching ability of the predator–prey particle swarm optimization, the optimal cluster center could be obtained by iterative optimization, and the image segmentation could be accomplished. Using fuzzy clustering algorithms such as FCM and Possibilistic FCM along with competitive neural network to segment any color image was proposed by Sowmya and Rani [142] which could find the number of clusters automatically.

In [7] Zhao et al. presents novel outcomes associated to the Voronoi Tessellation (VT) and Hidden Markov Random Field (HMRF) based FCM method named as VTHMRF-FCM for texture image subdivision. The objective function of is defined by adding a regularization term of Kullback–Leibler (KL) divergence information to FCM objective function. Cao [69] presents an adaptive FCM (AFCM) method used for the segmentation of M-FISH images. An enhanced AFCM cataloging technique (IAFCM) with a new objective function, which yields improved background compensation and outcomes in improved chromosome segmentation and classification, was considered in this work, also discriminated from other FCM-based algorithms, which directly simulate the bias field.

4.2.4 Discussion

Though traditional FCM with its weakness of not including spatial domain within its objective function a number of its variants has been deployed for segmenting compel real world images. Adding spatial function with FCM makes it's a significant method in recent time for segmenting an image and this method outperforms the traditional fuzzy set or fuzzy logic theory. FCM combines with rough theory, self-organizing feature map (SOFM), hidden markov random field (HMRF), bias functions, level set equation (LSE), Lattice Boltzmann method (LBM), student t-distribution, weighted patches, Discrete wavelet transform (DWT), local membership relative entropy (MRE) along with variants of FCM like including spatial domain into objective function, kernelized versions, intuitionistic etc. Threshold value in FCM also plays an important role, once it is stable than it's become easy to perform the research. The subsequent parameter plays vital role working with FCM is fuzziness factor generally denoted by m its ranges from 0 to 3. The value of m by default is 2. Neighbourhood window denoted by nw and number of cluster denoted by c are parameters working with FCM is considered. Tables 6 and 7 shows summary of the various papers used for segmentation using FCM.

Table 6 Summary of FCM articles with parameter

Ref no.	Methodology	Parameters	Domain	Dataset/result
[8]	SEEFC	Neighbourhood window nw = 3 × 3, fuzziness index m = 2, threshold ε = [0, 1]	Segmentation of various images	BSD500/The avg. Sensitivity = 84.56%, Accuracy = 88.1%, Q index = 0.0798 ± 0.41
[62]	IAMTHFCM	m = 2, neighbour radius r = 1, ζ = 400, threshold ε = 0.75, L = 15, cluster c = 4	For brain MRI segmentation	BrainWeb, IBSR/JS = 73.29 ± 8.12
[59]	RPT2FCM	$\eta_1 = \eta_2 = 2$, relative no. for probalistic membership a and b = 0.5, no. of tree for RF = 1000, $f_{LW} = 0.95$ and $f_{BN} = 0.05$, m = 2	MRI segmentation	BrainWeb, SBD/Avg. DB = 0.38358, ARI = 0.72755, Minkowski Score MS = 0.64725, Percentage of Correct Pair %, CP = 85.82549
[49]	RCLFCM	c = m=2, p = 2, q = 1.5, basis function = 20, nw = 3 × 3	To segment image brain MRI	BrainWeb/Results were evaluated on SA, V_{pc} and V_{pe} proposed algorithm outperforms others 5 algorithms
[7]	VTHMRF-FCM	β = 0.5, λ = 0.04, $T_c = 0.001$, m = 96, no. of iterations = 5000	Texture image sub division	RADARSAT II/SA and the kappa coefficient are up to 99% and 0.99
[11]	FCM with spatial constraints	Step time Δt = 0.1, constant for regularity terms μ = 1, thresholding coefficient α = 0.3, SD of Gaussian filter σ = 3	Various images with spatial constraints	BSD500/compared with 5 algorithms on RMSE and DSC the proposed method outperforms others
[50]	FCM based ABC optimization as FABC algorithm	c = 5, iterations = 50, no. of individuals N = 10	To segment various images	Brodatz album/based on Davies–Bouldin, Xie–Beni, β-index, and Dunn index compared with PSO, GA and Expectation maximization (EM) proposed FABC gives better results
[53]	CKS_FCM	m = 2, threshold e = 0.01, nw = 3 × 3, no. of iterations = 500, weighting parameter α = 5	SAR images and noise removal	The mean and SD of the partition coefficient Vpc and partition entropy Vpe is 0.8622 ± 0.165 and 0.2801 ± 0.158
[63]	LMREFCM and LDMREFCM	m = 2, c = 4, nw = 3 × 3, no. of iterations = 25, weighting parameter α = 5	Natural image segmentation	Lena image and 2 images from BSD/the V_{pc} for LMREFCM = 0.9511 ± 0.0004 and for LDMREFCM = 0.9589 ± 0.0002, V_{pe} for LMREFCM = 0.0768 ± 0.0008 and for LDMREFCM = 0.0633 ± 0.0003
[127]	BCEFCM	m = 5, d = 1, q = 2, λ1 = 1.7, λ2 = 1.0, λ3 = 0.8, smoothness in the bias field ρ = [16, 23]	Brain tissues from MR images	BrainWeb, IBSR
[41]	ACM and FCM	No. of iterations = 150, c = 3, m = 2, α = 4, δ = 1, threshold = 0.3	Segmentation of lung nodules	LIDC-IDRI/The proposed method achieved SA of 98.95%, For lesion, the average volume error obtained is 0.968%. The spatial overlap, RMSE, coefficients of similarity, average over and under-segmentation ratio are 0.584, 0.10 mm, 0.914, 0.63 and 0.015% respectively
[128]	BCPNFCM and BCSPNFCM	m = 2, nw = 3 × 3	MR image	BrainWeb/ME for BCPNFCM and BCSPNFCM = 4.2302 and 4.6967, JS for BCPNFCM and BCSPNFCM = 0.4166 ± 0.06 and 0.3866 ± 0.11
[138]	HPKRCM, HPKRFCM, HPKR Intuitionistic FCM	m = 2, best value λ = 2	Algorithm for various image segmentation	Four different types of images

Table 6 (continued)

Ref no.	Methodology	Parameters	Domain	Dataset/result
[137]	FCM and kNN (HFCM-kNN)	kernel parameter $\lambda = 10^{-3}$, penalty parameter of the error term $= 10^4$	Identification of TCFA in VH-IVUS image	599 Gray-scale IVUSimages/TCFA detection with accuracy rate of 98.02% Compared with the 76.5% obtained by the cardiologist decision. Moreover, by validation of VH-IVUS images and their corresponding Optical Coherence Tomography (OCT) images, accuracy of 92.85% is achieved
[47]	IVIFSs	c = 3, m = 2, threshold $\varepsilon = 0.001$, n = 9, nw = 3 × 3	For brain tumor segmentation	Dataset with 55 slices from Advanced MR and CT Scan
[56]	FCM algorithm	m = 1.75, threshold = 1e−5, no. of iterations = 100, q = 0 or 0.25, $\lambda_G = 3$	Partial volume effect with noise removal	BrainWeb, synthetic image/SA of proposed method = 0.8897
[129]	IIFCM	m = 2, c = 4, nw = 3 × 3, $\lambda = 1.5$, $\alpha = 0.2$	Brain image segmentation	Synthetic image, IBSR/Avg. DSC = 0.7433, SE = 0.1788, SP = 0.3076
[130]	csFCM	m = 2, nw = 3 × 3, p = q=2	MRI segmentation	Brainweb/Average $V_{pc} = 0.960$ $V_{pe} = 0.064$
[44]	NS_FCM	threshold $= 10^{-6}$, no. of iterations = 200, m = 2, nw = 5 × 5	SAR images with removal of noise	Images of Swabian Jura and Rio Grande River/NLS on synthetic image Segmentation Accuracy = for NS_FCM is 0.9728, clustering time = 595 ms. SA using NS_FCM for real images is 0.9188 and 0.9057
[131]	NIFCMGA	m = [1.5, 3.0], c = 5, $\alpha = 2$, SD = 4	Medical image	Two MRI images and two CT images
[45]	Lattice Boltzmann method (LBM) and FCM	m = 2, diffusion coefficient $\lambda = 15$	Segmentation of medical (blood vessels) and real world images	BSD300, MRI of Knee
[139]	Fuzzy C-Means (FCM) based Hierarchical Approach (HA)	m = 2	Color image segmentation	7 and 140 images/MSE = 2.1309, F (I) = 2.7968 F' (I) = 2.8508, Q (I) = 0.6546 MSE, F(I), F'(I), Q(I) for 140 images are 0.6890, 0.5710, 1.2400, 0.5690
[140]	RFHA	m = 2, threshold $\varepsilon = 0.001$, c = adaptive	Color image segmentation	7 and 140 standard images/For 7 images MSE = 2.0932, F(I) = 0.5346, F'(I) = 0.5421, Q(I) = 1.8521, for 140 images = 3.0900, 7.5600, 7.6600, 0.4900
[3]	AMFCM	m = 2, nw = 3 × 3, $\delta = 0.1$, threshold $\varepsilon = 1e{-}5$	To provide automatic segmentation	The cameraman, pixels brain and the Lena image/V_{pc} and $V_{pe} = 0.9219$ and 0.1744
[133]	modified FCM	m = c = 2, $\eta = 0.01$	Noisy image segmentation	Real and Brain images
[141]	Two-dimensional FCM clustering method (PSO + FCM)	size of predalar particle swarm = 25, size of prey particle swarm = 25, c1 = c2 = 1.49, $\omega_{max} = 0.9$, $\omega_{min} = 0.2$, Pf = 0.02	Noisy image segmentation	Synthetic image/SA = 99%
[58]	2-D adaptive FCM (2-D AFCM)	weighting factor q = 1	Segmentation of 2D, 3D MR images	BrainWeb

4.3 Segmentation Using Artificial Neural Network and Its Variants

4.3.1 Medical Images Segmentation

Demirhan et al. [98] presents a new tissue subdivision method that segments MR brain images into the tumor (glial), edema, CSF, WM, and GM. The segmentation is accomplished using SOM that is trained with unsupervised learning approach and fine-tuned with LVQ. In [143] Hassanien et al. presents a hybrid approach using fuzzy sets, ant-based clustering and MLPNN classifier, in combination with statistical-based feature extraction technique to identify Benign or Malignant from breast cancer MRI imaging. In [144] Ortiz et al. presents two methods the first one is founded on the use of relevant information mined

Table 7 Summary of FCM articles without parameters

Ref no.	Methodology	Domain	Dataset/result
[54]	MRFFCM	Underwater or Waterlogged image subdivision	Fish4Knowledge Project/The accuracy was 13% higher than FCM and FFCM
[52]	FCM	Clustering of noisy data and to remove from MRI	IBSR/For synthetic image Accuracy = 98.79%, for MRI = 98.73%
[57]	Modified strategy of fuzzy clustering algorithm	Infrared and synthetic images	Synthetic image and real image/ME of the proposed
[69]	Adaptive FCM using a gain field	To segment M-FISH	M-FISH database of 20 cells with 120 images/Correct detection rate (CR) = 89.5 ± 10.5% and false detection rate (FR) = 3.6 ± 2.8%
[134]	WIPFCM	Synthetic and MR images	BrainWeb/The average SA of WIPFCM is 99.81%
[142]	FCM, Possibilistic FCM and competitive NN	Color image segmentation	101 object categories database
[135]	FCM S1, FCM S2 (including Spatial Constraints), KFCM_S, KFCM S1, KFCM S2 (kernelized versions)	Robust image clustering	Artificial and real T1-weighted MR images datasets
[136]	FCM + NN	Fuzzy segmentation of brain tissue	Synthetic, BrainWeb, and IBSR

from the whole volume histogram which is processed by using SOM used for getting relevant information from the entire histogram and then second one divided into 4 phases that is overlapping windows is used for first and second order feature extraction, evolutionary computing-based feature assortment and lastly, map units are gathered by means of an innovative SOM clustering algorithm. Alirezaie et al. [145] has work on feature mapping and generating a set of codebook vectors using SOFM, ANN for segmenting the cerebrum from MRI brain images. WPNN (Weighted Probabilistic NN) algorithm for general normal brain tissue segmentation from MRI images by Song et al. [99] has been presented which is modified version of the probabilistic NN (PNN) and probabilistic density function (pdf) estimation is done by an SOM-WPNN structure.

Vorontso et al. [71] presents a Voxel classifier based on a MLP deformable model for segmentation of liver tumor in CT images. This deformable model considers vertex displacement towards apparent tumor boundaries and regularization that promotes surface smoothness. Makes it is easy to identify the targeted tumor and the network then form the MLP processed image automatically. Chang [93] proposed a method for automatic thyroid segmentation and volume estimation based on progressive learning vector quantization NN (PLVQNN) combined with a preprocessing procedure.

In [146] Xie et al. presented a novel approach for classifying melanocytic tumors as benign or malignant by the analysis of digital Dermoscopy images along with lesion boundaries. The proposed works in three steps using two databases. Franklin and Rajan [147] presented an automated retinal vessel segmentation method using the neural network, for analysis of retinal images to automatically identify and classify the image pixels as vessels or non-vessels and also for analysis of vascular structures of the human retina. Veredas et al. [148] uses NN and Bayesian Classifiers for spontaneous tissue extraction in wound images with the help of a mean shift technique and a region-growing approach for improved region extraction. In [149] Wang and Wang used the ANN for rapid void detection from the X-ray image. The image is divided into small blocks using an image processing method for multi-threshold image cutting and feature extraction. Then finding and locating the block that contains void is done. Working in an unsupervised manner for finding an affinity graph using CNN Turaga et al. [150] adopted a machine knowledge method. Cheng et al. [151] uses a Competitive Hopfield NN (CHNN) with winner-takes-all learning mechanism forming a network that evades the time-consuming process of defining values for the weighting factors in the energy function for medical image segmentation. In addition, its training structure permits the network to acquire quickly and efficiently. Chen et al. [152] has worked on solving the problem of medical image segmentation using Constraint Satisfaction NN (CSNN) by considering each pixel as an object. They had worked on MRI/CT/PET images for carrying out their work. The same label is assigned to pixels belonging to the same homogenous region.

4.3.2 Satellite Images Segmentation

Taravat et al. [94] a new approach for automated dark spot recognition from satellite images with the amalgamation of Weibull multiplicative model based filter is created which is applied to each sub-image and then PCNN technique is used for segmenting that filtered sub-image. Singha et al. [153] for verifying oil spills or/and look-alikes from SAR images and efficiently detecting and classification of oil spills, authors had used two different ANN sequentially. The first ANN is used to segment the SAR image for identifying pixels belonging to candidate oil spill features. And second ANN classifies objects into oil spills and look-alikes with the help of extracted statistical feature parameters. Rizvi and Mohan [154] presented multi-resolution watershed transform-based for image segmentation followed by a modified Cloud Basis Function (CBF) has been used in OBIA of high-resolution satellite images. The author focuses on the performance of a kernel called CBF by investigating with some modification for classification. For post processing, probabilistic relaxation labelling is used which improved the results further. Karvonen et al. [96] uses PCNNs which is trained and tested using a logarithmic scale and full-resolution (100 m) Radarsat-1 ScanSAR wide mode images over the Baltic Sea ice for segmentation and classification. Cellular Neural Networks (CNN) based architecture used for statistical image segmentation. First-order MRF for the probability distribution of region label at a given pixel is applied in [155] by Sziranyi and Zerubia. Baraldi and Parmiggiani [156] uses a Simplified Adaptive Resonance Theory NN (SARTNN) to perform unsupervised identification.

4.3.3 Segmentation for Different Applications

In [92] Konar et al. have used Quantum bi-directional self-organizing NN (QBDSONN) architecture which is a quantum version of a classical bi-directional self-organizing NN (BDSONN) architecture composed of three second order neighbourhood topology based inter-connected layers of neurons (represented by qubits) arranged as input, intermediate and output layers to acquire true output as extracted binary image from noisy background by converting the quantum bit into one of the classical bit 0 or 1 depending on the probability. The efficiency in terms of time and extraction of shapes of an image as compared to classical BDSONN has been increased when the result was observed on real life spanner image with different degrees of uniform and Gaussian noises and evaluation being done on 2 sample one-sided Kolmogorov–Smirnov test. Arumugadevi and Seenivasagam [157] presents an unsupervised hybrid technique using FCM with feedforward networks for color image segmentation on CIE L × a × b × color reduced image for automatic segmentation. The network is trained with 15 images in different sizes and colors. For determining the number of clusters method named cooccurrence and for the cluster validation the silhouette index values used. The labels obtained from FCM are used as a target of the supervised FFNN. The network is trained by the Levenberg–Marquardt back-propagation algorithm. SOM as the preprocessing step for initial classification then PCNN is used for limiting over segmentation from high-resolution images using the Shift Invariant Shearlet Transform (SIST) in [158] Helmy and El-Taweel introduced a hybrid method for image subdivision. A method named Simplified PCNN with Region-Based Object Recognition (SPCNN-RBOR) for segmenting real world complex images in order to extract object with good texture and less texture was proposed by Chen et al. [95]. De et al. [159] presented a parallel self-organizing NN (PSONN) model and a parallel version of the optimized MUSIG (ParaOptiMUSIG) activation function for subdivision of true color images in. The issue of parameter selection has been addressed by Meftah et al. [160]. For image segmentation and edge detection, Spiking neuron networks (SNNs) is used which prevail over the computational power of neural networks made of threshold efficient results are obtained if parameters are set correctly. In [161] a self-supervised multilayer self-organizing NN (MLSONN) and a supervised pyramidal neural network (PyraNet) for the segmentation of real life multilevel intensity images and also presented a bi-directional self-organizing NN (BDSONN) model suitable for multilevel image partitioning given by Bhattacharyya et al. Boskovitz and Guterman [162] proposed a feedforward architecture comprises of a Multilayer perceptron look alike network that accomplishes image subdivision by adaptive thresholding and for handling error of the segmentation Fuzzy entropy is used. The system works with no apriori assumptions about type, features, contents, stochastic model, etc. whatsoever are made for an image. Kuntimad and Ranganath [97] mentioned that even when there is a substantial overlap in the intensity ranges of next to regions of digital images, PCNN along with an inhibition receptive field to the neuron, perfectly segments the image. Using this method boundary geometries of the objects in the image and the optimal values for and based on the intensity probability density function can be determined of an image.

In [72] Trujillo et al. presents segmentation of carbon nanotube images which is important in nanotechnology. NN and Perona–Malik filter are the two algorithms compromising of 3 steps i.e. preprocessing, segmentation and post processing, used for segmentation. Relaxed Otsu's threshold and ANN are also the part of the segmentation phase. In [163] Fu and Chi uses the ANN and a

thresholding method to extract leaf veins. A hybrid DNN (HDNN), by dividing the maps of the last Convolutional layer and the max-pooling layer of DNN into several blocks of variable receptive field sizes or max-pooling field sizes, to permit the HDNN to extract variable-scale features was proposed by Chen et al. [164].

4.3.4 Discussion

Artificial neural network with its alternatives like Multilayer perceptron (MLP), Self-organizing map (SOM), Pulse coupled neural network (PCNN) etc. performs segmentation working geniality with radial basis function (RBF), affinity graph, cloud basis function (CBF), Shift Invariant Shearlet Transform (SIST), Markov random field (MRF), learning vector quantization (LVQ), Weibull multiplicative model (WMM), competitive Hopfield has been used for segmentation. The parameters like learning rate, momentum are most common while working with NN. Tables 8 and 9 summarize the related work.

4.4 Segmentation Using Convolutional Neural Network and Its Variants

4.4.1 Medical Images Segmentation

As a pre-processing phase for intensity normalization Pereira et al. [166] proposed CNN for brain tumor segmentation. Training the data set by revolving the patches in addition to by sampling from classes of HGG that were under-represented in LGG which in order gives higher adeptness to segment image. An effective and vigorous technique to automatically detect CMBs from MR volumes leveraging 3D CNNs was proposed in [84] by Dou et al. having a two-stage framework to reduce its computational cost and improve the detection performance. A number of candidates with high probabilities of being CMBs by leveraging a novel 3D FCN strategy are the first stage. A well-trained model is performed on the candidates to discriminate CMBs from hard mimics in the second stage. Rajchl et al. [89] proposed DeepCut, a new method to obtain pixel-wise segmentations, given a database of bounding box annotations and studied variants employing an iterative dense CRF formulation and CNN models. DeepCut is able to segment both the fetal brain and lungs from an image database of the large variation in the anatomy and is readily applicable to similar problems on medical images. Working with an MRI (anatomical) for classifying tissues automatically to obtain multiscale statistics by using multiple convolution kernel sizes and patch sizes Moeskops et al. [167] proposes a CNN. For the segmentation of glioblastomas (tumor) from MR images by using Deep Neural Networks (DNNs) was proposed by Havaei et al. [168].

In order to address the challenging task of automatically characterizing plaque composition in carotid ultrasound Lekadir et al. investigated a deep learning approach in [169]. The proposed method does not require the pre-definition of intensity thresholds or imaging features. Instead, they built a Convolutional NN that can extract automatically from a training sample of imaging patches around each pixel position the image information in the ultrasound data that are optimal for the discrimination of the different plaque constituents. Roth et al. [170] present a probabilistic bottom-up approach for pancreas segmentation in abdominal CT scans. Tajbakhsh et al. [78] presents extensive experiments, based on 4 distinct medical imaging applications from 3 different imaging modality systems, have demonstrated that deeply fine-tuned CNNs are useful for medical image analysis, performing as well as fully trained CNNs and even outperforming the latter when limited training data are available. To segment individual glands (instances) in colon histology images by Xu et al. [171] a new image instance segmentation method is proposed using deep multichannel NN. A fully automatic method for skin lesion segmentation by leveraging 19-layer deep convolutional neural networks (CNNs) that are trained end to-end and does not rely on prior knowledge of the data was proposed by Yuan et al. [172]. Zhang et al. [173] utilized DCNN for EFL they proposed specific fine-tuning method for cascaded regression, named cascade transfer. The capacity of DCNN, as a generic feature extractor for regression, and the effectiveness of fine-tuning were used. In [174] Kumar et al. develops a new feature extractor by fine-tuning CNNs that have been initialised on a large dataset of medical images. van Grinsven et al. [175] proposed a method using CNN to substantially speed up the time-consuming training process of CNN with a selective sampling strategy, named SeS, embedded in the training procedure. The SeS CNN used for the identification of hemorrhages on color fundus images. Lawrence et al. [176] have presented a fast, automatic system for face recognition system combines local image sampling, a SOM neural network, and a CNN. Present results using the Karhunen–Loeve (KL) transform in place of the SOM, and a MLP in place of the convolutional network. With an adaptive implementation of 1D CNN Kiranyaz et al. [177] proposed a patient-specific ECG heartbeat classifier which fuses the two major blocks of the traditional ECG classification into a single learning body: feature extraction and classification. The proposed method only requires 1D convolution that makes any hardware implementation simpler and cheaper. The variations on the beat resolution with different CNN settings and raw data representations are not degrading and can be desirable for even lower computational complexity.

Table 8 Summary of ANN articles with parameter

Ref no.	Methodology	Parameter	Domain	Dataset/result
[71]	Multilayer perceptron (MLP)	Momentum = 0.9, feature weight = [0, 1], SVM soft margin parameter C and RBF parameter γ decided using grid search	Liver tumours segmentation in CT images	40 abdominal CT scans with 95 colorectal images/ DSC = 0.80 ± 0.11
[146]	Neural network	parameters C and r for the SVM with RBF were 2048 and 0.0313 for the xanthous race dataset, and 64 and 0.25 for the caucasian race dataset	Melanocytic tumors as benign or malignant by from digital dermoscopy images	A xanthous race dataset and a caucasian race dataset/for xanthous race dataset sensitivity = 95.00, specificity = 93.75, accuracy = 94.17, caucasian race dataset sensitivity = 83.33, specificity = 95.00, accuracy = 91.11
[158]	SIST + SOM + PCNN	For SOM Training sets = Sequential, No. of neurons 7 × n 0.5341, Initialization = Random, Learning rate = [0.5 0.05], Learning rate function = Sigmoid, for PCNN $\alpha = 0.2$, $\beta = 0.089$, V_θ, = 10, $V_L = 0.01$	For high resolution images	BSD and Quick-Bird Satellite images/ improved in computational efficiency and F(I) F'(I), Q(I), were also improved as compared to other methods
[98]	SOM + LVQ	Running length = 1000, learning rate = 0.5, window width parameter = 0.2, relative learning parameter = 0.3, no. of clusters = 5, mapping unit = 5 × data_length$^{0.54321}$	Tissue segmentation of MRI	IBSR, BRATS12/Efficiency of this method is much effective as it requires only 20 s time for each MR volume
[147]	ANN	NN has 1 input, 5 hidden, 1 output layer	Retinal vessel segmentation	DRIVE/the ROC curve between TPF and FPF is about 0.96% on average
[143]	FS, ant-based clustering with MLPNN	Fuzziness m = 1.7, parameter q = [0, 1]	Benign or Malignant segmentation in MRI breast cancer diagnosis	25 medical images/Avg. accuracy = 95.1%
[144]	SOM EGS-SOM and HFS-SOM	No. of extracted features D = 24, Population P = 30, $P_c = 0.8$, $P_m = 0.03$,	MR image segmentation	IBSR and IBSR 2.0/avg. sensitivity = 75%, avg. specificity = 88%
[93]	PLVQNN	Leaning parameters $\eta 1$ and $\eta 2$ lies between [0, 1], adjusting level k = 40	Thyroid segmentation and volume estimation from CT images	241 CT images assimilated from 3 patients/Avg. sensitivity (OF) = 78.7%, spec (σ) = 94.7%, acc. (ρ) = 91.5%, avg. sensitivity score = 86.3%
[148]	Bayesian classifier + NN	Avg. convergence time of mean shift = 11.7 s, bandwidth $h^s = 20$, neighbour k = 300	Wound tissues segmentation	113 images/for SVM and SVM + Heuristics sensitivity = 77.53, 78.23, specificity = 94.38, 94.55, success = 85.95, 86.39 and accuracy = 91.01, 91.29 respectively
[163]	ANN	To balance speed and accuracy parameter B = 99	To extract leaf veins	24 sub-images/out of 1200 pixels, 1168 = correctly classified pixels with correct classification rate = 97.33%, computing time = 0.90 s
[145]	Self Organiaing Feature Map (SOFM)	Mapping = hexagonal lattice, map sizes = 6 × 6 to 13 × 13, clusters = 4, 5, 6	Segmentation of Cerebral MR Images	29 MRI

As a result, the proposed approach achieves the main design objectives, i.e. with a superior classification performance maintaining a fast patient-specific and robust system. A CNN for fingerprint liveness detection, was proposed by Nogueira et al. [178]. Brosch and Tam [179] have evaluated the running time improvements using two standard benchmark data sets, showing a speed-up of up to 8 times on 2D images and up to 200 times on 3D volumes

Table 9 Summary of ANN articles without parameters

Ref no.	Methodology	Domain	Dataset/result
[92]	QBDSONN	Object extraction in real time from noisy background	Random images
[157]	Feedforward Neural Networks with FCM	Color image segmentation	BSD
[72]	ANN	Carbon nanotube images	41 carbon nanotube images
[149]	ANN	Rapid void detection from X-ray image	25 binary images
[94]	WMM + PCNN	Automated dark-spot detection using SAR imagery	60 Envisat and ERS2 images/an avg. accuracy of 93.66% was obtained working with 60 Envisat and ERS2 images
[95]	Simplified PCNN(SPCNN) + RBOR	To identify objects from complex real-world scenes	Texture and real world images
[164]	HDNN	Extracting multiscale features from vehicle database	Vehicle dataset of the city of San Francisco
[153]	ANN	Classification of oil spills from SAR	97 ERS2 SAR and ENVSAT ASAR
[159]	ParaOptiMUSIG + activation function	Color image	Lena and baboon
[154]	CBFNN	OBIA of high-resolution satellite images	A QuickBird satellite image and Indian Remote Sensing Satellite image/ Compared with CBF has CA = 4% higher to conventional RBF employed in artificial neural network
[160]	SNNs	Image segmentation and edge detection	50 images taken from the BSD
[161]	MLSONN + supervised pyramidal (PyraNet)	Multilevel image segmentation	Lena image, a brain slice
[150]	CN + Affinity graph	Computation of affinity graph	Images of retinal tissue
[99]	Modified PNN(WPNN)	Normal brain matter	Five real T1- and T2-weighted MR images
[96]	PCNN	Sea ice dissection	RADARSAT I ScanSAR over Baltic sea ice
[162]	MLP + Fuzzy clustering	Automatic Image Segmentation	Over 100 images of different types
[97]	PCNN	Digital Image Segmentation	–
[155]	Cellular NN (CNN)	Statistical image segmentation	SPOT satellite image
[165]	FHNN	Medicinal Image	5 medical images
[151]	CHNN	Medicinal Image	–
[156]	SARTNN	Satellite Image Clustering	–
[152]	CSNN	Medicinal Image	Several medical images obtained from CT, MRI and PET

from the OASIS data set. The algorithm makes training of Convolutional deep belief networks on 3D medical images with a resolution of up to 128 × 128 × 128 voxels practical, which opens new directions for using deep learning for medical image analysis.

4.4.2 Satellite Images Segmentation

Badrinarayanan et al. [180] motivated to develop a method named SegNet for semantic pixel-wise subdivision using a DCNN network which is effective in computational time and memory for indoor and road sight. This network compromises of 3 key components 1. An encoder network 2. Decoder network 3. A pixel-wise cataloguing level. In [181] Cheng et al. using DeconvNet as fundamental authors applied the prevalent deep convolutional neural networks to the sea–land segmentation problem. The proposed method is named as SeNet. The proposed local smooth regularization makes segmentation results spatially consistent. By integrating edge network with Deconvnet,

one can get more accurate edge results compared with traditional methods and DeconvNet. A 3-DCNN-based FE model which is a regularized deep feature extraction (FE) method through combined regularization to excerpt actual spectral–spatial features along with in order to additional advance the performance, a virtual sample enhanced technique for hyperspectral image (HSI) classification is proposed by Chen et al. [74]. In [82] Ding et al. have exploited the CNN for SAR target recognition with domain-specific data augmentation. Authors investigate the capability of a deep CNN combined with three types of data augmentation operations in SAR target recognition. Using the CNN trained by all types of augmentation operations, showing that it is a practical approach for target recognition in challenging conditions of target translation, random speckle noise, and missing pose demonstrate the usefulness of the proposed method. Kim et al. [86] shown a drone classification method based on CNN and micro-Doppler signature (MDS). GoogLeNet, a CNN structure, is utilized for the proposed image data set because of its high performance and optimized computing resources. The image data set is generated by the returned Ku-band frequency modulation continuous wave radar signal. FCNN with global output and input Li et al. [87] proposes a multi-task deep saliency model. The shared fully convolutional layers produces nominal features for object perception. In [75] for the classification of hyperspectral data Ghamisi et al. proposed a self-refining CNN. They also to tackle overfitting practices the notion of dither. Cheng et al. [77] presents a novel and effective approach to learning a rotation-invariant CNN (RICNN) model for advancing the performance of object detection. RICNN model is trained by optimizing a new objective function via imposing a regularization constraint. Depending on a downsample then upsample architecture for classification in [90] Volpi and Tuia presents a CNN-based system, involving the semantic labeling of aerial images of 9 and 5-cm resolution. Maggiori et al. [91] proposes an end-to-end framework for the dense, pixel-wise classification of satellite imagery with CNN. Zhou et al. [182] proposed a polarimetric SAR (POLSAR) images terrain classification framework using DCNN. The result of the San Francisco case shows that slant built-up areas, which are conventionally mixed with the vegetated area in polarimetric feature space, can be successfully distinguished after taking into account spatial features. Zhang et al. [183] proposed a CNN for aircraft recognition which combines a candidate region proposal network (CRPnet) and a localization network (LOCnet) to extract the proposals and simultaneously locate the aircraft, which is more efficient and accurate, even in large scale VHR images. For objects detection from aerial images incorporating a two phase method for training of network and verification a content base analysis approach which is automatic has been used by Sevo and Avramovic [88]. In [81] CNN has been used by Wang et al. to estimation of ice concentration by means of SAR extracts seized through the melt time of year on twofold-polarized SAR (HH and HV) images to generate ice concentration estimates. These dual-pol RADARSAT-2 satellite images are used as input, and the ice concentration is the direct output from the CNN Image analysis charts are used for training. CNN is a robust method that can model the effect of incidence angle, SAR image noise, and the effect of the wind on water and melt and Low-ice-concentration regions are also captured by the CNN model used.

4.4.3 Segmentation for Different Applications

In [85] Liu et al. have presented a novel visual analytics system to help machine learning experts better understand, diagnose, and refine CNNs along with a hybrid visualization consisting of rectangle packing, matrix ordering, and bi-clustering based edge bundling, the system allows experts to explore and understand a deep CNN from different. A DCNN for human parsing cataloguing grounded on Doppler radar was proposed by Kim and Moon [83]. The network does not use any explicit domain knowledge for extracting features, and the spectrogram itself served as input data to the DCNN. A novel Co-CNN architecture for the human parsing task, which integrates the cross-layer context, global image label context, semantic edge context and local super-pixel contexts into a unified network, was proposed by Liang et al. [76]. A deep learning method for single image super-resolution (SR) proposed by Dong et al. [184] named as SRCNN, which learns an end-to-end mapping between low- and high-resolution images, with little extra pre/post-processing beyond the optimization. The idea is to capture the driver gestures in order to detect postures of normal driving, functioning the shift gear, smoking or eating, and busy with a cell phone have been substantiated using CNN by Yan et al. [185]. Wang et al. [186] weighted hierarchical depth motion maps (WHDMM) with three-channel deep CNN (3ConvNets), for human action recognition from depth maps. Working with sparse Laplacian filter for unlabeled data and softmax classifier as output phase for labeled data Dong et al. [187] proposed a semisupervised CNN for the vehicle category sorting. Liu et al. [188] proposed a deep Convolutional neural field model for estimating depths from single monocular images, aiming to jointly explore the capacity of deep CNN and continuous CRF. Wu et al. [189] have proposed DDNN with HMM. DDNN is used to learn high-level spatiotemporal representations and automatically extract the relevant information from the data. The input to this network is multimodal whereas HMM is used to solve the temporal dependencies which segments and classifies

the multimodal data stream. It has two feature learning methods (1) for processing of skeleton features: Deep Belief Networks. (2) For RGB-D data: 3D Convolutional Neural Networks. In [190] Dosovitskiy et al. by training 'up-convolutional' neural networks which are capable of generating images of objects given object style, color, and viewpoint and trained on rendered 3D models of chairs, tables, and cars. A practical theory for designing very deep convolutional neural network and developed an inception module for multi-scale input was proposed by Py et al. [79]. By casting design of DCNN into a constrained optimization problem and found an optimal solution under certain condition.

Fakhry et al. [191] proposes a simple yet powerful model named as a residual deconvolutional network (RDN). Having capability of naturally balancing the trade-off between increasing contextual window required for multi-scale reasoning and the ability to preserve pixel level resolution and accuracy expected for dense output prediction. Identification and classification of handwritten numbers is of great interest among researchers. In this article Neubauer had used two variations of CNN named as neocognitron and an amendment of neocognitron along with FCFF (fully connected feedforward) layers in [192]. In [193] Anthimopoulos et al. proposed and evaluated a convolutional neural network (CNN), designed for the classification of ILD patterns. In [194] Tang and Wu proposed a new method for scene text recognition and subdivision based on cascaded convolution neural networks. In this method, a text-aware CTR extraction model and a CTR refinement model are devised to extract CTRs and obtain precise text segmentation results, which can overcome the above problems. The text-aware CTR extraction model detects regions of text (or the coarse CTRs) in the scene images and the CTR refinement model precisely segments the detected regions (or the coarse CTRs) into text in order to get the refined CTRs. Finally, the refined CTRs are fed into a CTR classification model to filter out non-text regions and obtain the final text regions. All of these models are based on a powerful CNN model (i.e. VGGNet-16). In [195] Chen et al. describes a fruit counting pipeline based on deep learning that correctly counts fruit in unstructured environments. They proposed a novel technique that uses deep learning to map from input images to total fruit counts. The pipeline utilizes a custom crowdsourcing platform to quickly label large data sets. A blob detector based on a fully convolutional network extracts candidate regions in the images. A counting algorithm based on a second Convolutional network then approximates the number of fruit in each region. Finally, a linear regression model maps that fruit count estimate to a final fruit count. In [196] Tang et al. emphasizes on the applications of maritime security and traffic control for ship detection on space borne images. The JPEG2000 compressed domain is used for fast ship candidate extraction, DNN is utilized for high-level feature representation and classification, and ELM is employed for efficient feature pooling and decision making. The difficulties of the higher resolution results in larger data volume and results which get affected by weather conditions like clouds and ocean waves.

4.4.4 Discussion

Convolutional neural network (CNN) or deep neural network (DNN) has been most widely adopted segmentation approach which has been deployed in number of applications. The architecture of CNN consists of input layer, convolutional layers, max-pooling layers, fully connected layer and an output layer termed as to be softmax layer. The novel neural network because of its deep structure itself is so powerful that it does not necessarily needs other functions or models, in some articles its was found that it has been incorporated with conditional random field (CRF), weighted hierarchical depth motion maps (WHDMM). CNN has been used in mostly complex applications compromising segmentation of SAR images, to find out objects from real world images, human activity recognition task and so on. Learning rate, momentum, batch size are its common parameters. Tables 10 and 11 depicts the summary of CNN and its variants.

4.5 Segmentation Using Genetic Algorithm and Its Variants

4.5.1 Medical Images Segmentation

Hung and Wu [103] proposes a novel parallel FCM method that integrates two algorithms, a GPU-based FCM and a genetic algorithm on multiple NVIDIA embedded GPU systems for brain MRI segmentation. The proposed algorithm consists of two parallel programming models—the MPI and CUDA. The GA presented in [101] by Ghosh et al. accomplishes derivative-free optimization of a level set function for image subdivision. Representing candidate explanations of the GA as segmenting contours and assessing their performance by means of a fitness function eradicates the need for defining an energy function and simplifies the optimization procedure needed for image subdivision. This permits the incorporation of different kinds of priors for exploring the fitness landscape. Shapes, regional properties and relative position of objects into a single framework to accomplish automated three-dimensional subdivision has also been targeted in this article. Image subdivision is typically accomplished manually by a physician to delineate gross tumor volumes for treatment

Table 10 Summary of CNN articles with parameter

Ref. no.	Methodology	Domain	No. of convolutional layer	No. of Maxpooling	Fully cone-cted layer	Softmax classifier/ output layer	Type of classificatio-n/ rectifier/cost function/ activation function	Training using BPA or SGD/other parameters	Dataset/result
[85]	BaseCNN	Visual analytics system to help machine learning experts	4C	1P	2F	1softmax	ReLU	BPA	CIFAR10, handwritten digit dataset, ImageNet dataset
[180]	SEGNET	For road and indoor scene	13C	5P (2 × 2)	–	1softmax	ReLU	SGD, learning rate = 10^{-3}, batch size = 5, 4, momentum = 0.9, dropout = 0.5, epochs = 100	CamVid road scenes dataset SUN RGB-D dataset
[181]	SENET	Sea–land segmentation	3C	3P	–	2softmax	ReLU/batch normalization (BN)	SGD, learning rate = 0.01, batch size = 4	A set of natural-colored images from Google Earth/Land precision (LP), land recall (LR), overall precision (OP), and overall recall (OR) = 99.69, 98.15, 98.12 and 98.11, Avg. F1-MEASURE (%) = 92.78
[171]	Deep multichannel NN	To segment glands	2C	5P	–	–	ReLU	BPA/Learning rate = 10^{-3}, weight decay = 0.002, momentum = 0.9	MICCAI 2015 Gland Segmentation/F1 score for part A and part B are 0.843, 0.893, DSC for A and B are 0.908, 0.833, object Hausdrofff for A and B are 44.129 and 116.821
[166]	Convolutional neural networks	Brain Tumor (gliomas) from MRI	For HGG = 6C (3 × 3) For LGG = 4C (3 × 3)	For HGG = 2P (3 × 3) For LGG = 2P (3 × 3)	HGG = 2F LGG = 2F	HGG = 1 LGG = 1	LeakyReLU	BPA	BRATS13 and BRATS13/ DSC = 0:78, 0:65, 0:75

Table 10 (continued)

Ref. no.	Methodology	Domain	No. of convolutional layer	No. of Maxpooling	Fully cone-cted layer	Softmax classifier/ output layer	Type of classificatio-n/ rectifier/cost function/ activation function	Training using BPA or SGD/other parameters	Dataset/result
[74]	Convolutional neural networks	Hyperspectral image (HSI) classification for 1D, 2D, 3D	5C (1 × 5, 1 × 5, 1 × 4, 1 × 5, 1 × 4)	5P (1 × 2, 1 × 2, 1 × 2, 1 × 2, 1 × 1)	1F	1 output (1 × 16)	Logistic regression/mini batch	BPA	IndianPine, University of Pavia, Kennedy space center dataset/ Accuracy for 1D = 85.09 + −1.20, 2D = 89.09 + −1.18, 3D = 98.00 + −1.10
			3C (1 × 8, 1 × 7, 1 × 8)	3P (1 × 2, 1 × 2, 1 × 2)	1F	1 output (1 × 9)	Logistic regression		
			4C (1 × 9, 1 × 9, 1 × 9, 1 × 10)	4P (1 × 2, 1 × 2, 1 × 2, 1 × 2)			Logistic regression		
[82]	Convolutional neural networks	SAR target recognition with domain-specific data augmentation	3C each C = 3 × 3	2P	1F (with 1000 units)	1softmax	ReLU	SGd and BPA	MSTAR/accuracy = 89.26
[86]	Convolutional neural networks + MDS	A drone classification method	GoogLeNet with 22 layers				ReLU	SGD, learning rate = 0.001, batch size = 4	Dataset from the anechoic chamber and outdoor measurement, 53 410 and 13 560 images/accuracy from 89.3 to 94.7%, the Two types of drone at the 50 and 100 m height are classified and showed 100% accuracy
[87]	FCNN(fully)	Object perception with feature extraction	15C (each 3 × 3)	5P	1F	1softmax	ReLU/Squared Euclidean loss/ cross entropy loss	BPA and SGD	ImageNet, ASD, DUTOMRON, CSSD, PASCAL-S, THUR, THUS, SED2, SOD
[83]	DCNN	Human detection and activity classification	2C (5 × 5)	2P (2 × 2, 4 × 4)	1F	–	Mini batch	BPA and SGD	12 human subjects performing seven activities/ Accuracy = 97.6% for human detection, accuracy = 90.9% for human activity classification

Table 10 (continued)

Ref. no.	Methodology	Domain	No. of convolutional layer	No. of Maxpooling	Fully cone-cted layer	Softmax classifier/ output layer	Type of classificatio-n/ rectifier/cost function/ activation function	Training using BPA or SGD/other parameters	Dataset/result
[84]	3D CNNs	CMBs from MRI	For 3DFCN 3C ($5 \times 5 \times 3$, $3 \times 3 \times 3$, $3 \times 3 \times 1$) For 3DCNN 2C ($7 \times 7 \times 5$, $5 \times 5 \times 3$)	1P ($2 \times 2 \times 2$)	For 3DFCN 2F ($2 \times 2 \times 2$, $1 \times 1 \times 1$) For 3DCNN 3F	1softmax	ReLU	BPA/learning rate = 0.03, momentum = 0.9, dropout rate = 0.3, batch size = 100	320 volumetric MR scans/ Sensitivity = 93:16%, avg. no. of false positives per subject = 2:74
[75]	SICNN	Classification of hyperspectral data	3C (4×4, 5×5, 4×4)	2P (each 2×2)	1F	1softmax	LR/ReLU/Mini batch	BPA and matconvnet-1.0 beta 18 with CUDA conf.	Indian Pines and Pavia University
[89]	CNN	To segment fetal brain and lungs	2 set of C	P for each C	–	–	ReLU	BPA	MR images of 55 fetal subjects/ brain (DSC 80.7 + −4.9% and lungs (DSC 58.6 + −19.0%)
[77]	CNN	Object detection in remote sensing	5C	3P	3F	1softmax		RICNN	VHR object detection dataset/ Accuracy = 90%
[78]	CNN	Segmentation of medical images	3C	P for each C	3F	–	ReLU	BPA	Database of 40 short colonoscopy videos, 121CTPA datasets, database of 92 CIMT videos
[90]	CNNPC (patch classification)	CNNPC for patch classification and CNNSPL for subpatch labeling from aerial images	4C	1P	1F	–	ReLU	BPA	Vaihingen and Potsdam sub-decimeter resolution/ accuracy = 85.8%
	CNNSPL(subpatch labelling)		4C	Replaced by $C = 1 \times 1$	Replaced by $C = 1 \times 1$		ReLU	BPA	
[81]	Convolutional neural networks	Ice concentration in SAR images	2 pair of C	2 pair of P	2 pair of F	–	ReLU/sigmoidal or linear activation	BPA/SGD	RADARSAT-2

Table 10 (continued)

Ref. no.	Methodology	Domain	No. of convolutional layer	No. of Maxpooling	Fully cone-cted layer	Softmax classifier/ output layer	Type of classificatio-n/ rectifier/cost function/ activation function	Training using BPA or SGD/other parameters	Dataset/result
[91]	CNN	Pixel wise classification of satellite imagery	3C	–	1F	Softmax	Mini batch	SGD	Pleiades images from CNES 2012 and CNES 2013/accuracy = 94.87%
[178]	CNNVGG	For fingerprint liveness detection	16C	–	3F	Softmax	ReLU	SGD	50,000 real and fake finger prints/Accuracy = 97.1%, and for Fingerprint Liveness Detection Competition (LivDet) 2015 with an overall accuracy of 95.5%
	CNNAlexnet		8C	–	3F	Softmax	ReLU	SGD	
[182]	DCNN	POLSAR images terrain classification	2C	2P	2F	Softmax	ReLU	BPA/SGD	AIRSAR records of San Francisco CA and Flevoland Netherland/San Francisco accuracy = 99.43 and 90.23% and Flevoland = 99.20 and 97.66%
[37]	Deep neural networks	Cancer segmentation from brain, breast images	2C (6×6, 4×4)	2P (2×2, 2×2)	2F	Softmax	ReLU	SGD/repulsion weight $\omega = 0$ to 2.5, nearest neighbour size M = 0 to 200, dictionary size is 5–100%	Several images/DSC for brain, NET, breast is 0.93, 0.92, 0.98, HD is 6.37, 3.14, 13.08 and MAD 4.41, 2.10 and 9.61 respectively, evaluation were also made on dictionary rate
[173]	Deep Convolutional neural networks	Facial landmark localization	4C	3P	2F	Softmax	ReLU	SGD/Learning rate = 2e−4, 1e−4	300 w challenge
[174]	Convolutional neural networks	Classification of medical images	Alexnet with 5C and GoogLeNet with 22 or 27 overall layers	2P	1F	Softmax	ReLU	SGD/learning rate $\eta = 5 \times 10^{-6}$, batch size = 256, momentum $\alpha = 0.9$	ImageCLEF 2016/classification accuracy of 82.48, 96.59
[183]	Coupled CNN	For aircraft detection from VHR	2C	2P	1F	Softmax	ReLU	BPA	Sydney International/Airport data set, the Tokyo Haneda Airport data set, and the Berlin Tegel Airport database

Table 10 (continued)

Ref. no.	Methodology	Domain	No. of convolutional layer	No. of Maxpooling	Fully cone-cted layer	Softmax classifier/ output layer	Type of classificatio-n/ rectifier/cost function/ activation function	Training using BPA or SGD/other parameters	Dataset/result
[175]	CNN	Color fundus image segmentation for hemorrhages	5C	5P	1F	Softmax	ReLU	BPA	From 2 databases 1. The Diabetic Retinopathy/Detection challenge database from Kaggle1 2. Messidor database/ $A_z = 0.894$ and 0.972
[193]	Deep CNN	Classification of ILD patterns	5C (2 × 2 each)	–	–	Softmax	ReLU +Leaky ReLU	gradient descent, BPA	14,696 image patches, derived from 120 CT scans/ accuracy = 85.5%
[172]	Deep Convolutional neural networks	Skin lesion segmentation	5C (5 × 5, 3 × 3, 4 × 4, 4 × 4, 5 × 5) and 4D (5 × 5, 4 × 4, 4 × 4, 3 × 3) 2P (2 × 2, 2 × 2) and 2U (2 × 2, 2 × 2) 1F (5 × 5)			–	ReLU	SGD/learning rate $\alpha = 0.003$, batch size = 18, dropout p = 0.5	ISBI 2016 Skin Lesion Analysis towards Melanoma Detection challenge, and the other is the PH2 database/ accuracy = 0.955, DSC = 0.912, JI = 0.843, SE = 0.918, SP = 0.966
[184]	SRCNN	Color image segmentation with super resolution	3C	–	–	–	ReLU	BPA, Mean Squared error, blur kernel	Set5, Set14, BSD200
[185]	CNN	To automatically learn and predict pre-defined driving postures	3C	1P (2 × 2)	3F	1softmax	ReLU/Mini batch	BPA	SEU driving dataset/Overall Accuracy = 99.47%
[177]	1D CNN	Patient-specific ECG heartbeat classifier	3C	2P	–	–	ReLU	BPA	Datasets from the MIT/BIH arrhythmia database
[170]	Deep ConvNets	Pancreas subdivision in abdominal CT	5C	3P	3F	Softmax	ReLU	–	CT images of 82 patients/A DSC of 83.6 ± 6.3% in training and 71.8 ± 10.7%

Table 10 (continued)

Ref. no.	Methodology	Domain	No. of convolutional layer	No. of Maxpooling	Fully connected layer	Softmax classifier/ output layer	Type of classificatio-n/ rectifier/cost function/ activation function	Training using BPA or SGD/other parameters	Dataset/result
[186]	WHDMM	For human action recognition from depth maps	5C	–	3F	–	ReLU	–	MSRAction3D, MSRAction3DExt, UTKinect-Action, and MSRDailyActivity3D/ accuracy = 85%
[187]	Semisupervised CNN	Vehicle type classification method	5C	1P	–	Softmax	Sparse laplacian filter learning(SLFL)	BPA	9850 Vehicle images/ accuracy = 88.11%
[176]	Convolutional neural networks	For face recognition system	2C (21 × 26, 9 × 11)	2P (11 × 13, 5 × 6)	1F	–	–	–	ORL database images/overall error rate of about 1.87% on avg.

planning and diagnosis De et al. [197] proposed, an application of a genetic algorithm (GA) based segmentation algorithm for automatic grouping of unlabelled pixels of the MR images into different homogeneous clusters. MRI segmentation is achieved using two automatic segmentation algorithms, viz. the fuzzy inter-cluster hostility index based genetic algorithm and the automatic clustering differential evolution (ACDE) algorithm and one supervised fixed number of class levels based algorithm, viz. Chabrier's algorithm. McIntosh and Hamarneh [198] have proposed a novel method for medical image segmentation that combines genetic algorithm (GA) with nonconvex, localized, medial-based shape statistics. Combining the GA and VEM algorithms a hybrid GA-VEM algorithm for GMM-based brain MR image segmentation proposed by Tian et al. [199]. GMM is investigated using VEM, and initialization of the hyperparameters of the conjugate prior distributions of GMM parameters involved in the VEM algorithm was done with the help of the GA. To optimize the settings of the automated segmentation of the MR Analytical Software System (MASS) package in [200] Angelie et al. uses Genetic Algorithm (GA) as a tuning method. Yeh and Fu [201] proposes a hierarchical genetic algorithm with fuzzy learning vector quantization network (HGALVQ), to segment multi-spectral human brain MRI. The objective of HGALVQ is to formulate and partition a set of feature vectors of multi-spectral brain MRIs into a relatively small number of clusters, each represented by a vector called a prototype. Each feature vector contains the elements T1, T2, and SD parameters at a certain image location called voxels. Then the HGALVQ searches for the best partition of the feature vectors so that the segmented image is obtained by representing each feature vector by its closest prototype. This paper describes a new approach to segmentation of brain MRIs for three types of images (T1, T2, PD). Since the proposed algorithm does not employ exhaustive searches, the solution generated is near optimal. Because the number of final clusters is not fixed, the algorithm can locate different types of brain tissues (e.g. tumors or meningiomas). An experimental design is used to specify the initial number of prototypes, in the same way that other parameters are predetermined. Once the number is specified, it is not changed. The input vectors, after processed by HGALVQ, are clustered into several groups and then mapped to a synthetically coloured image for visualization. The region of abnormal tissue is specified to represent the location of the tumor or meningioma. A real-coded genetic algorithm with an application of RGA with SBX crossover based multilevel thresholding to medical brain image is used by Manikandan et al. [202]. To segment the lateral ventricles from magnetic resonance brain images in [203] Fan et al. presents a corresponding GA-based active model. First, an objective function is defined then one instance

Table 11 Summary of CNN articles without parameters

Ref no.	Methodology	Domain	Dataset/result
[167]	Convolutional neural networks	Automatic segmentation of MR brain images	Five different databases/the avg. DSC for different age groups was 0.87, 0.82, 0.84, 0.86 and 0.91
[189]	DDNN and HMM	Gesture separation and classification	ChaLearn LAP/JI = 0.81
[76]	Co-Convolutional neural networks	Human parsing task	ATR dataset and the Fashionista dataset/the F−1 score on the large dataset reaches 81:72% by Co-CNN, significantly higher than 62:81% and 64:38% by the state-of-the-art algorithms, MCNN and ATR, respectively, By utilizing newly collected large dataset for training, Co-CNN can achieve 85:36% in F−1 score
[88]	Convolutional neural networks	Objects from high-resolution images	UCMerged dataset/Accuracy = 98.6%
[79]	CNN	Plankton classification	Plankton set 1.0
[190]	Convolutional neural networks	3D models of chairs, tables, and cars	ShapeNet dataset
[191]	Residual deconvolutional network	Electron Microscopy (EM) image segmentation	2D neurite segmentation challenge dataset
[169]	Convolutional neural networks	Characterizing plaque composition in carotid ultrasound	56 test images
[194]	Cascaded CNN	Scene text detection and segmentation	ImageNet dataset, ICDAR 2011, ICDAR2013, the Street View Text dataset (SVT)
[195]	Deep learning network	Counting apples and oranges	Data sets of oranges in day and green apples at night/best ROC is 0:03, yielding a TPR of 0:957 and FPR of 0:051. TPR with threshold is 0:961 and the FPR is 0:033. The mean IU is 0:838 at the 0:37 threshold
[168]	DNN	Fully automatic brain tumor segmentation method	2013 BRATS/avg. DSC = 0.85 ± 0.5, avg. Specificity = 0.90 ± 0.5, avg. Sensitivity = 0.86 ± 0.5
[196]	DNN + ELM	Ship detection on space borne images	Space borne artificial images
[179]	Convolutional neural networks	For medical images	OASIS data set
[192]	Convolutional neural networks	Classification of handwritten digits	Four datasets

surface was extracted using the finite-difference method-based active model and used to initialize the first generation of a parallel genetic algorithm. Finally, to refine result the parallel genetic algorithm is employed. 2-D method which is used as the initial surface for the evolution equation, an estimated object is segmented from one image data slice by slice and for the final result in the second stage the objective function is optimized by the parallel GA.

Aim of this study was to find a semi-automatic method of bone segmentation on the basis of computed tomography (CT) scan series in order to recreate corresponding 3D objects was done by Janc [204]. In [205] Rogai et al. presents an unseeded segmentation system applied to ultrasound imaging is presented, based on a compact segmentation method. A real-valued genetic algorithm and an ant colony algorithm are two nature inspired algorithms which are used for specialization for the present clinical application and its behavior is represented by fuzzy rule system. The final refinement of the region, using the GrowCut algorithm, also allows one to reduce the discrepancy between the human segmentation and the system output. Detection of suspect masses from Mammograms images is a critical issue in medical diagnosis. Pereira et al. [206] uses a set of computational tools such as GA, wavelet transform thresholding, wiener filter. Xie and Bovi proposed a new Dermoscopy image subdivision method using a amalgamation of a self-generating NN (SGNN) and the GA in [104]. A hybrid approach of the genetic algorithm is used for feature selection in medical images by Nagarajan et al. [207] consist of three phases. In the first phase, three distinct algorithms are used to extract the vital features from the images they are Texton-based contour gradient extraction algorithm, intrinsic pattern extraction algorithm and modified shift invariant feature transformation algorithm. In the second phase to identify the potential feature vector GA-based feature selection is done, using a hybrid approach of "Branch and Bound Algorithm" and "Artificial Bee Colony Algorithm". In the third phase to improve the performance of the hybrid content-based medical image retrieval system, diverse density based relevance feedback method is used. Ye [208] proposed GA in amalgamation with PSO, a fusion method for medical image diagnosis forming GAPSO-FS also GAFOA-FS. Dokur and Olmez [209] for the segmentation of tissues in ultrasound images presents a genetic based incremental neural network (GINeN). Use of wavelet transform and genetic based incremental neural network together in order to increase the segmentation performance was also proposed in this work.

4.5.2 Satellite Images Segmentation

Mylonas et al. proposes an object-based classification scheme for handling remotely sensed images in [105]. The method combines the results of a supervised pixel-based classifier with spatial information extracted from image segmentation. Using spectral and textural features of pixels, pixel-wise classification is implemented by a fuzzy output SVM classifier at first. This classification results in a set of fuzzy membership maps. Genetic Sequential Image Segmentation (GeneSIS) algorithm is then developed to partition the image into homogeneous regions by operating on this transformed space. GeneSIS follows a sequential object extraction approach, whereby at each iteration a single object is extracted by invoking a GA-based object extraction algorithm. Saha and Bandyopadhyay [210] used a newly developed genetic clustering technique named multicenter-based automatic clustering technique (MCVGAPS) for automatically segmenting remote sensing satellite images was proposed. In [211] Awad et al. have presented a new multicomponent image segmentation method using a nonparametric unsupervised ANN called SOM and HGA. SOM is used to identify the main features that are there in the image; then, HGA is used to cluster the image into homogeneous regions without any a priori knowledge. A technique for the detection of roads in a space borne SAR image using a genetic algorithm (GA) was proposed by Jeon et al. [212]. In [213] Izadi et al. presents a new approach which is portrayed for roads damage detection and assessment by vector map and both pre-event and post-event high-resolution satellite images. Various texture and spectral features are considered and a genetic algorithm is used to find the optimal features. The new semi-automatic approach is proposed. After roads masking, A GA-based algorithm was engaged to find the best subset of features. This increases the automation and makes damage detection more accurate. The SVM-based classification which achieves higher accuracy than traditional MLL was chosen. Singh and Singh [214] proposed a semi-supervised method for classification of flooded areas in satellite images based on Genetic Algorithm (GA) and Radial Basis Function Neural Network (RBFNN). The seed selection is done using spectral indices like NDVI, NDBI, NDWI and PC-1. The proposed method trains the radial basis function network with Genetic Algorithm and thus combines the advantages of both. The RBFNN provides easy design, good generalization, strong tolerance to input noise, and online learning ability. The neural network handles a large amount of data present in satellite images. The use of GA makes the search optimal as it is a powerful optimization tool and works well when the exploration space is enormous in satellite images. In [215] Mylonas et al. uses Genetic Sequential Image Segmentation (GeneSIS) algorithm for segmenting the satellite images by extracting a single object at each iteration. The suggested fitness function encompasses three fuzzy components: the coverage, the consistency and smoothness criteria, used to

accommodate the size, the homogeneity and the shape of extracted objects.

4.5.3 Segmentation for Different Applications

In [216] Ishak for image segmentation ha considered the rigorous formulation of the two-dimensional multilevel thresholding approach. Then, to determine efficiently the required thresholding values the two optimizers QGA and DE are used. Based on the 2D gray-level histogram and maximum Renyi and Tsallis entropies authors have proposed a multilevel thresholding approach. The main contribution of this article is to the significance of the proposed work, on multimodal images, noisy images with shadow or reflection. The problem of color image segmentation is considered as a clustering problem and a fixed length genetic algorithm (GA) used for handling it by Khan and Jaffar [217]. A self-organizing map (SOM) is used to determine the number of segments in order to set the length of a chromosome automatically. Using a permutation-coded genetic algorithm (GA) identifying regions in hue–saturation–intensity (HSI) color space (GAHSI) for desired and undesired raisin detection in various conditions was successfully implemented by Abbasgholipour et al. [218] for supervised color image segmentation. In the experiment, GAHSI performance was measured by comparing the GAHSI-segmented image with a corresponding hand-segmented reference image. The GAHSI method when compared with cluster analysis based segmentation results, showed no significant difference. The GA-based segmentation scheme described in this article is a novel and simple approach to robustly segment an image of raisin into desired, undesired and background regions under variable conditions has been taken. Hammouche et al. [219] presents a new multilevel thresholding method based on a genetic algorithm, which enables determining the appropriate number of thresholds, as well as the adequate threshold values. The length of the original histogram is reduced by using a wavelet transform. Based on this lower resolution version of the histogram, the optimal threshold values are determined by using a standard GA. In this GA is used a new string representation of the chromosome, which is different from current representations. A binary encoding is used and the threshold values are directly determined without requiring the use of encoding and decoding operations. In order to improve the performance of the GA, a learning strategy was used and a new mutation operator, that handles problem dependent characteristics, was also proposed. Melkemi et al. [220] presents a new distributed image segmentation algorithm, in which several techniques are carefully combined to achieve different tasks in the segmentation process. The algorithm is structured as a multiagent system (MAS) composed of a set of segmentation agents interconnected around a coordinator agent. Segmentation agent uses the MRF-based iterated conditional modes (ICM) method to accomplish their segmentation tasks. The proposed approach is very amenable to parallel implementation which can potentially result in great speed-ups over conventional optimization techniques.

In [100] Abdel-Khalek et al. proposes a novel two-dimensional image segmentation approach based on the flexible representation of Tsallis and Renyi entropies and employing the GA. The GA is utilized to make the most of the entropy in order to segment efficiently the image into object and background. The comparison has been done of segmentation method with the classical thresholding approach using Renyi and Tsallis entropies. The present method defines a new form of shape representation, which uses the FCSs discovered by a GA in [221] Wei and Tang. This representation shows the essential structural logic of a contour. (1) GAs are used and redesigned for learning the conceptual shape representation and achieving object recognition, respectively. (2) The present representation shows a symbolic description of the geometric features of contour. The proposed method contributes to the formation of conceptual definitions based on geometric structure. It can also be used for shape retrieval and shape recognition. Spatial fuzzy genetic algorithm (SFGA) for the unsupervised segmentation of color images [222] Khan et al. in this article. The SFGA adds diversity to the search process to find the global optima. The performance of SFGA is influenced by two factors: first, K no. of clusters should be known in advance; second, the initialization of the cluster centers. To overcome these issues, a progressive technique based on the SOM is presented to find out the optimal K number of clusters automatically. To handle the initialization problem, peaks are identified using the image color histograms. The genetic algorithm with fuzzy behavior maximizes the fuzzy separation and minimizes the global compactness among the segments. The segmentation is performed on wavelet transform image which not only reduces the dimensionality and computational cost but also makes more compact segments. A novel pruning technique is proposed to handle the problem of over-segmentation. Andrey [223] describes an unsupervised image segmentation method based on a fine-grained distributed genetic algorithm. The method does not require the definition of an objective fitness function evaluating candidate segmentation results. Kim et al. [224] presents a hierarchical distributed genetic algorithm (HDGA) which is unsupervised and parallel for segmenting noisy and blurred images. [225] in this paper Song and Ciesielski describes a texture segmentation method using genetic programming (GP). The work presented shows that a fast and accurate texture segmentation method can be developed based on classifiers

evolved by GP. Adopting a distributed genetic algorithm gray level image subdivision has been performed by Andrey and Tarroux [226]. In [106] Wang et al. have presented an improved adaptive GA (IAGA) for the image subdivision and vision alignment of the solder joints in the microelectronic chips. GA was enhanced using Hill-climbing, randomizing, and modified mutation operators, leading to what is called hybrid dynamic genetic algorithm (HDGA) was proposed by Awad et al. [227]. Integrating HDGA and FCM create an automatic segmentation method that successfully segments two types of multi-component images. A novel method employing an improved robust estimator to iteratively detect and extract distinct planar and quadric surfaces was proposed by Gotardo et al. [228] for range image segmentation. A genetic algorithm was specifically designed to accelerate the optimization process of surface extraction while avoiding premature convergence.

4.5.4 Discussion

Genetic algorithm has been deployed mostly with other soft computing approaches like fuzzy c means (FCM), ant colony optimization, particle swarm optimization, artificial neural network, self-organizing map (SOM), learning vector quantization (LVQ), Markov random field (MRF) etc. The most common parameters for genetic algorithm are population, no. of generations, crossover probability and mutation probability denoted by P, N, P_c, and P_m respectively. Tables 12 and 13 summarize various articles.

5 Outcomes

The soft computing approaches used for partitioning of an image has clutched a great deal of courtesy amongst scholars and academicians. These approaches for Image segmentation have facilitated to condense user collaboration and manual clarification to an excessive amount. Robustness, efficiency, and effectiveness has been enriched when associated with traditional and mathematical methods [254–256, 261]. Here in this section we intended to present the various findings by categorizing them into the problems researches working on with different images, databases used, evaluation parameters, noises used etc. for research purposes.

A lot of work has been done specially on two types of images medical and SAR images, but recently the interest of researchers has been shift from those to other images including natural scenes, other complex real world images such as Leaf veins extraction from images of plant, Document page segmentation from like newspapers, Road and indoor scenes, etc. the region of interest among the different classification of images as for example in MRI images most of the authors are willing to classify the given brain MRI image into 4 regions 1. GM 2. WM 3. CSF and 4. Background in order to extract tumor along with extraction of Endorrhachis from MRI, breast cancer from MRI images, Retinal images are segmented into vessels and non-vessels pixels for diagnosis of diabetic retinopathy and for analysis of vascular structures of the human retina, CT images has been used for thyroid segmentation, tumor regions, suspect nodules, Pancreas segmentation, Skin images has been used for lesion segmentation and other dermatology problems, Masses of region of interest (cancer) from mammographic images and other images such as lip images for lip classification, tissue identification from wound images, segmentation of knee images into blood vessels of interest, Void detection from X-ray images, ECG images for heart beat classification, Leukocytes in blood smear images etc.

The region of interest of researchers in satellite images of SAR images lies in generally to classify the objects into two types of classes (1) Man-made class (2) Natural class in order to identify road, building, vegetation, tree, water, and land area etc. Number of authors recently have also focused on texture segmentation from SAR images while detection of oil spills or dark spot are also topic of interest. Segmentation of SAR images has also been carried out for ocean or sea images for the extraction of ice concentration in the sea for different period of time along with sea land classification, terrain classification. Again a novel work has been seen for the subdivision of flooded area and non-flooded area before the flood and after the flood.

Coming to the third category of our subdivision for carrying segmentation in several image includes underwater image segmentation permissible to classify fishes, M-fishes, species etc. Segmentation of Carbon nanotube images, Identification of TCFA from VH-IVUS image, Infrared ship image segmentation. The segmentation of natural real world complex images has been the area of attention for academician in identifying real world objects such as table, chair, road and indoor scenes such as sign board subdivision etc. the work has also been carried out for the document segmentation so as to identify handwritten characters, digits from a hand written document, segmenting newspaper into number of classes such as headings, sub-headings, pictures, paragraph etc.

More complex work was carried out to identify or classify human being activities like actions, movements or gestures. Ship detection from space borne images, vehicle type classification, natural color image segmentation, Drone classification, geographic map image segmentation, agricultural or plant images segmentation etc. are some other areas Table 14 shows segmentation applications for the images in different fields. In this table we have

Table 12 Summary of GA articles with parameter

Ref no.	Methodology	Parameter	Domain	Dataset/result
[205]	Genetic algorithm + Ant Colony Algorithm	Mutation probability $P_m = 0.05$	Ultrasound images segmentation	BreastDS, AnesthAnnulusDS, AnesthVascularDS, GynFolliclesDS
[103]	GPU-based FCM and a genetic algorithm	Population P = 30, 60, 90, 120, 150, 180	Brain MR image	BrainWeb
[101]	Genetic algorithm	Crossover probability $P_c = 50\%$/gene, $P_m = 10\%$/gene, P = 50 for 2D and P = 25 for 3D	2 and 3 Dimensional CT and MRI	Oregon Health and Sci. Univ. (OHSU)/DSC for 2D = 0.45 and for 3D = 0.69
[216]	Genetic algorithm	No. of generations N = 100, $P_c = 1.0$	Gray-level image segmentation	20 benchmark images
[105]	GeneSIS	$P_c = 0.8$, $P_m = 0.20$, N = 1000, P = 20	Satellite images	University of Pavia, Indiana, Karonia lake images/For Univ. of Pavia OA = 95.46, AA = 97.21, k = 93.95, For Indiana OA = 95.33, AA = 97.41, k = 94.65, For Karonia lake agriculture area OA = 81.47, AA = 86.31, k = 74.24, For Karonia lake wet land area OA = 94.85, AA = 92.45, k = 91.85
[217]	Fixed length genetic algorithm (GA)	$P_c = 0.8$, $P_m = 0.05$, P = 20	Various images	BSD/Avg. PRI 0.8332 and VoI 1.9239
[197]	Genetic algorithm (GA)	$P_c = 0.5$ to 1.0, $P_m = 0.01$, P = 100	MR image	Correlation coefficient (ρ) = 0.9896 Empirical measure (Q) = 0.0014
[106]	Improved adaptive genetic algorithm (IAGA)	$P_c = 0.9$ and 0.6, $P_m = 0.09$ and 0.01, P = 20	Solder joints from microelectronic chips	–
[206]	Multiple thresholding, wavelet transform, and genetic algorithm	$P_c = 0.9$, $P_m = 0.001$, N = 100, $P = 150/2^j$ (where j = resolution level)	Mammogram mass segmentation	The average AOM achieved by algorithms is 0.79 ± 8% equivalent to approx. 79% on average. A FP rate of 1.35 FP/image was acquired for a sensitivity of 95%
[204]	Genetic algorithm (GA)	$P_c = 0.8$, $P_m = 0.002$, 0.005, 0.1 N = 400, 300, 200, P = 10, 25, 50	Bone segmentation from CT images	J. Morita Mfg. Corporation/80/SA = 0.761
[229]	GeneSIS	$P_c = 0.8$, $P_m = 0.01$ and 0.25, N = 1000, P = 20	Object-based classification scheme for handling remotely sensed images	University of Pavia, Indiana, Karonia lake images
[230]	Bell fuzzy multilayer perceptron (BF-MLP) optimized with GA	$P_c = 0.75$, $P_m = 0.02$, N = 20, P = 10	Medical image segmentation	44 images from National Biomedical images with 3 class labels/CA of 95.5% and by 2.3% increased when NN optimization has been performed
[198]	GA	P = 24	Medical image	50 mid-sagittal MRI
[104]	Self-generating NN (SGNN) and the GA	$P_c = 0.6$, $P_m = 0.08$, N = 40, P = 25	Dermoscopy images	Caucasions 125 Dermoscopy images from a hospital
[199]	GA-VEM	P = 500	MRI segmentation	IBSR/Accuracy = 0.7702 ± 0.1435, for 17 high resolution T1-wieghted = 0.8570 ± 0.0458
[210]	Multicenter-based automatic clustering (MCVGAPS)	$P_c = 0.8$, $P_m = 0.2$, N = 30, P = 50	Satellite Images	2 numeric image, SPOT-3D of part of city of Kolkata India, Landsat-V/Avg. ARI MCVGAPS = 0.75 ± 0.01, for the SPOT image 0.72 ± 0.01, Landsat image = 0.71 ± 0.01

Table 12 (continued)

Ref no.	Methodology	Parameter	Domain	Dataset/result
[218]	Permutation-coded genetic algorithm (GA)	$P_c = 0.8$, $P_m = 0.16$, N = 100, P = 12, 24, 36 and 48	Color images	–
[227]	Hybrid dynamic genetic algorithm (HDGA)	$P_c = 60\%$, $P_m = 0.15$ and 0.05	Satellite Image	Landsat ETM + , IKONOS II/For Landsat ETM + acc (ρ) = 97%, For IKONOS Accuracy = 90%
[231]	Genetic Algorithm (GA)	$P_c = 0.8$, $P_m = 0.005$, P = 100	Medical Image	–
[225]	Genetic programming (GP)	$P_c = 90\%$ and 10%, P = 500	Texture Image	The segmentation performance on two patterns with multiple regions was 99.83% and when segmenting for Brodatz textures, D21, D24, D35 and D57 was found to be 97.48%
[201]	Fuzzy learning vector quantization network (HGALVQ)	$P_c = 1.0$, $P_m = 0.01$ to 0.05, N = 100, P = 24	Multi-spectral human-brain MRI	Database collected form a hospital in Taiwan/SP = 0.9739, SE = 0.9220, JS = 0.4266
[211]	SOM–HGA	$P_c = 60\%$, $P_m = 10\%$, P = 90	Satellite Image	ISODATA, IKONOS/SA = 92.66%
[219]	Genetic Algorithm (GA)	$P_c = 0.9$, $P_m = 0.001$, N = 100, P = 100	Various images	8 images/Uniformity U = 1.1007
[220]	Genetic Algorithm (GA)	$P_c = 0.9$, $P_m = 0.005$	Various images	–
[200]	Genetic Algorithm (GA)	$P_c = 0.5$	Automatic tuning of left ventricular from MRI	–
[212]	Genetic Algorithm (GA)	N = 200, P = 100	Detection of roads in SAR	an acc. (ρ) = 92.2%, with an avg. error = 0.13 pixels
[203]	Parallel genetic algorithm	$P_c = 0.9$, P = 80	Lateral ventricles from magnetic resonance brain images	–

Table 13 Summary of GA articles without parameter

Ref no.	Methodology	Domain	Dataset/result
[213]	ANFIS using Genetic algorithm (GA)	Roads damage detection after earthquake	QuickBird pan-sharpened images from the Bam earthquake
[100]	Genetic Algorithm (GA)	Various images	–
[214]	Genetic Algorithm (GA) and RBFNN	Flooded areas in satellite images	LandSat 8 OLI images of Dongting Lake in south China/the total flooded area is about
[207]	GA + BBA + ABC	Medical images	–
[208]	GA +PSO or FOA (fruit fly optimization) GAPSO-FS, GAFOA-FS	Analysis of Parkinson's disease, breast cancer, diabetes	UCI machine learning data repository
[215]	GeneSIS	For the classification of remotely sensed images	Taxiarchis, Kerkini and Center of Pavia images
[221]	Genetic algorithms	Shape extraction and object classification	CE-Shape-1 dataset, INRIA horses dataset, ETHZ shape classes dataset
[202]	RGA with SBX crossover based multilevel thresholding with GA	Medical brain image	–
[222]	SFGA-Spatial fuzzy GA	Color images subdivision	BSD
[209]	GINeN	Tissues in ultrasound images	Phantom and Drgdiaz
[232]	Genetic Algorithm (GA)	Real range images	ABW and Perceptron DB, the Cyberware DB
[233]	Genetic Algorithm (GA)	Texture image segmentation	–
[223]	Fine-grained distributed (GA)	Various images	–
[234]	Genetic Algorithm (GA)	Texture image segmentation	–
[224]	HDGA	Segmenting noisy and blurred images	The evaluation function F for number of regions = 23 was resulted as 50.8

categorized set of images into 3 parts i.e. medical, satellite and others.

The role of database is one of the important issues which the number of researcher has to face off. Although most of the authors have work on generally available databases few of them has also used databases either by crating of their own or by taking it from the other organisations to conduct their research. In this part we would like to introduce some of the enormously used databases like Berkeley Segmentation dataset (BSD), Internet Brain Segmentation Repository (IBSR), BrainWeb, Digital Retinal Images for Vessel Extraction (DRIVE), Structured Analysis of the Retina Project (STARE), LIDC-IDRI—Lung Image Database Consortium image collection, Karolinska Directed Emotional Faces (KDEF), Indian Pines, Pavia Centre and University, RADARSAT-1 and 2 [267], PlanktonSet 1.0, KSC-Kennedy Space Center, Fish4Knowledge etc. These databases are publically obtainable databases some of them are direct available to download while some of them requires permission for accessing them. Though the user just always has to cite them.

BSD300 with 300 images and BSD500 with 500 is the most popular database in today's era which contains set of gray and color images for BSD300 200 images are for testing and 100 for testing and BSD500 included with additional 200 test images. It contains images of several scenes (natural). IBSR compromises of MRI which is being classified into different subjects. BrainWeb contains realistic MRI data volumes obtained from MRI simulator, accessible into 2 groupings Normal Brain and MS Lesion Brain Database. DRIVE and STARE both containing about 400 images which are used for the subdivision of blood vessels from the retinal images so that further diagnosis can be carried out. LIDC-IDRI is a collection of approx. 1018 such cases which of CT images having lung cancer and diagnostic problems. KDEF database is a collection of about 4900 images with different facial expression which is intended for psychological and other medical diagnosis but can be used for other applications also. Fish4Knowledge database has been the database available for the shake of underwater image subdivision into fish species and other complex regions extraction. PlanktonSet 1.0 has been collected from subtropical Straits of Florida in order to help biophysical drivers upsetting fine-scale connections among larval fish, their prey, and predators. Indian Pines among the SAR dataset compromise of images are classified into 3 categories about 2/3 images of agriculture, 1/3 of forest or other natural recurrent flora. Pavia Centre and University 42776 samples classify into 9 classes images of Pavia a place in north Italy. RADARSAT-1 and 2 dataset consists of SAR images. RADARSAT-1 temporal coverage Nov 1993 to Mar 2013 and RADARSAT-2 temporal coverage Dec 2007 to present. KSC acquired over the Kennedy Space Center (KSC), Florida, on March 23, 1996 is a set of another form of SAR images.

Another important aspect of the literature survey is noise which plays a very important for the evaluation of different algorithms for checking their effectiveness and performance [269, 273]. Based on the review we have found mostly 2 noises have been used, they are Gaussian noise and Salt and Pepper noise, some authors has also worked with yet another type of noise that is Poisson noise. The noises are mixed with original images and then using the algorithm results of original image and noised image has been compared under different variations of noise. A Gaussian noise is termed as to be a statistical noise which is having a PDF equivalent to that of normal distribution or Gaussian distribution [276, 277]. The Gaussian noise is independent of the intensity of the pixels from an original image so it can be termed as additive noise. The Gaussian noise can be removed with the help of a spatial filter. The probability density function p of a Gaussian random variable z is given by Eq. 7:

$$P_R(g) = \frac{1}{s\sqrt{2\pi}} e^{-\frac{(g-m)^2}{2s^2}} \tag{7}$$

where g = gray level, m = mean value and s = standard deviation.

Salt and Pepper noise in the form of white and black pixels it presents on images as sparsely occurring one. This noise can be removed by using a morphological or median filter and when either of the one has to be removed than it's done with the help of contra-harmonic mean filter. Poisson noise is the noise that is reliant on the intensity of the pixels of an original image, hence we can say that it is correlated with the intensity of each pixel. It is very rare to have such kind of noise.

The performance of any work is patterned by two ways as it has been seen from the literature survey (1) Computational efficiency (time) and (2) Some evaluation parameters. This in fact is another effort to present important aspects for validating the segmentation performance of the proposed algorithms or methods. Number of evaluation parameters was seen through this work and we had tried to introduce some of them along with providing the mathematical functions given in Table 15. Though these parameters could be utilized for finding out the segmentation accuracy but a high performance system to diminish the computational load is a much researched domain for segmenting an image and it is one of the major criteria for evaluating any method.

The function like Dice Similarity coefficient (DSC), Jaccard coefficient (JC) or Tanimoto index, Overall accuracy (OA), Kappa coefficient (κ), Peak signal to noise ratio (PSNR), Signal to noise ratio (SNR), Root mean square error (RMSE), Standard Deviation (STD), Segmentation

Table 14 Segmentation applications

Medical images	Satellite images	Other images application
Segmenting brain image into GM, WM, CSF from MRI [256, 259]	To segment road, building, vegetation, tree, water, and land area	From forest environments Stereovision matching in hemispherical images
Multiple tumor region from CT images	Texture image segmentation	Document page segmentation
Suspect nodules from CT images	Urban information from VHSR images	Synthetic image segmentation
Retinal vessel segmentation	Automated dark-spot detection	Text graphics segmentation
Masses of region of interest from mammographic images	Classification of oil spills	Infrared ship image segmentation
Leukocytes in blood smear images	Sea ice concentration segmentation	Geographic map images
Lip image segmentation	Sea land segmentation	Underwater image segmentation
Liver image segmentation	Flood area classification	Identification of TCFA in VH-IVUS image
Segmentation of knee images into blood vessels of interest	Terrain classification	M-FISH segmentation
Endorrhachis from MRI		Color image segmentation [253, 271]
Rapid void detection from X-ray images		Carbon nanotube images segmentation
Thyroid detection from CT images		Objects from complex real world scenes [270]
Tissue identification from wound images		Leaf veins extraction
To segment glands		Visual analytics for categorization of handwritten digits [257]
Fingerprint detection		Identification of 3D objects such as chair, tables etc.
Skin lesion segmentation		Road and indoor scenes
ECG heart beat classification		Gesture segmentation
Pancreas segmentation from CT images		Human activity, Human face classification [263]
Breast cancer diagnosis from MRI		Drone classification
		Plankton classification
		Counting objects such as apple and oranges from real world scene
		Ship detection in space borne images
		Driving postures segmentation
		Vehicle type, Vehicular plate [258, 266, 272] classification

Table 15 Evaluation parameters

Reference	Evaluation parameters	Mathematical equation	Description
[11, 47, 64, 70, 89, 98, 101, 108, 113, 122, 134, 158, 166–168, 170–172, 235–238]	Dice index or Dice Similarity coefficient (DSC)	$D(R,S) = \frac{2\lvert R \cap S\rvert}{\lvert R\rvert + \lvert S\rvert}$	Provides a measure of degree of overlap between two segmentation, if R and S are images where R = segmenting contour and S = ground truth resulted from manual segmentation, if DSC = 1 perfect match, DSC = 0 no match
[62, 64, 68, 70, 104, 107, 108, 120, 122, 127, 128, 134, 144, 158, 172, 189, 199, 201, 236, 237, 239]	Jaccard similarity (JS) or Jaccard coefficient (JC) or Tanimoto index	$J(R,S) = \frac{\lvert R \cap S\rvert}{\lvert R \cup S\rvert}$	Used to compare similarity and diversity of image, where R = segmented image, S = ground truth, a higher JS better segmentation
[70, 74, 75, 199, 213, 262, 266, 274]	Overall accuracy (OA)	$OA = \sum_{i=1}^{M} P_{ii}$	Higher OA better segmentation
[55, 70, 74, 75, 115, 121, 137, 154, 175, 201, 214]	Kappa coefficient (κ)	$\kappa = \frac{(OA - EA)}{1 - EA}$ where, $EA = \sum_{i=1}^{M} P_{i+} P_{+i}$	Higher Kappa better segmentation
[100, 108, 119, 142, 160, 184, 216]	Peak signal to noise ratio (PSNR)	$PSNR(i,j) = 20\log_{10}\left(255/RMSE(i,j)\right)$	Higher PSNR better segmentation, or the PSNR is used to compare the similarity of segmented image against original image depending on the MSE for each pixel
[11, 41, 105, 143, 188, 229, 237]	Root mean square error (RMSE)	$RMSE = \sqrt{\frac{\sum_{i=1}^{ro}\sum_{j=1}^{co}\left(I_o^c(i,j) - I_{th}^c(i,j)\right)}{ro \times co}}$	Where I_o^c is the original image, I_{th}^c is the segmented image, c depends on the image (RGB or gray scale) and ro, co are the total number of rows and columns of the image, respectively
[57, 115]	Signal to noise ratio (SNR)	$SNR = 10\log\left[\frac{\sum_{x\in\Omega} I_x^2}{\sum_{x\in\Omega}(I_x - N_x)^2}\right]$	I_x and N_x represent the grey intensity of pixel x between the reference besides test image, higher SNR better segmentation
[119, 240, 265, 277]	Standard Deviation (STD)	$STD = \sqrt{\sum_{i=1}^{Max_iter} \frac{(\theta_i - \epsilon)^2}{Max_iter}}$	If the STD value increases the algorithms becomes more instable
[43, 118, 217, 222, 241]	Probability Rand Index (PRI)	$PRI(Z_{test}, Z) = \frac{2}{N(N-1)}\sum_{f,g}\alpha_{f,g}\beta_{f,g} + (1 - \alpha_{f,g})(1 - \beta_{f,g})$	PRI measures the agreement of the computed segmentation result with the ground truth, where Z = true image, Z_{test} is segmented result, f ≠ g, N(N−1) is unique pixel pairs out of total N data points, $\alpha_{f,g}$ refers to situation where identical label exists in Z_{test}, $\beta_{f,g}$ refers to probability where identical label in Z, when PRI = 0 and PRI = 1 referred to no and total similarity between Z_{test} and Z
[44, 49, 53, 56, 86, 94, 107, 130, 134, 135, 141, 153, 174, 182, 185–187, 214, 225, 230, 242–244]	Segmentation accuracy (SA)	$SA = \sum_{k=1}^{K} \frac{A_k \cap C_k}{\sum_{i=1}^{K} C_i}$	Where K = no. of cluster, A_k = pixel belonging to the *k-th* cluster, c_k = the pixels in the *k-th* cluster for ground u_{ik} = membership value of pixel i belonging to *k-th* cluster, N is the number of total pixel the best clustering result is achieved when SA = 1
[52, 57, 66, 99, 116, 128, 131, 233, 264]	Misclassification Error (ME)	$ME = 1 - \frac{\lvert B_O \cap B_T\rvert + \lvert F_O \cap F_T\rvert}{\lvert B_O\rvert + \lvert F_O\rvert}$	Where B_O and F_O = no. of background and desired area pixels of the main image, BT and FT are the no. of background and desired area pixels of the image computed by algorithm, 0 is best classification and 1 is enormous classification
[202, 219]	Uniformity Measure (U)	$U = 1 - 2(k-1)\frac{\sum_{j=0}^{k-1}\sum_{i\in R_{ji}}(f_i - m_j)^2}{N(f_{max} - f_{min})^2}$	Where (k−1) is number of threshold R = segmented region j, f_i = grey level of pixel I m_j = mean of the grey levels of those pixels in segmented region j, N = no. of total pixel in given image, f_{max} = maximal grey level of pixels in the given image, f_{min} = minimal grey level of pixels in the given image, U value lies between 0 and 1 a higher value a better segmentation
[52, 66]	Regional area error (RAE)	$RAE = \begin{cases} \frac{A_O - A_T}{A_O} if A_T < A_O \\ \frac{A_T - A_O}{A_T} if A_T \geq A_O \end{cases}$	Computing accuracy of the desired region area measurement, AO = area of the desired region in image, AT = area of the desired region after application of the algorithm. RAE will be equal to zero is best state of segmentation

Table 15 (continued)

Reference	Evaluation parameters	Mathematical equation	Description
[3, 49, 53, 63, 130, 134]	Validation evaluation partition coefficient (V_{pc})	$V_{pc} = \sum_{k=1}^{K}\sum_{i=1}^{N}\frac{u_{ik}^2}{N}$	Where u_{ik} is the membership value of pixel i belonging to the k-th cluster, K is the number of clusters and N is the total number of image pixels, When Vpc is high and Vpe is low, it implies the membership values are less fuzzy in segmentation results and the tissues are classified correctly or when $V_{pc} = 1$ and $V_{pe} = 0$
[3, 49, 53, 63, 130, 134]	Validation evaluation partition entropy (V_{pe})	$V_{pe} = -\sum_{k=1}^{K}\sum_{i=1}^{N}\frac{u_{ik}\log(u_{ik})}{N}$	
[40, 139, 140, 158, 161, 275]	Segmentation quality F(I) function	$F(I) = \sqrt{M}\times\sum_{j=1}^{M}\frac{e_j^2}{\sqrt{N_j}}$	I is an image and N is the total pixels in I. Cj denotes the set of pixels in region j, whereas Nj = |Cj| denotes the number of pixels in Cj. The value of ej, which represents homogeneity within a region, is defined as the Euclidean distance between the RGB color vectors of the pixels of region j and the color vector attributed to region j in the segmented image. Finally, S(a) denotes the number of regions in image I that has an area of exactly a and MaxArea denotes the largest region in the segmented image. Although the three formulae differ, these functions are used to penalize the segmentation that form too many regions and have non-homogeneous regions by giving them larger values. The smaller value of three function indicates the better segmentation result
[40, 139, 140, 158, 161]	F'(I) function	$F'(I) = \frac{\sum_{j=1}^{M} e_j^2\sqrt{\sum_{a=1}^{MaxArea}[S(a)]^{1+(\frac{1}{a})}}}{(1000\times N)\sqrt{N_j}}$	
[8, 40, 139, 140, 158, 161, 271]	Q(I) function	$Q(I) = \frac{1}{1000\times N}\sqrt{M}\sum_{j=1}^{M}\left[\frac{e_j^2}{1+logN_j} + (S(N_j)/N_j)^2\right]$	
[46, 51, 70–72, 78, 93, 98, 108, 114, 122, 137, 144, 146, 148, 157, 168, 169, 172, 174, 175, 177, 201, 205, 208, 237, 245–247]	Specificity (σ) or True negative ratio (TNR)	$= \frac{TN}{TN+FP}$	TP = True Positive is the exact classification FP = False positive is misclassification or misidentification FN = False Negative is region undetected or misclassified TN = True Negative Specificity defines the competence of an algorithm to segment the normal regions present in the input image also termed as false alarm rate, FAR = 0 better segmentation OF or sensitivity values refer to the proper classification or segmentation of the input image or Sensitivity is also termed as object recognition rate SI defines the identical value among the segmented image and input image, higher SI better results Accuracy also termed as segmentation accuracy is an evaluation parameter used to assess the efficacy of the segmentation algorithm ROC is a graph which renders the relationship between TPR and FPR along with the varying threshold or cut-off limits for a classifier, it shows that TPR cannot increase without an increasing FPR EF denotes the number of voxels falsely detected as tumor region
[8, 46, 47, 51, 64, 70–72, 76–78, 84, 93, 95, 98, 108, 114, 115, 120, 122, 130, 137, 144, 146, 148, 157, 164, 166, 168, 171, 177, 181, 194, 201, 205, 207, 208, 230, 235, 237, 238, 245, 246, 248, 260]	Sensitivity or Recall or Overlap Function (OF)	$Sensitivity\,or\,OF = \frac{TP}{TP+FN}$	
[247]	Similarity Index (SI)	$SI = \frac{2\times TP}{2\times TP+FP+FN}$	
[8, 46, 51, 64, 71, 72, 74–76, 88, 93, 95, 108, 115, 137, 143, 146, 148, 157, 172, 177, 183, 193, 196, 208, 237, 245, 247–249, 268]	Accuracy (ρ)	$\frac{TP+TN}{TP+TN+FP+FN}$	
[46]	Negative predictive ratio (NPV)	$\frac{TN}{TN+FN}$	
[46, 64, 70, 78, 147, 193, 195, 244, 250]	Region under curve (ROC)	Graph	
[108]	Extra Function (EF)	$EF = \frac{FP}{TP+FN}$	
[46, 47, 64, 76, 77, 84, 95, 120, 157, 164, 166, 171, 174, 177, 181, 193, 194, 207, 230, 235, 238, 246, 251, 252]	Positive predictive value (PPV) or Precision	$\frac{TP}{TP+FP}$	
[47, 64, 84, 115, 127, 129, 130, 183, 196, 250]	False positive rate (FPR)	$\frac{FP}{Total\,negative}$	
[114]	Balanced accuracy (BAC)	$\frac{Sensitivity+Specificity}{2}$	
[70, 164]	False acceptance rate (FAR)	$\frac{No.\,of\,false\,acceptances}{No.\,of\,identifcation\,task}$	High FAR, GAR higher accuracy with low FRR
[70]	False rejection rate (FRR)	$\frac{No.\,of\,false\,rejections}{No.\,of\,identifcation\,task}$	
[70]	Genuine acceptance rate (GAR)	$GAR = 1 - FRR$	
[78]	Segmentation error (SE)	$SE = P(R).P(S\|R) + P(S).P(R\|S)$	P(R) and P(B) probability object and background, P(S|R) is the probability of classifying background as object, P(R|S) is the probability of classifying object as background, SE = 0 accurate segmentation
[43, 76, 115, 120, 171, 174, 194, 252, 260]	F measure	$F_{measure} = \frac{2N_{TP}}{2N_{TP}+N_{FP}+N_{FN}}$	N = no. of pixels NTP = true positive, NTN = true negative, NFP = false positive, NFN = false negative, A_z indicates performance of system and its high rate indicates proportion of sensitivity and specificity and consequently high relative accuracy
[115, 175]	Area under the ROC curve (A_z)	$A_z = \frac{1}{N_{TP}N_{TN}}\sum_{v=1}^{N_{TP}}\sum_{nv=1}^{N_{TN}} I(N_{TP_v}, N_{TN_{nv}})$	

Table 15 (continued)

Reference	Evaluation parameters	Mathematical equation	Description
[45]	The Hausdorff distance	$HAU(I_C, I_{ref}) = \max\left(h(I_C, I_{ref}), h(I_{ref}, I_C)\right)$ where $h(I_c, I_{ref}) = max_{aeI_C}\left(min_{beI_{ref}}\|a-b\|\right)$	Measure the similarity between two images, the lower value the better segmentation
[45]	Local consistency error (LCE)	$LCE(R,V) = \frac{1}{A}\sum_s min\{E(s), E'(s)\}$	Where I is the image, V is the ground truth, R is the segmentation result of the method to evaluate, A is the number of pixels in the image with V_j as the region of the ground truth to which the pixels belongs and R_i as the region of the segmented image to which the pixel s belongs. This measure produces a real-valued output in the range of [0, 1] where 0 signifies no error and 1 signifies worst segmentation
[45]	Global consistency error (GCE)	$GCE(I,V) = \frac{1}{A}min\left\{\sum_s E(s), \sum_s E'(s)\right\}$ where, $E(s) = \frac{card\left(\frac{V_j}{R_i}\right)}{card(V_j)}$ $E'(s) = \frac{card\left(\frac{R_i}{V_j}\right)}{card(R_i)}$	
[51]	Homogeneity index	$HOM = \sum_{i=0}^{n}\sum_{i=0}^{n}\frac{1}{1+(i-j)^2}h_c(i,j)$	NIR = Near-infrared spectral response where A_{Hull} and P_{Hull} are area and perimeter of the convex Hull polygon where A and P area and perimeter of the exterior border
[67]	Normalized difference vegetation index (NDVI)	$NDVI = NIR\text{-}R/NIR + R$	
[67]	Brightness index	$I_{br} = \frac{1}{6}(B + V + 2R + 2NIR)$	
[67]	Compactness index	$I_{compactness} = \frac{4\pi A_{Hull}}{P_{Hull}^2}$	
[67]	Convexity index	$I_{convexity} = \frac{A}{A_{Hull}}$	
[43, 217, 222, 241]	Variation of information (VoI)	$VoI(S_{test}, \{S_k\}) = \frac{1}{K}\sum_k [H(S_{test}) + H(S_k) - 2I(S_{test}, S_k)]$ where	H and I denote the entropy and mutual information
[126]	False negative volume fraction (FPVF)	$\frac{\lvert C_{gt} \cap C_O' \rvert}{\lvert C_{gt} \rvert} \times 100$	Here C_{gt}, represents the number of pixels in C_{gt} with value 1, and the complements of Co and C_{gt} are represented as C_o and C_{gt}', respectively. FNVF indicates the fraction of Cgt missed by the method and FPVF denotes the number of pixels falsely identified by the method, while TPVF denotes the number of pixels correctly identified by the method
[126]	True positive volume fraction (TPVF)	$\frac{\lvert C_O \cap gt \rvert}{\lvert C_{gt} \rvert} \times 100$	
[41]	Coefficient of Similarity	$1 + \frac{(GS \cap S)}{GS}$	Gold Standard (GS), S denotes the automated segmented image, less than 5% volume error is more likely suitable, Coefficient of similarity shows the resemblances between the segmented and gold standard images. Spatial overlap is the accurate measure of spatial properties of segmented images
[41]	Overall segmentation rate V	$\lvert S - (S \cap GS) \rvert$	
[41]	Spatial overlap	$\frac{2(GS \cap S)}{(S \cup GS)}$	
[41]	Volume error	$\frac{2(S-GS)}{(S+GS)}$	
[41, 136]	Under segmentation rate, U	$GS - (S \cap GS)$	
[104]	XOR	$\frac{Area(A \cup B) - Area(A \cap B)}{Area(A)}$	The lower XOR the better segmentation Area denotes the no. of pixel in binary image A(*I*)

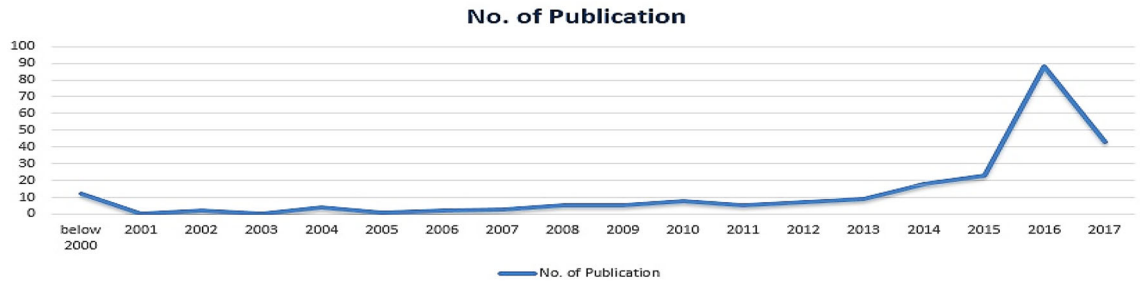

Fig. 10 Year wise development of SC techniques for image segmentation

accuracy (SA), Probability Rand Index (PRI), Misclassification Error (ME), Validation evaluation partition coefficient (V_{pc}), Validation evaluation partition entropy (V_{pe}), Specificity (σ) or True negative ratio (TNR), Sensitivity or Recall or Overlap Function (OF) or True positive ratio (TPR), Accuracy (ρ), Positive predictive value (PPV) or Precision, Region under curve (ROC), False positive rate (FPR) are the most common and most widely used recent evaluation functions which is being considered by number of authors for checking the segmentation performance. There are another validation functions has been used like also Segmentation quality F (I) function, F' (I) function, Q (I) function, Variation of information (VoI), F measure etc.

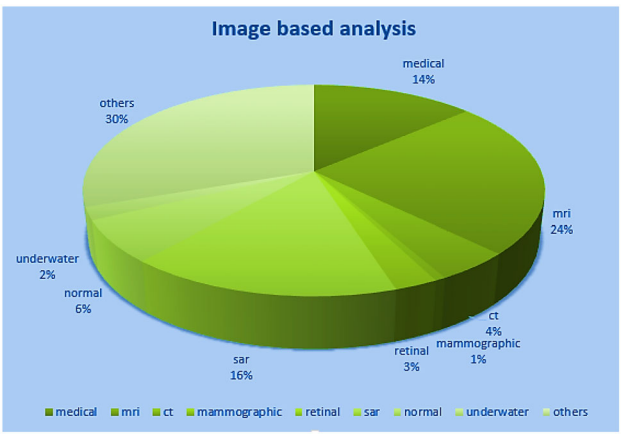

Fig. 11 Impact of SC techniques for segmentation on various categories

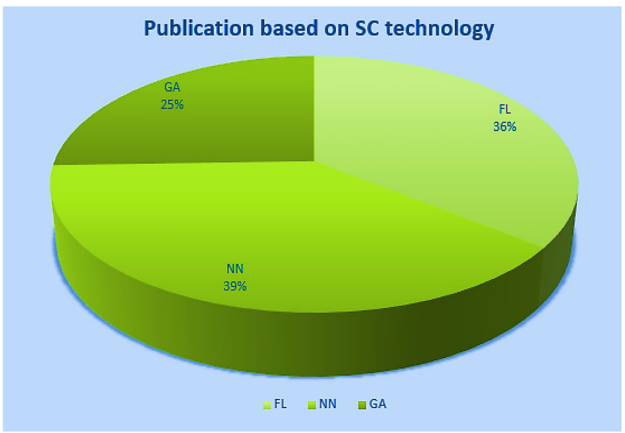

Fig. 12 Publications by SC techniques

6 Discussions

Survey on image segmentation using soft computing approaches are an extensive category of research area in artificial intelligence along with image processing. Category wise classification of SC based object extraction methodologies help in solving and understanding specific problems in numerous applications. Various soft computing methodologies have made it easier to solve typical problems of segmenting an image in faster way and authors are giving much more attention to use those process. From this review work it is clear that various SC developments were focused as author's research fields, expertise and problem domains were different. It is found that several authors are having common concept and methodologies along with common and different application fields. However, some authors work with hybrid techniques and methodologies. Designates that the inclination of expansion on approaches is also dissimilar due to author's research interests and abilities in the methodology and domain. This shows that the development of SC methodologies and domains is absorbed toward expertise orientation as the world is heading towards computational intelligence. There are many applications in image segmentation such as for medical diagnosis to segment tumor region, thyroid region from CT images, analysis of retinal blood vessels, tissues from MRI brain images etc., for SAR images to detect oil spills, ice concentration, flood analysis, land and water region etc.

In this review work, utmost of the articles of dissimilar categories are mainly retrieved from IEEE Xplore, Elsevier, and Springer online database. This paper has also

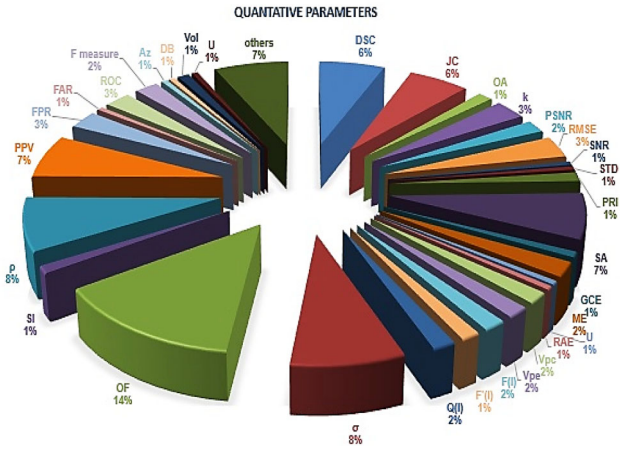

Fig. 13 Quantative parameters

Fig. 14 Resources utilization

gone through a number of conference proceedings from IEEE Xplore for the recent year only for investigating various methods and applications for image segmentation using SC. Figure 10 Shows year wise development of SC techniques for image segmentation. According to the collected articles from various online databases, journals and conference proceedings, it is seen that from the year 2010 onward researchers mainly focused on the SC techniques rather than conventional techniques for image segmentation. But from the year 2014 a lot of usages of SC techniques have been noticed especially in the year 2016 a tremendous work on image segmentation using SC approaches has been observed. From the year 2009 a new direction in the fuzzy logic filed was noticed with the application of soft computing technique and advanced learning algorithms. Authors were interested in the domain of medical system using fuzzy logic for identification of diseases, prediction and diagnosis. Based on the survey we can say that applications of neural network has been deployed for complex scene detection such as human activity identification, classification of hyperspectral data, classification of objects from real world scenes. Genetic algorithms have also shown promising results in the field of medical, SAR and other images. Though these SC techniques are sufficient enough to solve complex real world problems but from the year 2010 it has been observed that hybridization of SC techniques shown results more accurately and efficiently. In this review work we had try to enlighten the recent approaches of SC that is FCM for FL family, CNN or deep learning for NN family as well.

There are some applications under medical image segmentation such as MRI image subdivision, CT image subdivision, Mammographic image subdivision, Retinal image segmentation, Satellite or SAR image segmentation, Real complex or natural images segmentation, underwater image segmentation and others are all topic of different methodologies and applications. It can be stated that the applications are at the most important inclination of image segmentation focussing different problems. This may help development of segmentation methodologies and articles type toward problem domain orientation. Figure 11 shows the impact of segmentation techniques for image segmentation on different applications. About 24% of the work was carried on MRI images segmentation along with 16% for SAR images shows that this is the area of curiosity for number of authors.

A great deal of research was conceded on by using SC techniques for the purpose of subdividing an image into the regions of interest. As we have considered only the main methodologies of soft computing approaches that is FL, NN and GA, Fig. 12 shows the preference of the methodologies being adopted by the researchers. NN and FL are sharing approximately near number of publications of about 39 and 36% but NN does have higher preference than FL due to their adaptive nature to face the real world problems on the other hand GAs being used for about 25% which is less than the other two shows that it has been less chosen for performing image subdivision task.

There are numeral of evaluation parameters which are used by the researchers. Among them Dice similarity coefficient (DSC), Jaccard similarity (JS) or Tanimoto index, Signal to noise ratio, Segmentation accuracy, Mean square error, Standard deviation, Specificity, Sensitivity, Precision, Accuracy are some evaluation parameters which has been used most widely for the assessment of the proposed work. Figure 13 shows the frequency of them used.

There are enormous of frameworks containing wide-ranging image segmentation implementations. A probable

Table 16 Publication by journals

Journal name	Frequency	Percentage
IEEE Trans. on Visualization And Computer Graphics	1	0.43
IEEE Trans. on Pattern Analysis And Machine Intelligence	6	2.55
IEEE Geoscience and Remote Sensing Letters	6	2.55
IEEE Trans. on Biomedical Engineering	3	1.28
IEEE Trans. on Medical Imaging	18	7.66
IEEE Trans. on Geoscience And Remote Sensing	18	7.66
IEEE Trans. on Image Processing	7	2.98
IEEE Trans. on Information Forensics and Security	1	0.43
IEEE Signal Processing Letters	4	1.70
IEEE Journal of Biomedical and Health Informatics	2	0.85
IEEE Robotics and Automation Letters	2	0.85
IET Computer Vision	1	0.43
IEEE Trans. on Human–Machine Systems	1	0.43
IEEE Trans. on Intelligent Transportation Systems	1	0.43
IEEE Trans. on Components, Packaging and Manufacturing Technology	1	0.43
IEEE Trans. on Neural Networks and Learning Systems	1	0.43
IEEE Computational Intelligence Magazine	3	1.28
IEEE Journal of Selected Topics in Applied Earth Observations and Remote Sensing	4	1.70
IEEE Trans. on Neural Networks	4	1.70
IEEE Trans. on Information Technology in Biomedicine	3	1.28
IEEE Trans. on Fuzzy Systems	2	0.85
IEEE Trans. on Nuclear Science	3	1.28
IEEE Trans. on Circuits And Systems	1	0.43
IEEE Access	1	0.43
IEEE Trans. on Aerospace and Electronic Systems	1	0.43
IEEE Trans. on Cybernetics	2	0.85
IEEE Trans. on Systems, Man, and Cybernetics	4	1.70
IEEE Trans. on Evolutionary Computation	3	1.28
IET Biometrics	1	0.43
IEEE/ASME Trans. on Mechatronics	1	0.43
IET Image Processing	3	1.28
Applied Soft Computing	46	19.57
Medical Image Analysis	1	0.43
Pattern Recognition	7	2.98
Archives of Computation Methods in Engineering	1	0.43
Future Generation Computer Systems	1	0.43
Pattern Recognition Letters	3	1.28
Computer Methods and Programs in Biomedicine	4	1.70
Neurocomputing	3	1.28
Knowledge Based Systems	3	1.28
Alexandria Engineering Journal	1	0.43
ISPRS Journal of Photogrammetry and Remote Sensing	1	0.43
Journal of Visual Communication and Image Representation	2	0.85
Renewable and Sustainable Energy Reviews	1	0.43
Information Processing in Agriculture	1	0.43
Journal of Ocean Engineering and Science	1	0.43
Journal of Hydrology	1	0.43
Information Fusion	1	0.43

Table 16 (continued)

Journal name	Frequency	Percentage
Expert Systems with Applications	4	1.70
Computers and Electronics in Agriculture	1	0.43
Optik-International Journal for Light and Electron Optics	1	0.43
Computers and Electrical Engineering	1	0.43
Measurement	1	0.43
Computer Vision and Image Understanding	1	0.43
Image and Vision Computing	2	0.85
International Journal of Automation and Computing	1	0.43
Journal of medicinal system	1	0.43
Soft Computing	8	3.40
Solar Energy	1	0.43
Journal Of Computer Science and Technology	1	0.43
Automatic Control and Computer Sciences	1	0.43
Signal, Image and Video Processing	3	1.28
Artificial Intelligence Review	1	0.43
Egyptian Informatics Journal	1	0.43
Advanced Engineering Informatics	1	0.43
International Journal of Machine Learning and Cybernetics	1	0.43
Frontiers of Electrical and Electronic Engineering	1	0.43
IRBM	1	0.43
Multimedia Tools and Applications	1	0.43
Progress in Artificial Intelligence	1	0.43
Knowledge-Based Systems	3	1.28
IEEE Journal Of Selected Topics In Signal Processing	1	0.43
Journal of Central South University Technology	1	0.43
Electronics Letters	2	0.85
Medical and Biological Engineering and Computing	1	0.43
Neural Computation	2	0.85
Neural Processing Letter	1	0.43
Journal of Indian Society Remote Sensing	1	0.43
Total	234	100

researcher can select from proprietary software, open source libraries, and tool boxes in C/C++, JAVA, MATLAB, PYTHON or CUDA. Figure 14 shows the percentages of resources used for the simulation or implementation purpose. This part has been dominated by MATLAB tool with approx. 49%.

Classification of research work in number of years from most sited journals being listed in Table 16. As we have considered some conference papers our number of article for journals are listed for total of about 235. Out of them the journals which has mostly published this kind of work includes Applied Soft Computing with 46 articles and percentage share is about 19.57%, IEEE Transactions on Medical Imaging with 18 articles and percentage share is about 7.66%, IEEE Transactions on Geoscience and Remote Sensing 18 articles and percentage share 7.66%, Soft Computing with 8 articles and percentage share is about 3.40%, IEEE transactions on Image Processing, Pattern Recognition with 7 articles and percentage share 2.98%, IEEE Transactions on Pattern Analysis and Machine Intelligence, IEEE Geoscience and Remote Sensing Letters with 6 articles and percentage share 2.55%, IEEE Signal Processing Letters, IEEE Journal of Selected Topics in Applied Earth Observations and Remote Sensing, IEEE Transactions on Neural Networks, IEEE Transactions on Systems, Man, and Cybernetics, Computer Methods and Programs in Biomedicine, Expert Systems with Applications each with 4 articles and percentage share 1.70% and so on.

Table 17 Proposed future work

Ref no.	Future work
[2]	Incorporation of spatial and frequency feature, having spatial correlation between blocks/pixels, small object detection or working with detail preserving technique
[43]	Working with texture and edges in unsupervised manner to have accurate results
[8]	For hand segmentation
[113]	Automatic selection of seed pixels, working with several tumors, classifying them as benign or malignant for diagnosis
[119]	Enhancement on GWO algorithm
[54]	By adjusting cluster size can be applied to more images and videos for large scale problems and focusing aforementioned tissue
[62]	Various enhancement like improvement in objective function, intensity of noise in image can be used for choosing a radius, automatically selecting size of neighbour patch
[59]	Automatically finding number of clusters, working with multi-objective version of algorithm
[118]	Segmentation of forest and urban areas
[49]	To reduce computational time
[7]	Working with other datasets
[64]	To implement fuzzy thresholding to find initial contour
[70]	With different pattern extraction to increase the label of image classification
[11]	To segment brain MRI and tumor PET images, using multilevel set formation, processing more complex medical images
[50]	To work with satellite images
[51]	Accuracy can further be improved
[52]	Algorithm can be spatially utilized
[53]	Number of cluster to be known before-hand in CKS_FCM
[63]	Computational complexity and noise robustness
[65]	The recognition rates can further be improved
[46]	To combine statistical features with spectral and morphological features, designing deep neural network classifier
[127]	Can be used for other medical images for detection of tumor etc.
[41]	Can be tested on MR images
[66]	Improvement in computational intricacy
[55]	To remove time complexity and use it in some application
[107]	Can be applied for feature reduction which is needed in classification, content-based image retrievals etc.
[115]	Working with real-time 3D modelling of the retina vessels
[128]	Parameter choosing criteria is to be improved
[138]	Can be adopted in various fields of computer and information technology
[120]	Working with complex scenes by making approach automatic and finding out edges, texture, shapes and other features
[137]	In the direction of measuring the threat of TCFA and CaTCFA, degree of NC abutting in the lumen and positive remodelling index will be extracted from VH-IVUS images
[47]	This work can be tested on other databases
[56]	Work with the medical images and SAR images
[42]	Evolutionary algorithms can be implemented to improve the classification performance
[129]	Improvement in computational intricacy
[121]	Improvement in fitness function by using the extracted shape and edges of processed image or working with other effective fitness function like fuzzy cluster validity indexes
[130]	The improvement in membership function of the proposed algorithm can be done by using features like intensity inhomogeneity, spatial information
[108]	Results can further be improved in terms of evaluation criteria and time complexity. This proposed approach can be deployed in pre and post application for surgical assistance
[114]	To fragment tumors from different medicinal images
[44]	Introduction of kernel-induced distance and knowing cluster number
[57]	To solve drift of cluster centers, performance improvement in terms of time, parameter setting such as λ
[9]	Can be utilised for more nature and texture images
[131]	Working with different Heuristic functions and on different medical images

Table 17 (continued)

Ref no.	Future work
[132]	Governing the features of tumour such as thickness, size, type etc.
[45]	Adding spatial information to FEF
[67]	Working with spatial information, finding geometric specifications of objects, working with high spectral images
[61]	Can be applied to 3D object localization problem
[139]	Evaluating results with different algorithms as well as performing results with evaluation parameters like rand index, F-measure etc.
[68]	Robustness and computational complexity
[69]	Incorporation of preprocessing and post processing steps
[134]	Automatic selection of noise patches based on noise present and adaptive selection of parameters used in algorithm
[140]	Can be adopted for application where areas of concern is well-thought-out
[48]	Can be tested on medical images
[125]	HNN, simulated annealing like optimization techniques can be utilized
[116]	Accuracy can further be tested on SAR images
[40]	Improvement in processing time and other variant images
[109]	Working with spatial information and optimizing tools excluding NSGA-II
[142]	Incorporating GA, weight matrix for CNN and for fuzzy clustering a partition matrix
[3]	Accuracy can further be tested on SAR images
[110]	Working with low intensity dataset of CT images
[133]	Working with modifies FCM or introducing kernalized version of FCM
[123]	Introducing wavelet coefficient for safety measure avoiding misclassification and refining efficacy. Also working with other classification of headings, titles, pictures etc.
[126]	Thresholding precluding and introducing affinity components
[135]	Working with original FCM objective function by introducing some penalty terms
[117]	Computational efficiency can further be improved
[60]	Taking clusters of different shape and size
[112]	Segmentation of hippocampus and the cerebral sulcus
[58]	Markov random fields or atlas evidence with spatial information, also selecting their values randomly can improve efficiency, can be used for clinical study
[124]	Improvement in computational time
[85]	Working with RNN like deep network which cannot be a DAG
[180]	Learning of deep extraction approaches can be further improved
[171]	Case in point subdivision of further medical images
[166]	CT images or lungs cancer segmentation
[167]	CT images or lungs cancer segmentation
[189]	Working with multimodal approaches, in order to improve the effectiveness CRF or further innovative variants probabilistic model should be adopt like RNN, probably by means of long short-term memory
[92]	Subdivision of intense color, grey level images
[157]	Can work with different dataset
[71]	DNN for improving speed and scalability, can be used for MR images, can be also used in organ segmentation and statistical shape information
[72]	Gabor filter bank, Steerable filter bank can be used, Deep learning with NN, SVM, ELM like supervised learning methods can be used, can be adopted for Road network extraction in satellite images, vessel detection in medical images, river detection in satellite images and many more application
[74]	3 layer-CNN network with kernel size 4×4 or 5×5 for convolution layer, 2×2 kernel size for pooling for HSI FE, for enhancing mapping performance a post-classification processing
[82]	Working with other databases
[86]	By means of abandoning Doppler frequency of drone's frame extending classification of moving drones
[83]	The computational complexity of DCNNs should be carefully considered in applications that require real-time processing for achieving higher efficiency
[84]	Can be used for biomarker recognition errands as of volumetric medicinal information or other object extraction task

Table 17 (continued)

Ref no.	Future work
[75]	Adopting morphological profile, attribute profiles, and segmentation approaches for improving classification accuracy
[76]	Co-CNN architecture further can be extend for nonspecific image analysing jobs such as object semantic extraction
[88]	With Multi-GPU configuration implementation the computation time can be reduce and with combination of different CNN architectures can be used for a large-scale aerial data analysis
[89]	Can be tested for SAR images
[77]	Focus on learning RICNN model by embedding the rotation invariant regularizer into the objective function of the CNN model without introducing additional layers to improve the computational efficiency can be its future work
[78]	Working with more images
[79]	Working with ImageNet type datasets
[81]	Improvement in graphic cards, optimization techniques could improve in efficiency. A lot of work during different time of year as well as study is needed
[91]	A lot of work at pre-processing step like learning of shapes is needed
[178]	Image alterations can be encompassed, for further evaluation
[37]	By adopting cloud computing techniques so that the method could available to large scale images
[173]	In future, for improving speed and accuracy optimize the patch cropping and network structure
[174]	Modification of loss function so as to improve the performance
[193]	Making it a helping tool for radiologists for diagnosis ILDs by working with 3-D information delivered by CT volume scans along with assimilating the projected technique hooked on a CAD scheme
[172]	To other medical image segmentation tasks
[190]	Learning and training network with different classification of objects
[191]	We believe this method can generalize well to other similar dense output prediction tasks
[169]	Working with larger dataset in order to taring and improve the results
[194]	Proposed method also has the ability to find some text which is not annotated in the ground truth due to the power of all of the CNN networks used
[195]	Method is susceptible to errors in the human-generated labels one can minimize these errors by calibrating human-generated labels with ground truth per-tree fruit counts obtained after harvest. Methodology can be applied beyond precision agriculture to applications such as plant phenotyping (identifying as well as counting plants), phytopathology (identifying and monitoring visual disease symptoms), and even microbiology cell counting
[196]	Can be used for ship detection from multiple sensors, the resolution with higher resolution could be taken as this work is conducted on images with 5 m, the work can be extended to other remote sensing images as this work is carried out on panchromatic images
[184]	To cope with different up scaling factors proposed system can cope up with more filters, numerous trainings
[185]	Can be tested for other human activities recognition task
[177]	Hardware implementation of the proposed approach
[170]	Can be adopted for multi-organ classification
[186]	Results can be verified by working with images with difficult or mess up backgrounds
[158]	Working with SAR and MRI images
[98]	To improve efficiency by adding additional feature like prior knowledge, shape and models
[149]	Work can be done with variable block size
[94]	Space borne C-band SAR image segmentation can be performed by just making some changes in the parameters
[95]	Texture segmentation of an image can be performed by using proposed method
[147]	Used for Diabetic retinopathy detection in the initial stage
[143]	Implementing this work on mobile devices with the help of cloud computing
[154]	CBF based technique can be applied for urban area segmentation or other applications
[93]	Method can be utilized for segmentation of other types of CT image thyroid volume
[148]	Can be applied on tissue identification on skin tumor images or burn wound
[160]	Applying this approach to sequences of image for edge detection
[161]	Color images subdivision
[150]	SA is to be improved for the proposed work
[99]	Thoroughly investigation and comparison with other algorithms and segmentation
[163]	Based on the extracted veins the leaf vein pattern recognition

Table 17 (continued)

Ref no.	Future work
[96]	A bigger database by big enough window size
[162]	Real-life images on validity and convergence of the segmentation
[97]	The boundary geometries of the objects in the image and the optimal values for and grounded on the intensity PDF for the image can be determined, development of digital and optical hardware and for processing multispectral and time varying images multilayer PCNN's and PCNN's can be developed
[155]	A hierarchical model in the CNN architecture and implementation on real VLSI CNN chips
[165]	Automatic segmentation needed as this method requires the radiologist
[151]	For real-time applications has great potential in parallel implementation
[152]	Same approach can be applied in other applications and with modifications images with different sizes can be taken and iterative and parallel computing making
[213]	In Future, this work can be continued towards finding the optimal path. Furthermore, discriminating simple limbs (impedance) and troublesome damaged trees needs further works and could improve this study. Moreover, wind may scatter dust on the road surface which can be misidentified as obstacles. In other words, using 'Lidar' data will increase the reliability of this algorithm
[205]	Can be used for different image with despeckling filter
[100]	Working with different entropies and large dataset of actual world images
[103]	Computational cost and time
[214]	Can be extend for other flooded areas detection
[207]	Using more advanced algorithms
[101]	Can be used in planning of radiation therapy observation and patient dominant models can also be developed
[216]	Working with different entropies and large dataset of actual world images
[208]	Working with several classifiers like Naive Bayes along with ANN for medical judgement. Multiphase classification of actual world images and working with several EA incorporating swarm optimizing method
[215]	The future research can be to examine different forms of fitness functions, in an attempt to represent more efficiently the spectral similarity between Objects. A final observed drawback of the method lies on the semi supervised case, where the classification results are clearly inferior to those obtained under the supervised mode
[105]	Working with BSFs such as polygonal shapes along with considering more effective methods
[217]	Summing up the features like texture, geometrical by means of color feature to increases the efficiency
[206]	Working with curvelet and shearlet transforms to improve the efficiency and investigation of false positive reduction algorithms evaluated by means of FROC curves
[221]	Can be extended to grammatical arrangement acknowledgement task by adopting top-down approach for object recognition
[204]	Parallelization taking place graphics card units and improvement in calculation of neighbourhood filters
[202]	Thresholding criteria should be enhanced for improving performance
[229]	Representation of chromosomes can be made flexible, working with rotating rectangles or similar methods
[230]	Collaborating FPGA (field programmable gate array) with classification algorithm to increase in efficiency
[198]	Working with 3D images
[104]	Improvement in cluster legitimacy indices for Dermoscopy images
[222]	Working with multifaceted texture properties in order to improve accuracy
[199]	Working with PET-CT images
[218]	Using several image devices, color representations, different GA parameters
[227]	To accept multiple images by FCM-HDGA
[231]	The proposed method can be hybridize with soft computing approaches like NN, FL etc.
[225]	Can work with non-texture images by using the proposed approach
[211]	Introducing FCM or other alike methods and evaluating it with SAR images
[232]	Initialization problem and working with large dataset
[219]	Working with complex images
[200]	Parallel implementation
[212]	Unsupervised approach segmentation and making it feasible to detect long and continuous roads
[233]	With the improvement on operators and parameter tuning, can improve segmentation quality and performance in time
[224]	Computational efficiency and working with natural images

Fig. 15 Images of plant leaf

7 Future Work

A lot of emphasis has been to be made by the researchers for selecting their area of interest for conducting their research work. Our aim in this portion is to present some of the future work, as suggested by the authors and also which has been excerpt while doing this review work. As we have gone through number of papers for reviewing, we will try to discuss the interesting areas of application which can be explored in future. Interesting domains like geographic map images in order to identify geographic regions, underwater images for underwater species or other objects like boats or ships etc. floods and other type of natural disasters in order to evaluation of the damage, segmentation of fruits from the tree from real world images, Stereovision matching in hemispherical from Forest environment images, classification of objects from drone images of natural scenes, recognition of sign boards or other road scenes objects etc. are some topics in which one can explore further research. Moreover in Table 17 we are presenting future work for the various articles.

8 Proposed Work

In our proposed work we are willing to work on agricultural images for identification and evaluation of various regions of interest. The main objectives of proposed our work are as follows

1. Performing image segmentation using some soft computing along with optimization approach.
2. Diversification of the proposed work to the area including agriculture, cultivation, plantation.
3. Predetermination of the crop utilization based on the perilous climatic conditions that deleterious the vegetation.
4. Medical capabilities enhanced delivering the desired results naturally.
5. Comparison of the existing techniques with the algorithm proposed highlighting the manner in which it superimposes the existing ones using evaluation parameters like Sensitivity, Specificity, Precision, Accuracy etc.

Expected significance

1. Predicts the crop cultivation failure due to untoward rainfall.
2. Apply the delineated algorithm on the other fields apart from crops and vegetation.
3. The assessment of the products related to the quality can be achieved.
4. The cost of the products can be determined with greater accuracy.
5. The utilization of the product leading to its reliability for masses.
6. Metric formation using parameters related to product such as durability, future needs, quality assurance, etc.
7. Farmer's cognizance regarding the fertilizers to be adopted.
8. Succour the actual cost leading to the confirmation of the pay per quality leading to define appropriate cost.

Some of the images of plant leaf are shown in Fig. 15.

9 Conclusion

This article presents a number of SC approaches and their utilizations in segmentation. The motivation behind soft computing is to simulate human style of decision making and reasoning. The interest of researchers is to use SC methodologies for image segmentation from complex applications, which are capable of handling uncertainty and imprecision due to which the intelligent system gets flexibility and adaptability. SC with its capability for handling real life ambiguous situations with flexibility serves the need for making a system intelligent which could think like human. This in fact can overcome the insufficiencies of the conventional approaches that are based on traditional and statistical models for solving problems. Information which are ambiguous, inaccurate and imperfect during the decision making procedure, SC approaches can even processes them. SC methodologies do have some pros and cons and no such guarantee is provided by for an application oriented domain to apply specific SC method to generate results. Surely by noticing the recent trends hybridization, metaheuristic, deformable models are improving performance of SC and even in the future hybridizing such techniques can be adopted to understand the thinking power alike human.

Compliance with Ethical Standards

Conflict of interest On behalf of all authors, the corresponding author states that there is no conflict of interest.

References

1. Mesejo P, Ibanez O, Cordon O, Cagnoni S (2016) A survey on image segmentation using metaheuristic-based deformable models: state of the art and critical analysis. Appl Soft Comput 44:1–29. https://doi.org/10.1016/j.asoc.2016.03.004
2. Choy SK, Lam SY, Yu KW, Lee WY, Leung KT (2017) Fuzzy model-based clustering and its application in image segmentation. Pattern Recogn 68:141–157. https://doi.org/10.1016/j.patcog.2017.03.009
3. Li Y-l, Shen Y (2014) An automatic fuzzy c-means algorithm for image segmentation. Soft Comput 14:123–128. https://doi.org/10.1007/s00500-009-0442-0
4. Jiao L et al (2010) Natural and remote sensing image segmentation using memetic computing. IEEE Comput Intell Mag 5:78–91. https://doi.org/10.1109/MCI.2010.936307
5. Jothi JAA, Rajam VMA (2017) A survey on automated cancer diagnosis from histopathology images. Artif Intell Rev 48:31–81. https://doi.org/10.1007/s10462-016-9494-6
6. Martin D, Fowlkes C, Tal D, Malik J (2001) A database of human segmented natural images and its application to evaluating segmentation algorithms and measuring ecological statistics. In: Proceedings of 8th international conference on computer vision, vol 2, pp 416–423
7. Zhao Q-H, Li X-L, Li Y, Zhao X-M (2017) A fuzzy clustering image segmentation algorithm based on hidden Markov random field models and Voronoi tessellation. Pattern Recogn Lett 85:49–55. https://doi.org/10.1016/j.patrec.2016.11.019
8. Aghajaria E, Chandrashekhar GD (2017) Self-organizing map based extended fuzzy C-means (SEEFC) algorithm for image segmentation. Appl Soft Comput 54:347–363. https://doi.org/10.1016/j.asoc.2017.01.003
9. Borges VR et al (2015) An iterative fuzzy region competition algorithm for multiphase image segmentation. Soft Comput 19:339–351. https://doi.org/10.1007/s00500-014-1256-2l
10. Bhaumik H, Bhattacharyya S, Nath MD, Chakraborty S (2016) Hybrid soft computing approaches to content based video retrieval: a brief review. Appl Soft Comput 46:1008–1029. https://doi.org/10.1016/j.asoc.2016.03.022
11. Jiang X-L, Wangb Q, He B, Chen S-J, Li B-L (2016) Robust level set image segmentation algorithm using local correntropy-based fuzzy c-means clustering with spatial constraints. Neurocomputing 207:22–35. https://doi.org/10.1016/j.neucom.2016.03.046
12. Ibrahim D (2016) An overview of soft computing. In: 12th international conference on application of fuzzy systems and soft computing, ICAFS 2016, Vienna, Austria, Procedia Comput Sci, vol 102, pp 34–38, 29–30. https://doi.org/10.1016/j.procs.2016.09.366
13. Yardimci A (2009) Soft computing in medicine. Appl Soft Comput 9:1029–1043. https://doi.org/10.1016/j.asoc.2009.02.003
14. Huang Y et al (2010) Development of soft computing and applications in agricultural and biological engineering. Comput Electron Agric 71(2):107–127. https://doi.org/10.1016/j.compag.2010.01.001
15. Agrawal S, Panda R, Dora L (2014) A study on fuzzy clustering for magnetic resonance brain image segmentation using soft computing approaches. Appl Soft Comput 24:522–533. https://doi.org/10.1016/j.asoc.2014.08.011
16. Indragandhi V, Subramaniyaswamy V, Logesh R (2017) Resources, configurations, and soft computing techniques for power management and control of PV/wind hybrid system. Renew Sustain Energy Rev 69:129–143. https://doi.org/10.1016/j.rser.2016.11.209
17. Singh V, Mishra AK (2017) Detection of plant leaf diseases using image segmentation and soft computing techniques. Inf Process Agric 4(1):41–49. https://doi.org/10.1016/j.inpa.2016.10.005
18. Dwarakish GS, Nithyapriya B (2016) Application of soft computing techniques in coastal study—a review. J Ocean Eng Sci 1(4):247–255. https://doi.org/10.1016/j.joes.2016.06.004
19. Chang F-J, Chang L-C, Huang C-W, Kao I-F (2016) Prediction of monthly regional groundwater levels through hybrid soft-computing techniques. J Hydrol 541:965–976. https://doi.org/10.1016/j.jhydrol.2016.08.006
20. Poria S et al (2017) A review of affective computing: from unimodal analysis to multimodal fusion. Inf Fusion 37:98–125. https://doi.org/10.1016/j.inffus.2017.02.003
21. Francis J, Anto Sahaya Dhas D, Anoop BK (2016) Identification of leaf diseases in pepper plants using soft computing techniques. In: 2016 conference on emerging devices and smart systems (ICEDSS), pp 168–173. https://doi.org/10.1109/icedss.2016.7587787
22. Sabzi S et al (2017) The use of soft computing to classification of some weeds based on video processing. Appl Soft Comput 56:107–123. https://doi.org/10.1016/j.asoc.2017.03.006
23. Kateriya B, Tiwari R (2016) River water quality analysis and treatment using soft computing technique: a survey. In: 2016 international conference on computer communication and

informatics (ICCCI), Coimbatore, India, pp 1–6. https://doi.org/10.1109/iccci.2016.7479942
24. Mojumder JC et al (2017) The intelligent forecasting of the performances in PV/T collectors based on soft computing method. Renew Sustain Energy Rev. https://doi.org/10.1016/j.rser.2016.11.225
25. Hiziroglu AK (2013) Soft computing applications in customer segmentation: state-of-art review and critique. Expert Syst Appl 40:6491–6507. https://doi.org/10.1016/j.eswa.2013.05.052
26. Waldchen J, Mader P (2017) Plant species identification using computer vision techniques: a systematic literature review. Arch Comput Methods Eng. https://doi.org/10.1007/s11831-016-9206-z
27. Balamurugan M et al (2017) Application of soft computing methods for grid connected PV system: a technological and status review. Renew Sustain Energy Rev. https://doi.org/10.1016/j.rser.2016.11.210
28. Riomoros I, Guijarro M, Pajares G et al (2010) Automatic image segmentation of greenness in crop fields. In: 2010 international conference of soft computing and pattern recognition, pp 462–467. https://doi.org/10.1109/socpar.2010.5685936
29. Ko M, Tiwari A, Mehnen J (2010) A review of soft computing applications in supply chain management. Appl Soft Comput 10(3):661–674. https://doi.org/10.1016/j.asoc.2009.09.004
30. Dileep G, Singh SN (2017) Application of soft computing techniques for maximum power point tracking of SPV system. Sol Energy 141:182–202. https://doi.org/10.1016/j.solener.2016.11.034
31. Saridakis KM, Dentsoras AJ (2008) Soft computing in engineering design—a review. Adv Eng Inform 22:202–221. https://doi.org/10.1016/j.aei.2007.10.001
32. Kamiya A, Ovaska SJ, Roy R, Kobayashi S (2005) Fusion of soft computing and hard computing for large-scale plants: a general model. Appl Soft Comput 5(3):265–279. https://doi.org/10.1016/j.asoc.2004.08.005
33. Chen Y et al (2016) Non-local-based spatially constrained hierarchical fuzzy C-means method for brain magnetic resonance imaging segmentation. IET Image Proc. https://doi.org/10.1049/iet-ipr.2016.0271
34. Liu G et al (2015) Incorporating adaptive local information into fuzzy clustering for image segmentation. IEEE Trans Image Process 24(11):3990–4000
35. Chiranjeevi P et al (2014) Neighborhood supported model level fuzzy aggregation for moving object segmentation. IEEE Trans Image Process 23(2):645–657
36. Zhou H et al (2009) Anisotropic mean shift based fuzzy C-means segmentation of dermoscopy images. IEEE J Sel Topics Signal Process 3(1):26–34. https://doi.org/10.1109/JSTSP.2008.2010631
37. Xing F et al (2016) An automatic learning-based framework for robust nucleus segmentation. IEEE Trans Med Imaging. https://doi.org/10.1109/TMI.2015.2481436
38. Shrivastavaa S, Singh MP (2011) Performance evaluation of feed-forward neural network with soft computing techniques for hand written English alphabets. Appl Soft Comput 11:1156–1182. https://doi.org/10.1016/j.asoc.2010.02.015
39. Badura P, Pietka E (2014) Soft computing approach to 3D lung nodule segmentation in CT. Comput Biol Med 53:230–243. https://doi.org/10.1016/j.compbiomed.2014.08.005
40. Sulaiman SN, Isa NAM (2010) Adaptive fuzzy-K-means clustering algorithm for image segmentation. IEEE Trans Consum Electron. https://doi.org/10.1109/TCE.2010.5681154
41. Nithila EE, Kumar SS (2016) Segmentation of lung nodule in CT data using active contour model and fuzzy C-mean clustering. Alex Eng J 55:2583–2588
42. Simhachalam B, Ganesan G (2016) Performance comparison of fuzzy and non-fuzzy classification methods. Egypt Inform J 2016(17):183–188. https://doi.org/10.1016/j.eij.2015.10.004
43. Yin S, Qian Y, Gong M (2017) Unsupervised hierarchical image segmentation through fuzzy entropy maximization. Pattern Recogn 68:245–269. https://doi.org/10.1016/j.patcog.2017.03.012
44. Ji J, Wang K-L (2014) A robust nonlocal fuzzy clustering algorithm with between-cluster separation measure for SAR image segmentation. IEEE J Sel Top Appl Earth Obs Remote Sens 7(12):4929–4936. https://doi.org/10.1109/JSTARS.2014.2308531
45. Balla-Arabe S, Gao X, Wang B (2013) A fast and robust level set method for image segmentation using fuzzy clustering and lattice Boltzmann method. IEEE Trans Cybern 43(3):910–920. https://doi.org/10.1109/TSMCB.2012.2218233
46. Barkana BD, Saricicek I, Yildirim B (2017) Performance analysis of descriptive statistical features in retinal vessel segmentation via fuzzy logic, ANN, SVM, and classifier fusion. Knowl Based Syst 118:165–176. https://doi.org/10.1016/j.knosys.2016.11.022
47. Ananthi VP, Balasubramaniam P, Kalaiselvi T (2016) A new fuzzy clustering algorithm for the segmentation of brain tumor. Soft Comput 20:4859–4879. https://doi.org/10.1007/s00500-015-1775-5
48. Choy SK (2011) Image segmentation using fuzzy region competition and spatial/frequency information. IEEE Trans Image Process 20(6):1473–1484. https://doi.org/10.1109/TIP.2010.2095023
49. Deng W-Q, Li X-M, Gao X, Zhang C-M (2016) A modified fuzzy C-means algorithm for brain MR image segmentation and bias field correction. J Comput Sci Technol 31(3):501–511. https://doi.org/10.1007/s11390-016-1643-5
50. Bose A, Mali K (2016) Fuzzy-based artificial bee colony optimization for gray image segmentation. Signal Image Video Process 10:109–1096. https://doi.org/10.1007/s11760-016-0863-z
51. Manikandan T, Bharathi N (2016) Lung cancer detection using fuzzy auto-seed cluster means morphological segmentation and SVM classifier. J Med Syst 40(7):1–9. https://doi.org/10.1007/s10916-016-0539-9
52. Bakhshali MA (2016) Segmentation and enhancement of brain MR images using fuzzy clustering based on information theory. Soft Comput. https://doi.org/10.1007/s00500-016-2210-2
53. Shang R et al (2016) A spatial fuzzy clustering algorithm with kernel metric based on immune clone for SAR image segmentation. IEEE J Sel Top Appl Earth Obs Remote Sens 9(4):1640–1652. https://doi.org/10.1109/JSTARS.2016.2516014
54. Li X, Zhang F, Ouyang X, Khan SU (2016) MapReduce-based fast fuzzy c-means algorithm for large-scale underwater image segmentation. Future Gener Comput Syst 65:90–101. https://doi.org/10.1016/j.future.2016.03.004
55. Zhang M et al (2016) Multi-objective evolutionary fuzzy clustering for image segmentation with MOEA/D. Appl Soft Comput 48(C):621–637. https://doi.org/10.1016/j.asoc.2016.07.051
56. Zhang X et al (2017) An improved fuzzy algorithm for image segmentation using peak detection, spatial information and reallocation. Soft Comput 21:2165–2173. https://doi.org/10.1007/s00500-015-1920-1
57. Zhou D, Zhou H (2015) A modified strategy of fuzzy clustering algorithm for image Segmentation. Soft Comput 19:3261–3272. https://doi.org/10.1007/s00500-014-1481-8
58. Pham DL, Prince JL (1999) Adaptive fuzzy segmentation of magnetic resonance images. IEEE Trans Med Imaging 18(9):737–752. https://doi.org/10.1109/42.802752

59. Sarkara JP, Saha I, Maulik U (2016) Rough possibilistic type-2 fuzzy C-means clustering for MR brain image segmentation. Appl Soft Comput 46:527–536. https://doi.org/10.1016/j.asoc.2016.01.040
60. Zhang M, Hall LO, Goldgof DB (2002) A generic knowledge-guided image segmentation and labeling system using fuzzy clustering algorithms. IEEE Trans Syst Man Cybern Part B Cybern 32(5):571–582. https://doi.org/10.1109/TSMCB.2002.1033177
61. Chen G-C, Juang C-F (2013) Object detection using color entropies and a fuzzy classifier. IEEE Comput Intell Mag 8(1):33–45. https://doi.org/10.1109/MCI.2012.2228592
62. Chen Y et al (2016) An improved anisotropic hierarchical fuzzy c-means method based on multivariate student t-distribution for brain MRI segmentation. Pattern Recogn 60:778–792. https://doi.org/10.1016/j.patcog.2016.06.020
63. Gharieb RR, Gendy G, Abdelfattah A (2017) C-means clustering fuzzified by two membership relative entropy functions approach incorporating local data information for noisy image segmentation. SIViP 11(3):541–548. https://doi.org/10.1007/s11760-016-0992-4
64. Ananthi VP, Balasubramaniam P (2016) A new thresholding technique based on fuzzy set as an application to leukocyte nucleus segmentation. Comput Methods Programs Biomed 134(C):165–177. https://doi.org/10.1016/j.cmpb.2016.07.002
65. Hernandez-Matamoros A et al (2016) Facial expression recognition with automatic segmentation of face regions using a fuzzy based classification approach. Knowl-Based Syst 110:1–14. https://doi.org/10.1016/j.knosys.2016.07.011
66. Bai X et al (2016) Feature based fuzzy inference system for segmentation of low-contrast infrared ship images. Appl Soft Comput 46(C):128–142. https://doi.org/10.1016/j.asoc.2016.05.004
67. Sebari I, He D-C (2013) Automatic fuzzy object-based analysis of VHSR images for urban objects extraction. ISPRS J Photogramm Remote Sens 79:171–184. https://doi.org/10.1016/j.isprsjprs.2013.02.006
68. Ji Z, Xia Y et al (2012) Fuzzy local gaussian mixture model for brain MR image segmentation. IEEE Trans Inf Technol Biomed 16(3):339–347. https://doi.org/10.1109/TITB.2012.2185852
69. Cao H (2012) Segmentation of M-FISH images for improved classification of chromosomes with an adaptive fuzzy c-means clustering algorithm. IEEE Trans Fuzzy Syst 20(1):1–8. https://doi.org/10.1109/TFUZZ.2011.2160025
70. Priya RMS, Prabu S, Dharun VS (2016) F-SIFT and FUZZY-RVM based efficient multi-temporal image segmentation approach for remote sensing applications. Autom Control Comput Sci 50(3):151–164
71. Vorontsov E et al (2017) Metastatic liver tumour segmentation with a neural network-guided 3D deformable model. Med Biol Eng Comput 55:127–139. https://doi.org/10.1007/s11517-016-1495-8
72. Trujillo MCR et al (2017) Segmentation of carbon nanotube images through an artificial neural network. Soft Comput 21:611–625. https://doi.org/10.1007/s00500-016-2426-1
73. Liu W et al (2017) A survey of deep neural network architectures and their applications. Neurocomputing 234:11–26. https://doi.org/10.1016/j.neucom.2016.12.038
74. Chen Y et al (2016) Deep feature extraction and classification of hyperspectral images based on convolutional neural networks. IEEE Trans Geosci Remote Sens 54(10):6232–6251. https://doi.org/10.1109/TGRS.2016.2584107
75. Ghamisi P et al (2016) A self-improving convolution neural network for the classification of hyperspectral data. IEEE Geosci Remote Sens Lett 13(10):1537–1541. https://doi.org/10.1109/LGRS.2016.2595108
76. Liang X et al (2017) Human parsing with contextualized convolutional neural network. IEEE Trans Pattern Anal Mach Intell 39(1):115–127. https://doi.org/10.1109/TPAMI.2016.2537339
77. Cheng G et al (2016) Learning rotation-invariant convolutional neural networks for object detection in VHR optical remote sensing images. IEEE Trans Geosci Remote Sens 54(12):7405–7415. https://doi.org/10.1109/TGRS.2016.2601622
78. Tajbakhsh N et al (2016) Convolutional neural networks for medical image analysis: fine tuning or full training? IEEE Trans Med Imaging 35(5):1299–1312. https://doi.org/10.1109/TMI.2016.2535302
79. Py O et al (2016) Plankton classification with deep convolutional neural networks neural networks. In: 2016 IEEE information technology, networking, electronic and automation control conference, pp 132–136. https://doi.org/10.1109/itnec.2016.7560334
80. Papandreou G et al (2015) Weakly- and semi-supervised learning of a deep convolutional network for semantic image segmentation. In: 2015 IEEE international conference on computer vision (ICCV). https://doi.org/10.1109/iccv.2015.203
81. Wang L et al (2016) Sea ice concentration estimation during melt from dual-pol SAR scenes using deep convolutional neural networks: a case study. IEEE Trans Geosci Remote Sens 54(8):4524–4533. https://doi.org/10.1109/TGRS.2016.2543660
82. Ding J et al (2016) Convolutional neural network with data augmentation for SAR target recognition. IEEE Geosci Remote Sens Lett 13(3):364–368. https://doi.org/10.1109/LGRS.2015.2513754
83. Kim Y, Moon T (2016) Human detection and activity classification based on micro-doppler signatures using deep convolutional neural networks. IEEE Geosci Remote Sens Lett 13(1):8–12. https://doi.org/10.1109/LGRS.2015.2491329
84. Dou Q et al (2016) Automatic detection of cerebral microbleeds from MR images via 3D convolutional neural networks. IEEE Trans Med Imaging 35(5):1182–1195. https://doi.org/10.1109/TMI.2016.2528129
85. Liu M et al (2017) Towards better analysis of deep convolutional neural networks. IEEE Trans Vis Comput Gr 23(1):91–100. https://doi.org/10.1109/TVCG.2016.2598831
86. Kim BK et al (2017) Drone classification using convolutional neural networks with merged doppler images. IEEE Geosci Remote Sens Lett 14(1):38–42. https://doi.org/10.1109/LGRS.2016.2624820
87. Li X et al (2016) Deepsaliency: multi-task deep neural network model for salient object detection. IEEE Trans Image Process 25(8):3919–3930. https://doi.org/10.1109/TIP.2016.2579306
88. Sevo I, Avramovic A (2016) Convolutional neural network based automatic object detection on aerial images. IEEE Geosci Remote Sens Lett 13(5):740–744. https://doi.org/10.1109/LGRS.2016.2542358
89. Rajchl M et al (2017) DeepCut: object segmentation from bounding box annotations using convolutional neural networks. IEEE Trans Med Imaging 36(2):674–683. https://doi.org/10.1109/TMI.2016.2621185
90. Volpi M, Tuia D (2017) Dense semantic labeling of subdecimeter resolution images with convolutional. IEEE Trans Geosci Remote Sens 55(2):881–893. https://doi.org/10.1109/TGRS.2016.2616585
91. Maggiori E et al (2017) Convolutional neural networks for large-scale remote-sensing image classification. IEEE Trans Geosci Remote Sens 55(2):645–657. https://doi.org/10.1109/TGRS.2016.2612821
92. Konar D et al (2016) A quantum bi-directional self-organizing neural network (QBDSONN) architecture for binary object

extraction from a noisy perspective. Appl Soft Comput 46:731–752. https://doi.org/10.1016/j.asoc.2015.12.040
93. Chang C-Y (2011) A neural network for thyroid segmentation and volume estimation in CT images. IEEE Comput Intell Mag 6(4):43–55. https://doi.org/10.1109/MCI.2011.942756
94. Taravat A et al (2014) Fully automatic dark-spot detection from SAR imagery with the combination of nonadaptive weibull multiplicative model and pulse-coupled neural networks. IEEE Trans Geosci Remote Sens 52(5):2427–2435. https://doi.org/10.1109/TGRS.2013.2261076
95. Chen Y et al (2015) Region-based object recognition by color segmentation using a simplified PCNN. IEEE Trans Neural Netw Learn Syst 26(8):1682–1697. https://doi.org/10.1109/TNNLS.2014.2351418
96. Karvonen JA et al (2004) Baltic sea ice SAR segmentation and classification using modified pulse-coupled neural networks. IEEE Trans Geosci Remote Sens 42(7):1566–1574. https://doi.org/10.1109/TGRS.2004.828179
97. Kuntimad G, Ranganath HS (1999) Perfect image segmentation using pulse coupled neural networks. IEEE Trans Neural Netw 10(3):591–598. https://doi.org/10.1109/72.761716
98. Demirhan A et al (2015) Segmentation of tumor and edema along with healthy tissues of brain using wavelets and neural networks. IEEE J Biomed Health Inform 19(4):1451–1458. https://doi.org/10.1109/JBHI.2014.2360515
99. Song T et al (2007) A modified probabilistic neural network for partial volume segmentation in brain MR image. IEEE Trans Neural Netw 18(5):1424–1432. https://doi.org/10.1109/TNN.2007.891635
100. Abdel-Khalek S et al (2017) A two-dimensional image segmentation method based on genetic algorithm and entropy. Optik 131:414–422. https://doi.org/10.1016/j.ijleo.2016.11.039
101. Ghosh P et al (2016) Incorporating priors for medical image segmentation using a genetic algorithm. Neurocomputing 195:181–194. https://doi.org/10.1016/j.neucom.2015.09.123
102. Sheta A et al (2012) Genetic algorithms: a tool for image segmentation. In: 2012 international conference on multimedia computing and systems, pp 84–90. https://doi.org/10.1109/icmcs.2012.6320144
103. Hung C-L, Yuan-Huai W (2016) Parallel genetic-based algorithm on multiple embedded graphic processing units for brain magnetic resonance imaging segmentation. Comput Electr Eng. https://doi.org/10.1016/j.compeleceng.2016.09.028
104. Xie F, Bovik AC (2013) Automatic segmentation of dermoscopy images using self-generating neural networks seeded by genetic algorithm. Pattern Recogn 46:1012–1019. https://doi.org/10.1016/j.patcog.2012.08.012
105. Mylonas SK et al (2015) Classification of remotely sensed images using the genesis fuzzy segmentation algorithm. IEEE Trans Geosci Remote Sens 53(10):5352–5376. https://doi.org/10.1109/TGRS.2015.2421640
106. Wang F et al (2014) An improved adaptive genetic algorithm for image segmentation and vision alignment used in microelectronic bonding. IEEE ASME Trans Mechatron 19(3):916–923. https://doi.org/10.1109/TMECH.2013.2260555
107. Namburu A, Samay SK, Edara SR (2017) Soft fuzzy rough set-based MR brain image segmentation. Appl Soft Comput 54(C):456–466. https://doi.org/10.1016/j.asoc.2016.08.020
108. Vishnuvarthanan G et al (2016) An unsupervised learning method with a clustering approach for tumor identification and tissue segmentation in magnetic resonance brain images. Appl Soft Comput 38:190–212. https://doi.org/10.1016/j.asoc.2015.09.016
109. Mukhopadhyay A, Maulik U (2011) A multiobjective approach to MR brain image segmentation. Appl Soft Comput 11:872–880. https://doi.org/10.1016/j.asoc.2010.01.007
110. Hata Y, Kobashi S (2009) Fuzzy segmentation of endorrhachis in magnetic resonance images and its fuzzy maximum intensity projection. Appl Soft Comput 9:1156–1169. https://doi.org/10.1016/j.asoc.2009.03.001
111. Kannan SR (2008) A new segmentation system for brain MR images based on fuzzy techniques. Appl Soft Comput 8:1599–1606. https://doi.org/10.1016/j.asoc.2007.10.025
112. Hata Y et al (2000) Automated segmentation of human brain MR images aided by fuzzy information granulation and fuzzy inference. IEEE Trans Syst Man Cybern Part C Appl Rev 30(3):381–395. https://doi.org/10.1109/5326.885120
113. Baazaouia A, Barhoumi W, Ahmed A, Zagrouba E (2017) Semi-automated segmentation of single and multiple tumors in liver CT images using entropy-based fuzzy region growing. IRBM 38:98–108. https://doi.org/10.1016/j.irbm.2017.02.003
114. Cordeiro FR et al (2016) An adaptive semi-supervised Fuzzy GrowCut algorithm to segment masses of regions of interest of mammographic images. Appl Soft Comput 46:613–628. https://doi.org/10.1016/j.asoc.2015.11.040
115. Rezaee K, Haddadnia J, Tashk A (2017) Optimized clinical segmentation of retinal blood vessels by using combination of adaptive filtering, fuzzy entropy and skeletonization. Appl Soft Comput 52:937–951. https://doi.org/10.1016/j.asoc.2016.09.033
116. Chaira T (2010) Intuitionistic fuzzy segmentation of medical images. IEEE Trans Biomed Eng 57(6):1430–1436. https://doi.org/10.1109/TBME.2010.2041000
117. Leung S-H, Wang S-L, Lau W-H (2004) Lip image segmentation using fuzzy clustering incorporating an elliptic shape function. IEEE Trans Image Process 13(1):51–62. https://doi.org/10.1109/TIP.2003.818116
118. Javed U, Raiz MM, Ghafoor A, Cheema TA (2016) SAR image segmentation based on active contours with fuzzy logic. IEEE Trans Aerosp Electron Syst 52(1):181–188. https://doi.org/10.1109/TAES.2015.120817
119. Li L et al (2016) Fuzzy multilevel image thresholding based on modified discrete grey wolf optimizer and local information aggregation. IEEE Access 4:6438–6450. https://doi.org/10.1109/ACCESS.2016.2613940
120. Mondal A, Ghosh S, Ghosh A (2016) Robust global and local fuzzy energy based active contour for image segmentation. Appl Soft Comput 47(C):191–215. https://doi.org/10.1016/j.asoc.2016.05.026
121. Zhao F et al (2015) A multi objective spatial fuzzy clustering algorithm for image segmentation. Appl Soft Comput 30:48–57. https://doi.org/10.1016/j.asoc.2015.01.039
122. Maj P, Roy S (2015) Rough fuzzy clustering and multiresolution image analysis for text-graphics segmentation. Appl Soft Comput 30:705–721. https://doi.org/10.1016/j.asoc.2015.01.049
123. Caponetti L et al (2008) Document page segmentation using neuro-fuzzy approach. Appl Soft Comput 8:118–126. https://doi.org/10.1016/j.asoc.2006.11.008
124. Chi Z, Yan H (1993) Map image segmentation based on thresholding and fuzzy rules. Electron Lett 29(21):1841–1843. https://doi.org/10.1049/el:19931225
125. Herrera PJ et al (2011) A segmentation method using Otsu and fuzzy k-means for stereovision matching in hemispherical images from forest environments. Appl Soft Comput 11:4738–4747. https://doi.org/10.1016/j.asoc.2011.07.010
126. Pednekar AS, Kakadiaris IA (2006) Image segmentation based on fuzzy connectedness using dynamic weights. IEEE Trans Image Process 15(6):1555–1562. https://doi.org/10.1109/TIP.2006.871165
127. Feng C, Zhao D, Huang M (2016) Segmentation of longitudinal brain MR images using bias correction embedded fuzzy c-means with non-locally spatio-temporal regularization. J Vis Commun

Image Represent 38(C):517–529. https://doi.org/10.1016/j.jvcir.2016.03.027
128. Aparajeeta J, Nanda PK, Das N (2016) Modified possibilistic fuzzy C-means algorithms for segmentation of magnetic resonance image. Appl Soft Comput 41(C):104–119. https://doi.org/10.1016/j.asoc.2015.12.003
129. Verma H et al (2016) An improved intuitionistic fuzzy c-means clustering algorithm incorporating local information for brain image segmentation. Appl Soft Comput 46:543–557. https://doi.org/10.1016/j.asoc.2015.12.022
130. Adhikari SK et al (2015) Conditional spatial fuzzy C-means clustering algorithm for segmentation of MRI images. Appl Soft Comput 34:758–769. https://doi.org/10.1016/j.asoc.2015.05.038
131. Huang C-W et al (2015) Intuitionistic fuzzy *c*-means clustering algorithm with neighborhood attraction in segmenting medical image. Soft Comput 19(459–470):2105. https://doi.org/10.1007/s00500-014-1264-2
132. Ain Q et al (2014) Fuzzy anisotropic diffusion based segmentation and texture based ensemble classification for brain tumor. Appl Soft Comput 21:330–340. https://doi.org/10.1016/j.asoc.2014.03.019
133. Yang Z (2009) Robust fuzzy clustering-based image segmentation. Appl Soft Comput 9:80–84. https://doi.org/10.1016/j.asoc.2008.03.009
134. Ji Z et al (2012) Fuzzy c-means clustering with weighted image patch for image segmentation. Appl Soft Comput 12:1659–1667. https://doi.org/10.1016/j.asoc.2012.02.010
135. Chen S, Zhang D (2004) Robust image segmentation using FCM with spatial constraints based on new kernel-induced distance measure. IEEE Trans Syst Man Cybern Part B Cybern 34(4):1907–1916. https://doi.org/10.1109/TSMCB.2004.831165
136. Shen S et al (2005) MRI fuzzy segmentation of brain tissue using neighborhood attraction with neural-network optimization. IEEE Trans Inf Technol Biomed 9(3):459–467. https://doi.org/10.1109/TITB.2005.847500
137. Rezaei Z et al (2017) Automatic plaque segmentation based on hybrid fuzzy clustering and k nearest neighborhood using virtual histology intravascular ultrasound images. Appl Soft Comput 53:380–395. https://doi.org/10.1016/j.asoc.2016.12.048
138. Tripathy BK, Mittal D (2016) Hadoop based uncertain possibilistic kernelized c-means algorithms for image segmentation and a comparative analysis. Appl Soft Comput 46(C):886–923. https://doi.org/10.1016/j.asoc.2016.01.045
139. Tan KS et al (2013) Novel initialization scheme for fuzzy C-means algorithm on color image segmentation. Appl Soft Comput 13:1832–1852. https://doi.org/10.1016/j.asoc.2012.12.022
140. Tan KS et al (2013) Color image segmentation using adaptive unsupervised clustering approach. Appl Soft Comput 13:2017–2036. https://doi.org/10.1016/j.asoc.2012.11.038
141. Zhou X-C et al (2008) New two-dimensional fuzzy C-means clustering algorithm for image segmentation. J Cent South Univ Technol 15:882–887. https://doi.org/10.1007/s11771-008-0161-1
142. Sowmya B, Rani BS (2011) Colour image segmentation using fuzzy clustering techniques and competitive neural network. Appl Soft Comput 11:3170–3178. https://doi.org/10.1016/j.asoc.2010.12.019
143. Hassanien AE et al (2014) MRI breast cancer diagnosis hybrid approach using adaptive ant-based segmentation and multilayer perceptron neural networks classifier. Appl Soft Comput 14:62–71. https://doi.org/10.1016/j.asoc.2013.08.011
144. Ortiz A et al (2013) Two fully-unsupervised methods for MR brain image segmentation using SOM-based strategies. Appl Soft Comput 13:2668–2682. https://doi.org/10.1016/j.asoc.2012.11.020
145. Alirezaie J et al (1998) Automatic segmentation of cerebral MR images using artificial neural networks. IEEE Trans Nucl Sci 45(4):2174–2182. https://doi.org/10.1109/23.708336
146. Xie F et al (2017) Melanoma classification on dermoscopy images using a neural network ensemble model. IEEE Trans Med Imaging 36(3):849–858. https://doi.org/10.1109/TMI.2016.2633551
147. Franklin W, Rajan SE (2014) Retinal vessel segmentation employing ANN technique by Gabor and moment invariants-based features. Appl Soft Comput 22:94–100. https://doi.org/10.1016/j.asoc.2014.04.024
148. Veredas F et al (2010) Binary tissue classification on wound images with neural networks and bayesian classifiers. IEEE Trans Med Imaging 29(2):410–427. https://doi.org/10.1109/TMI.2009.2033595
149. Wang F, Wang F (2014) Void detection in TSVs with X-ray image multithreshold segmentation and artificial neural networks. IEEE Trans Comp Packag Manuf Technol 4(7):1245–1250. https://doi.org/10.1109/TCPMT.2014.2322907
150. Turaga SC et al (2010) Convolutional networks can learn to generate affinity graphs for image segmentation. Neural Comput 22:511–538
151. Cheng K-S et al (1996) The application of competitive hopfield neural network to medical image segmentation. IEEE Trans Med Imaging 15(4):560–567. https://doi.org/10.1109/42.511759
152. Chen C-T et al (1991) Medical image segmentation by a constraint satisfaction neural network. IEEE Trans Nucl Sci 38(2):678–686. https://doi.org/10.1109/23.289373
153. Singha S et al (2013) Satellite oil spill detection using artificial neural networks. IEEE J Sel Top Appl Earth Obs Remote Sens 6(6):2355–2363. https://doi.org/10.1109/JSTARS.2013.2251864
154. Rizvi IA, Mohan BK (2011) Object-based image analysis of high-resolution satellite images using modified cloud basis function neural network and probabilistic relaxation labeling process. IEEE Trans Geosci Remote Sens 49(12):4815–4820. https://doi.org/10.1109/TGRS.2011.2171695
155. Sziranyi T, Zerubia J (1997) Markov random field image segmentation using cellular neural network. IEEE Trans Circuits Syst I Fundam Theory Appl 44(1):86–89. https://doi.org/10.1109/81.558448
156. Baraldi A, Parmiggiani F (1995) A neural network for unsupervised categorization of multivalued input patterns: an application to satellite image clustering. IEEE Trans Geosci Remote Sens 33(2):305–316. https://doi.org/10.1109/36.377930
157. Arumugadevi S, Seenivasagam V (2016) Color image segmentation using feedforward neural networks with FCM. Int J Autom Comput 13(5):491–500. https://doi.org/10.1007/s11633-016-0975-5
158. Helmy AK, El-Taweel GS (2016) Image segmentation scheme based on SOM–PCNN in frequency domain. Appl Soft Comput 40:405–415. https://doi.org/10.1016/j.asoc.2015.11.042
159. De S et al (2012) Color image segmentation using parallel OptiMUSIG activation function. Appl Soft Comput 12:3228–3236. https://doi.org/10.1016/j.asoc.2012.05.011
160. Meftah B et al (2010) Segmentation and edge detection based on spiking neural network model. Neural Process Lett 32:131–146. https://doi.org/10.1007/s11063-010-9149-6
161. Bhattacharyya S et al (2010) Multilevel image segmentation with adaptive image context based thresholding. Appl Soft Comput 11:946–962. https://doi.org/10.1016/j.asoc.2010.01.015
162. Boskovitz V, Guterman H (2002) An adaptive neuro-fuzzy system for automatic image segmentation and edge detection. IEEE Trans Fuzzy Syst 10(2):247–262. https://doi.org/10.1109/91.995125
163. Fu H, Chi Z (2006) Combined thresholding and neural network approach for vein pattern extraction from leaf images. IEEE

Proc Vis Image Signal Process 153(6):881–892. https://doi.org/10.1049/ip-vis:20060061
164. Chen X et al (2014) Vehicle detection in satellite images by hybrid deep convolutional neural networks. IEEE Geosci Remote Sens Lett 11(10):1797–1801. https://doi.org/10.1109/LGRS.2014.2309695
165. Lin J-S et al (1996) A fuzzy hopfield neural network for medical image segmentation. IEEE Trans Nucl Sci 43(4):2389–2398. https://doi.org/10.1109/23.531787
166. Pereira S et al (2016) Brain tumor segmentation using convolutional neural networks in MRI images. IEEE Trans Med Imaging 35(5):1240–1251. https://doi.org/10.1109/TMI.2016.2538465
167. Moeskops P et al (2016) Automatic segmentation of MR brain images with a convolutional neural network. IEEE Trans Med Imaging 35(5):1252–1261. https://doi.org/10.1109/TMI.2016.2548501
168. Havaei M et al (2017) Brain tumor segmentation with deep neural networks. Med Image Anal 35:18–31. https://doi.org/10.1016/j.media.2016.05.004
169. Lekadir K et al (2017) A convolutional neural network for automatic characterization of plaque composition in carotid ultrasound. IEEE J Biomed Health Inform 21(1):48–55. https://doi.org/10.1109/JBHI.2016.2631401
170. Roth HR et al (2015) Deeporgan: multi-level deep convolutional networks for automated pancreas segmentation. In: MICCAI 2015: medical image computing and computer-assisted intervention, pp. 556–564. https://doi.org/10.1007/978-3-319-24553-9_68
171. Xu Y et al (2017) Gland instance segmentation using deep multichannel neural networks. IEEE Trans Biomed Eng. https://doi.org/10.1109/TBME.2017.2686418
172. Yuan Y et al (2017) Automatic skin lesion segmentation using deep fully convolutional networks with jaccard distance. IEEE Trans Med Imaging. https://doi.org/10.1109/TMI.2017.2695227
173. Zhang S et al (2016) Transferred deep convolutional neural network features for extensive facial landmark localization. IEEE Signal Process Lett 23(4):478–482. https://doi.org/10.1109/LSP.2016.2533721
174. Kumar A et al (2017) An ensemble of fine-tuned convolutional neural networks for medical image classification. IEEE J Biomed Health Inform 21(1):31–40. https://doi.org/10.1109/JBHI.2016.2635663
175. van Grinsven MJJP et al (2016) Fast convolutional neural network training using selective data sampling: application to hemorrhage detection in color fundus images. IEEE Trans Med Imaging 35(5):1273–1284. https://doi.org/10.1109/TMI.2016.2526689
176. Lawrence S et al (1997) Face recognition: a convolutional neural-network approach. IEEE Trans Neural Netw 8(1):98–113. https://doi.org/10.1109/72.554195
177. Kiranyaz S et al (2016) Real-time patient-specific ECG classification by 1D convolutional neural networks. IEEE Trans Biomed Eng 63(3):664–675. https://doi.org/10.1109/TBME.2015.2468589
178. Nogueira RF et al (2016) Fingerprint liveness detection using convolutional neural networks. IEEE Trans Inf Forensics Secur 11(6):1206–1213. https://doi.org/10.1109/TIFS.2016.2520880
179. Brosch T, Tam R (2015) Efficient training of convolutional deep belief networks in the frequency domain for application to high-resolution 2D and 3D images. Neural Comput 27:211–227. https://doi.org/10.1162/NECO_a_00682
180. Badrinarayanan V et al (2017) SegNet: a deep convolutional encoder-decoder architecture for scene segmentation. IEEE Trans Pattern Anal Mach Intell. https://doi.org/10.1109/TPAMI.2016.2644615
181. Cheng D et al (2017) SeNet: structured edge network for sea-land segmentation. IEEE Geosci Remote Sens Lett 14(2):247–251. https://doi.org/10.1109/LGRS.2016.2637439
182. Zhou Yu et al (2016) Polarimetric SAR image classification using deep convolutional neural networks. IEEE Geosci Remote Sens Lett 13(12):1935–1939. https://doi.org/10.1109/LGRS.2016.2618840
183. Zhang F et al (2016) Weakly supervised learning based on coupled convolutional neural networks for aircraft detection. IEEE Trans Geosci Remote Sens 54(9):5553–5563. https://doi.org/10.1109/TGRS.2016.2569141
184. Dong C et al (2016) Image super-resolution using deep convolutional networks. IEEE Trans Pattern Anal Mach Intell 38(2):295–307. https://doi.org/10.1109/TPAMI.2015.2439281
185. Yan C et al (2015) Driving posture recognition by convolutional neural networks. IET Comput Vision 10(2):103–114. https://doi.org/10.1049/iet-cvi.2015.0175
186. Wang P et al (2016) Action recognition from depth maps using deep convolutional neural networks. IEEE Trans Hum Mach Syst 46(4):498–509. https://doi.org/10.1109/THMS.2015.2504550
187. Dong Z et al (2015) Vehicle type classification using a semisupervised convolutional neural network. IEEE Trans Intell Transp Syst 16(4):2247–2256. https://doi.org/10.1109/TITS.2015.2402438
188. Liu F et al (2016) Learning depth from single monocular images using deep convolutional neural fields. IEEE Trans Pattern Anal Mach Intell 38(10):2024–2039. https://doi.org/10.1109/TPAMI.2015.2505283
189. Wu D et al (2016) Deep dynamic neural networks for multimodal gesture segmentation and recognition. IEEE Trans Pattern Anal Mach Intell 38(8):1583–1597. https://doi.org/10.1109/TPAMI.2016.2537340
190. Dosovitskiy A et al (2017) Learning to generate chairs, tables and cars with convolutional networks. IEEE Trans Pattern Anal Mach Intell 39(4):692–705. https://doi.org/10.1109/TPAMI.2016.2567384
191. Fakhry A et al (2017) Residual deconvolutional networks for brain electron microscopy image segmentation. IEEE Trans Med Imaging 36(2):447–456. https://doi.org/10.1109/TMI.2016.2613019
192. Neubauer C (1998) Evaluation of convolutional neural networks for visual recognition. IEEE Trans Neural Netw 9(4):685–696. https://doi.org/10.1109/72.701181
193. Anthimopoulos M et al (2016) Lung pattern classification for interstitial lung diseases using a deep convolutional neural network. IEEE Trans Med Imaging 35(5):1207–1216. https://doi.org/10.1109/TMI.2016.2535865
194. Tang Y, Xiangqian W (2017) Scene text detection and segmentation based on cascaded convolution neural networks. IEEE Trans Image Process 26(3):1509–1520. https://doi.org/10.1109/TIP.2017.2656474
195. Chen SW et al (2017) Counting apples and oranges with deep learning: a data driven approach. IEEE Robot Autom Lett 2(2):781–788. https://doi.org/10.1109/LRA.2017.2651944
196. Tang J et al (2015) Compressed-domain ship detection on spaceborne optical image using deep neural network and extreme learning machine. IEEE Trans Geosci Remote Sens 53(3):1174–1185. https://doi.org/10.1109/TGRS.2014.2335751
197. De S et al (2016) Automatic magnetic resonance image segmentation by fuzzy intercluster hostility index based genetic algorithm: an application. Appl Soft Comput 47:669–683. https://doi.org/10.1016/j.asoc.2016.05.042
198. McIntosh C, Hamarneh G (2012) Medial-based deformable models in nonconvex shape-spaces for medical image

segmentation. IEEE Trans Med Imaging 31(1):33–50. https://doi.org/10.1109/TMI.2011.2162528
199. Tian GJ et al (2011) Hybrid genetic and variational expectation-maximization algorithm for gaussian-mixture-model-based brain mr image segmentation. IEEE Trans Inf Technol Biomed 15(3):373–380. https://doi.org/10.1109/TITB.2011.2106135
200. Angelie E et al (2003) Automatic tuning of left ventricular segmentation of MR images using genetic algorithms. Int Congr Ser 1256:1102–1107. https://doi.org/10.1016/S0531-5131(03)00351-0
201. Yeh J-Y, Fu JC (2008) A hierarchical genetic algorithm for segmentation of multi-spectral human-brain MRI. Expert Syst Appl 34:1285–1295. https://doi.org/10.1016/j.eswa.2006.12.012
202. Manikandan S et al (2013) Multilevel thresholding for segmentation of medical brain images using real coded genetic algorithm. Measurement 47:558–568. https://doi.org/10.1016/j.measurement.2013.09.031
203. Fan Y et al (2002) Volumetric segmentation of brain images using parallel genetic algorithms. IEEE Trans Med Imaging 21(8):904–909. https://doi.org/10.1109/TMI.2002.803126
204. Janc K et al (2013) Genetic algorithms as a useful tool for trabecular and cortical bone segmentation. Comput Methods Programs Biomed 111:72–83. https://doi.org/10.1016/j.cmpb.2013.03.012
205. Rogai F et al (2016) Metaheuristics for specialization of a segmentation algorithm for ultrasound images. IEEE Trans Evolut Comput 20(5):730–741. https://doi.org/10.1109/TEVC.2016.2515660
206. Pereira DC et al (2014) Segmentation and detection of breast cancer in mammograms combining wavelet analysis and genetic algorithm. Comput Methods Programs Biomed 114:88–101. https://doi.org/10.1016/j.cmpb.2014.01.014
207. Nagarajan G et al (2016) Hybrid genetic algorithm for medical image feature extraction and selection. In: International conference on computational modeling and security (CMS 2016), vol 85, pp 455–462. https://doi.org/10.1016/j.procs.2016.05.192
208. Ye F (2016) Evolving the SVM model based on a hybrid method using swarm optimization techniques in combination with a genetic algorithm for medical diagnosis. Multimed Tools Appl. https://doi.org/10.1007/s11042-016-4233-1
209. Dokur Z, Olmez T (2008) Tissue segmentation in ultrasound images by using genetic algorithms. Expert Syst Appl 34:2739–2746. https://doi.org/10.1016/j.eswa.2007.05.002
210. Saha S, Bandyopadhyay S (2010) Application of a multiseed-based clustering technique for automatic satellite image segmentation. IEEE Geosci Remote Sens Lett 7(2):306–308. https://doi.org/10.1109/LGRS.2009.2034033
211. Awad M et al (2007) Multicomponent image segmentation using a genetic algorithm and artificial neural network. IEEE Geosci Remote Sens Lett 4(4):571–575. https://doi.org/10.1109/LGRS.2007.903064
212. Jeon B-K et al (2002) Road detection in spaceborne SAR images using a genetic algorithm. IEEE Trans Geosci Remote Sens 40(1):22–29. https://doi.org/10.1109/36.981346
213. Izadi M et al (2017) A new neuro-fuzzy approach for post-earthquake road damage assessment using GA and SVM classification from quickbird satellite images. Remote Sens, J Indian Soc. https://doi.org/10.1007/s12524-017-0660-3
214. Singh A, Singh KK (2017) Satellite image classification using genetic algorithm trained radial basis function neural network, application to the detection of flooded areas. J Vis Commun Image Represent 42:173–182. https://doi.org/10.1016/j.jvcir.2016.11.017
215. Mylonas SK et al (2016) A local search-based genesis algorithm for the segmentation and classification of remote-sensing images. IEEE J Sel Top Appl Earth Obs Remote Sens 9(4):1470–1492. https://doi.org/10.1109/JSTARS.2016.2518403
216. Ishak AB (2016) A two-dimensional multilevel thresholding method for image segmentation. Appl Soft Comput 52:306–322. https://doi.org/10.1016/j.asoc.2016.10.034
217. Khan A, Jaffar MA (2015) Genetic algorithm and Self organizing map based fuzzy hybrid intelligent method for color image segmentation. Appl Soft Comput 32:300–310. https://doi.org/10.1016/j.asoc.2015.03.029
218. Abbasgholipour M et al (2014) Color image segmentation with genetic algorithm in a raisin sorting system based on machine vision in variable conditions. Expert Syst Appl 38:3671–3678. https://doi.org/10.1016/j.eswa.2010.09.023
219. Hammouche K et al (2008) A multilevel automatic thresholding method based on a genetic algorithm for a fast image segmentation. Comput Vis Image Underst 109:163–175. https://doi.org/10.1016/j.cviu.2007.09.001
220. Melkemi KE et al (2006) A multiagent system approach for image segmentation using genetic algorithms and extremal optimization heuristics. Pattern Recogn Lett 27:1230–1238. https://doi.org/10.1016/j.patrec.2005.07.021
221. Wei H, Tang X-s (2015) A genetic-algorithm-based explicit description of object contour and its ability to facilitate recognition. IEEE Trans Cybern 45(11):2558–2571. https://doi.org/10.1109/TCYB.2014.2376939
222. Khan A et al (2014) Color image segmentation: a novel spatial fuzzy genetic algorithm. SIViP 8(7):1233–1243. https://doi.org/10.1007/s11760-012-0347-8
223. Andrey P (1999) Selectionist relaxation: genetic algorithms applied to image segmentation. Image Vis Comput 17(3–4):175–187. https://doi.org/10.1016/S0262-8856(98)00095-X
224. Kim HJ et al (1988) MRF model based image segmentation using hierarchical distributed genetic algorithm. Electron Lett 34(25):2394–2395. https://doi.org/10.1049/el:19981674
225. Song A, Ciesielski V (2008) Texture segmentation by genetic programming 2008 by the Massachusetts Institute of Technology. Evol Comput 16(4):461–481. https://doi.org/10.1162/evco.2008.16.4.461
226. Andrey P, Tarroux P (1994) Unsupervised image segmentation using a distributed genetic algorithm. Pattern Recogn 27(5):659–673. https://doi.org/10.1016/0031-3203(94)90045-0
227. Awad M et al (2009) Multi-component image segmentation using a hybrid dynamic genetic algorithm and fuzzy C-means. IET Image Proc 3(2):52–62. https://doi.org/10.1049/iet-ipr.2007.0213
228. Gotardo PFU et al (2004) Range image segmentation into planar and quadric surfaces using an improved robust estimator and genetic algorithm. IEEE Trans Syst Man Cybern Part B Cybern 34(6):2303–2316. https://doi.org/10.1109/TSMCB.2004.835082
229. Mylonas SK et al (2013) GeneSIS: a GA-based fuzzy segmentation algorithm for remote sensing images. Knowl-Based Syst 54:86–102. https://doi.org/10.1016/j.knosys.2013.07.018
230. Chinnasamy S (2014) Performance improvement of fuzzy-based algorithms for medical image retrieval. IET Image Process 8(6):319–326. https://doi.org/10.1049/iet-ipr.2012.0510
231. Maulik U (2009) Medical image segmentation using genetic algorithms. IEEE Trans Inf Technol Biomed 13(2):166–173. https://doi.org/10.1109/TITB.2008.2007301
232. Tohka J et al (2007) Genetic algorithms for finite mixture model based voxel classification in neuroimaging. IEEE Trans Med Imaging 26(5):696–711. https://doi.org/10.1109/TMI.2007.895453
233. Li C-T, Chiao R (2003) Multiresolution genetic clustering algorithm for texture segmentation. Image Vis Comput 21:955–966. https://doi.org/10.1016/S0262-8856(03)00120-3

234. Tseng D-C, Lai C-C (1999) A genetic algorithm for MRF-based segmentation of multi-spectral textured images. Pattern Recogn Lett 20(14):1499–1510. https://doi.org/10.1016/S0167-8655(99)00117-8
235. Saha R, Bajger M, Lee G (2016) Spatial shape constrained fuzzy C-means (FCM) clustering for nucleus segmentation in pap smear images. In: 2016 international conference on digital image computing: techniques and applications (DICTA), pp 1–8. https://doi.org/10.1109/dicta.2016.7797086
236. Kumar SVA et al (2016) A picture fuzzy clustering approach for brain tumor segmentation. In: 2016 second international conference on cognitive computing and information processing (CCIP). https://doi.org/10.1109/ccip.2016.7802852
237. Al-Dmour H, Al-Ani A (2016) MR brain image segmentation based on unsupervised and semi-supervised fuzzy clustering methods. In: 2016 international conference on digital image computing: techniques and applications (DICTA), pp 1–7. https://doi.org/10.1109/dicta.2016.7797066
238. Pereira S et al (2017) On hierarchical brain tumor segmentation in MRI using fully convolutional neural networks: a preliminary study. In: 2017 IEEE 5th Portuguese meeting on bioengineering (ENBENG), pp 1–4. https://doi.org/10.1109/enbeng.2017.7889452
239. Wang C et al (2016) On semantic image segmentation using deep convolutional neural network with shortcuts and easy class extension. In: 2016 sixth international conference on image processing theory, tools and applications (IPTA), pp 1–6. https://doi.org/10.1109/ipta.2016.7821005
240. Gobikrishnan M, Rajalakshmi T, Snekhalatha U (2016) Diagnosis of rheumatoid arthritis in knee using fuzzy C means segmentation technique. In: International conference on communication and signal processing, pp 430–433. https://doi.org/10.1109/iccsp.2016.7754172
241. Xu M, Guo M, Shang L, Jia X (2016) Multi-value image segmentation based on FCM algorithm and graph cut theory. In: 2016 IEEE international conference on fuzzy systems (FUZZ), pp 1333–1340. https://doi.org/10.1109/fuzz-ieee.2016.7737844
242. Abedin MdZ et al (2016) Traffic sign recognition using hybrid features descriptor and artificial neural network classifier. In: 19th international conference on computer and information technology, Dec 2016. https://doi.org/10.1109/iccitechn.2016.7860241
243. Yamamoto Y et al (2016) An efficient classification method for knee MR image segmentation. In: 2016 12th international conference on signal-image technology and internet-based systems, pp 36–45. https://doi.org/10.1109/sitis.2016.15
244. Roy K et al (2015) Multibiometric system using fuzzy level set, and genetic and evolutionary feature extraction. IET Biom 4(3):151–161. https://doi.org/10.1049/iet-bmt.2014.0064
245. Khan ZF et al (2017) Automated segmentation of lung images using textural echo state neural networks. In: 2017 international conference on informatics, health and technology (ICIHT). https://doi.org/10.1109/iciht.2017.7899012
246. Zangeneh D, Yazdi M (2016) Automatic segmentation of multiple sclerosis lesions in brain MRI using constrained GMM and genetic algorithm. In: 2016 24th Iranian conference on electrical engineering (ICEE), pp 832–837. https://doi.org/10.1109/iraniancee.2016.7585635
247. Kaur A, Kaur P (2016) An integrated approach for diabetic retinopathy exudate segmentation by using genetic algorithm and switching median filter. In: 2016 international conference on image, vision and computing, pp 119–123. https://doi.org/10.1109/icivc.2016.7571284
248. Mistry VH, Makwana RM (2016) Computationally efficient vanishing point detection algorithm based road segmentation in road images. In: 2016 IEEE international conference on advances in electronics, communication and computer technology (ICAECCT)
249. Kampffmeyer M et al (2016) Semantic segmentation of small objects and modeling of uncertainty in urban remote sensing images using deep convolutional neural networks. In: 2016 IEEE conference on computer vision and pattern recognition workshops, pp 680–688. https://doi.org/10.1109/cvprw.2016.90
250. Benalcazar ME et al (2014) Automatic design of aperture filters using neural networks applied to ocular image segmentation. In: 2014 22nd European signal processing conference (EUSIPCO), pp 2195–2199
251. Lee G-G et al (2017) Traffic light recognition using deep neural networks. In: 2017 IEEE international conference on consumer electronics (ICCE), pp 277–278. https://doi.org/10.1109/icce.2017.7889317
252. Takeki A et al (2016) Detection of small birds in large images by combining a deep detector with semantic segmentation. In: 2016 IEEE international conference on image processing (ICIP), pp 3977–3981. https://doi.org/10.1109/icip.2016.7533106
253. Kumar S, Pant M, Kumar M, Dutt A (2015) Colour image segmentation with histogram and homogeneity histogram difference using evolutionary algorithms. Int J Mach Learn Cybernet. https://doi.org/10.1007/s13042-015-0360-7
254. Singh V, Gupta S, Saini S (2015) A methodological survey of image segmentation using soft computing techniques. In: 2015 international conference on advances in computer engineering and applications (ICACEA), pp 419–422. https://doi.org/10.1109/icacea.2015.7164741
255. Zhang J, Chen W-N, Zhan Z-H et al (2012) A survey on algorithm adaptation in evolutionary computation. Front Electr Electron Eng 7(1):16–31. https://doi.org/10.1007/s11460-012-0192-0
256. Li G (2016) Magnetic resonance image segmentation algorithm based on fuzzy clustering. In: 2016 eighth international conference on measuring technology and mechatronics automation, pp 379–382. https://doi.org/10.1109/icmtma.2016.97
257. Kuruvilla J, Sukumaran D, Sankar A, Joy SP (2016) A review on image processing and image segmentation. In: 2016 international conference on data mining and advanced computing (SAPIENCE), pp 198–203. https://doi.org/10.1109/sapience.2016.7684170
258. Bedruz RA et al (2016) Fuzzy logic based vehicular plate character recognition system using image segmentation and scale-invariant feature transform. In: 2016 IEEE region 10 conference (TENCON), pp 676–681. https://doi.org/10.1109/tencon.2016.7848088
259. Zhu W (2016) Segmentation algorithm for MRI images using global entropy minimization. In: IEEE international conference on signal and image processing (ICSIP), pp 1–5. https://doi.org/10.1109/siprocess.2016.7888212
260. Parvathi P, Rajeswari R (2016) A hybrid FCM-ALO based technique for image segmentation. In: 2016 IEEE international conference on advances in computer applications (ICACA), pp 342–345. https://doi.org/10.1109/icaca.2016.7887978
261. Tewari P, Surbhi P (2016) Evaluation of some recent image segmentation method's. In: 2016 international conference on computing for sustainable global development (INDIACom), pp 3741–3747
262. Naz S, Majeed H, Irshad H (2010) Image segmentation using fuzzy clustering: a survey. In: 2010 6th international conference on emerging technologies (ICET), pp 181–186. https://doi.org/10.1109/icet.2010.5638492
263. Vapenik R et al (2016) Human face detection in still image using Multilayer perceptron solution based on Neuroph framework. In: 2016 international conference on emerging elearning

technologies and applications (ICETA), pp 365–369. https://doi.org/10.1109/iceta.2016.7802049
264. Swietojanski P et al (2014) Convolutional neural networks for distant speech recognition. IEEE Signal Process Lett 21(9):1120–1124. https://doi.org/10.1109/LSP.2014.2325781
265. Duran-Rosal AM et al (2017) Identification of extreme wave heights with an evolutionary algorithm in combination with a likelihood-based segmentation. Prog Artif Intell 6:59–66. https://doi.org/10.1007/s13748-016-0105-1
266. Uy ACP et al (2016) Automated traffic violation apprehension system using genetic algorithm and artificial neural network. In: 2016 IEEE region 10 conference (TENCON)—proceedings of the international conference, pp 2094–2099. https://doi.org/10.1109/tencon.2016.7848395
267. Saqui D et al (2016) Methodology for band selection of hyperspectral images using genetic algorithms and gaussian maximum likelihood classifier. In: 2016 international conference on computational science and computational intelligence, pp 733–738. https://doi.org/10.1109/csci.2016.0143
268. Hiwa S et al (2016) Region-of-interest extraction of MRI data using genetic algorithms. In: 2016 IEEE symposium series on computational intelligence (SSCI), pp 1–7. https://doi.org/10.1109/ssci.2016.7850135
269. Hameed S, Hasan O (2016) Towards autonomous collision avoidance in surgical robots using image segmentation and genetic algorithms. In: 2016 IEEE region 10 symposium (TENSYMP), pp 266–270. https://doi.org/10.1109/tenconspring.2016.7519416
270. Dey J et al (2016) Moving object detection using genetic algorithm for traffic surveillance. In: International conference on electrical, electronics, and optimization techniques (ICEEOT), pp 2289–2293. https://doi.org/10.1109/iceeot.2016.7755101
271. Das S, De S (2016) Multilevel color image segmentation using modified genetic algorithm (MfGA) inspired fuzzy C-means clustering. In: 2016 second international conference on research in computational intelligence and communication networks (ICRCICN), pp 78–83. https://doi.org/10.1109/icrcicn.2016.7813635
272. Bedruz RA et al (2016) Philippine vehicle plate localization using image thresholding and genetic algorithm, pp 2822–2825. https://doi.org/10.1109/tencon.2016.7848557
273. Al-Sahaf H et al (2017) Automatically evolving rotation-invariant texture image descriptors by genetic programming. IEEE Trans Evolut Comput 21(1):83–101. https://doi.org/10.1109/TEVC.2016.2577548
274. Patra S et al (2013) A novel context sensitive multilevel thresholding for image segmentation. Appl Soft Comput 23:122–127. https://doi.org/10.1016/j.asoc.2014.06.016
275. Kim EY et al (2000) A genetic algorithm-based segmentation of markov random field modeled images. IEEE Signal Process Lett 7(11):301–303. https://doi.org/10.1109/97.873564
276. Yoshimura M, Oe S (2003) Evolutionary segmentation of texture image using genetic algorithms towards automatic decision of optimum number of segmentation areas. Pattern Recogn 32:2041–2054. https://doi.org/10.1016/S0031-3203(99)00004-7
277. Chun DN, Yang HS (1996) Robust image segmentation using genetic algorithm with a fuzzy measure. Pattern Recogn 29(7):1195–1211. https://doi.org/10.1016/0031-3203(95)00148-4